A proposed, three step model for Nodal's role in anterior neurulation involving FGF and Wnt Signaling

A THESIS
SUBMITTED TO THE FACULTY OF
UNIVERSITY OF MINNESOTA
BY

Lexy M Kindt

IN PARTIAL FULFILLMENT OF THE REQUIREMENTS
FOR THE DEGREE OF
MASTER OF SCIENCE

Jennifer O. Liang

June 2015

Acknowledgements

I would like to thank my advisor, Jennifer O. Liang, members of my committee Matthew Andrews and Marshall Hampton, and the UMD Biology faculty. I would also like to thank the Integrated Biosciences program and the UMD Department of Biology for funding and support. Lastly, I would like to thank all of the members of the Liang Lab, fellow students of the Integrated Bioscience program, and my family and friends for their continued support and encouragement throughout my education.

Abstract

Neurulation is a complex process in vertebrates that can be affected by environmental, nutritional, and genetic factors. Disruptions in primary neurulation result in an open neural tube and, thus, neural tube defects (NTDs). Previous research has shown Nodals are involved in anterior neurulation and suggest an indirect role through induction of the mesendoderm/mesoderm. Based on characterization of Nodal mutants, our laboratory previously proposed a model for Nodal's role in anterior neurulation with three basic steps: 1) Nodals induce the mesendoderm/mesoderm, 2) The mesendoderm/mesoderm then signals the overlying neurectoderm, and 3) This mesendodermal/mesodermal signal promotes proper adhesion between neural tube cells.

Some Nodal mutants, such as those lacking zygotically expressed one-eyed pinhead (*Zoep*), a component of the Nodal receptor, have an incompletely penetrant NTD. Our research shows penetrance of this NTD increases with exposure to high temperatures at or before mid-blastula stages (up to 4 hpf). From ANOVA analysis, genetic background also significantly contributed to penetrance of the NTD in *Zoep* mutants.

We found Nodal is required up to mid- to late-blastula stages for neurulation to occur properly. Mesendodermal/mesodermal tissues are induced by Nodal during the time Nodal is required for neurulation supporting the first step of our model. Statistical analysis indicates a strong correlation between many mesendodermal/mesodermal derived tissues and a closed neural tube.

However, none of these derived tissues were sufficient or necessary for proper neurulation suggesting a critical amount of mesendodermal/mesodermal precursors are required during gastrulation to promote proper neurulation.

Through RNA-sequencing embryos with Nodal inhibited during the requirement for Nodal in neurulation (would have open neural tubes) and after this requirement (would have closed neural tubes), we identified over 3,000 transcripts for involvement in neurulation. With further investigation, we found two of these candidates, FGF signaling and *dkk1b*, a member of the canonical Wnt signaling pathway, are involved in neurulation.

Table of Contents

List of Tables

Chapter II

Chapter III

Chapter IV

List of Figures

Chapter II:

Chapter III:

Chapter IV:

Introduction

Primary Neurulation in Vertebrates

The vertebrate neural tube forms by two mechanisms, primary and secondary neurulation. Primary neurulation forms the anterior portion of the neural tube up to the sacral region from an epithelial substrate that forms a tube by rolling, folding, or bending (Smith and Schoenwolf, 1997). Secondary neurulation forms the posterior portion of the neural tube through mesenchymal cells that come together to form a rod of cells that will become neuroepithelium (Griffith et al., 1992; Lowery and Sive, 2004). Disruptions in primary neurulation cause open Neural Tube Defects (NTDs).

NTDs are the second most common birth defect occurring in approximately 1/1000 births (Detrait et al., 2005). The most common NTDs are anencephaly and spina bifida. Spina bifida occurs when there is defective closure of the neural tube in the spinal column. Anencephaly occurs when the anterior neural tube fails to close (Detrait et al., 2005). Previous work in our laboratory found that zebrafish with decreased Nodal signaling display a phenotype analogous to humans with anencephaly (Aquilina-Beck et al., 2007).

Studies have been done regarding neurulation in chick, frog, zebrafish and mouse embryos among other vertebrate species. These studies demonstrate that, although specific mechanisms can vary, the basic steps of primary neurulation are the same across vertebrate species (Davidson and Keller, 1999; Lowery and Sive, 2004; Morriss-Kay et al., 1994). These basic steps begin with

formation of the neural plate from columnarization of ectodermal cells, neural fold formation from the thickening edges of the neural plate, convergent extension of the neural plate which assists with bending and extension, and closure to form a neural tube (Schoenwolf and Colas, 2001).

Since primary neurulation in zebrafish has the same basic steps as other vertebrate species, studying unknown mechanisms of primary neurulation in zebrafish will help with understanding these same mechanisms in other vertebrate species. In zebrafish, the neural plate forms from columnarization and pseudostratification of the ectoderm. Next, the neural plate lengthens in the anterior to posterior direction and the neuroepithelial midline cells become wedge shaped forming the neural keel (Lowery and Sive, 2004; Smith and Schoenwolf, 1997). The neural keel continues to move inward until the neural folds fuse at the dorsal midline and, in zebrafish, form the neural rod, a solid rod of cells which is zebrafish specific (Smith and Schoenwolf, 1997). Then the lumen begins to open, forming a complete neural tube (Lowery and Sive, 2004).

Using Zebrafish as a Model for Anencephaly

Zebrafish provide a good model for study of neurulation and NTDs. Mice and *Xenopus tropicalis* with phenotypes analogous to NTDs have already been defined and are also being used to try and determine mechanisms of neurulation (Chowanadisai et al., 2013; Harris and Juriloff, 2010). Zebrafish also provide a useful model for study because structures in developing zebrafish are completely

visible, embryos are easily collected and manipulated because eggs are fertilized externally, many embryos are laid at once, fish can spawn about once a week, and fish absorb substances from their environment. Therefore, since Nodal deficient zebrafish display a phenotype similar to human anencephaly, zebrafish are an efficient and useful model organism for studying the mechanisms of anencephaly.

Nodals are secreted proteins in the TGF-β signaling pathway that have many roles in development. The TGF-β family of signaling molecules induce mesoderm, mesendoderm, and endoerm (Schier and Shen, 2000). Along with induction of the mesoderm, roles of Nodals include regulating left-right asymmetry in visceral organs and the brain, and regulating anterior-posterior patterning of neurectoderm, patterning of the ventral neural tube. Nodals have also been implicated in subdividing the mesoderm into different tissue types (Raya and Izpisúa Belmonte, 2004; Schier, 2003). Cyclops, Squint, and Southpaw are the three Nodal signals in Zebrafish. These Nodals work through a receptor complex containing Activin Like Kinases (ALKs), Type II receptor, and the EGF-CFC protein Oep as an extracellular cofactor (Gritsman et al., 1999).

Embryos without Nodal signaling always have an open neural tube. Anterior mesendodermal and mesodermal tissues are completely lacking in embryos which have no Nodal signaling (Schier and Shen, 2000). Nodal deficient embryos also display reduced expression and localization to the membrane of the adhesion protein N-cadherin (Aquilina-Beck et al., 2007).

Previous work from our laboratory showed that activation of the Nodal pathway in the cells of Maternal Zygotic *oep* mutant embryos can rescue the formation of mesendodermal and mesodermal tissues resulting in a closed neural tube (Aquilina-Beck et al., 2007). All embryos with a closed neural tube had rescued mesendoderm, but the reverse was not true (Aquilina-Beck et al., 2007). These experiments suggested a model where Nodal signaling acts through induction of the head mesendoderm to promote neural tube closure. The mesendoderm would then regulate the N-cadherin levels at the cell-membrane which then helps the movements that bring the neural tube together for fusion (Aquilina-Beck et al., 2007).

Although it is not known if mesenchymal tissue in mice and mesendodermal tissue in zebrafish have similar roles, mesenchymal tissue is also necessary for the cranial neural tube to fold (Chen and Behringer, 1995). *Twist* and *Cart1* knockout mice both display cranial NTDs. Mesenchymal tissue with a high proportion of *Twist* $^{-/-}$ cells can lead to an exencephalic phenotype, while high proportions of *Twist* $^{-/-}$ cells in the neural plate does not cause a NTD (Copp et al., 2003a). This suggests a role for mesenchymal tissue in mice similar to the role of mesendodermal tissue in zebrafish where both are necessary for the first phase of neurulation.

Chapter II: Identification of Transcripts Involved in Neural Tube Closure Using RNA-sequencing

Lexy M. Kindt, Alicia R. Coughlin, Tianna R. Perosino, Marshall Hampton, Jennifer O. Liang

Anencephaly is a fatal human developmental defect in which the anterior neural tube remains open. When Nodal signaling is reduced, zebrafish display a disorder similar to anencephaly. Previous work from our laboratory suggests a model for neurulation where Nodal signaling acts through induction of the head mesendoderm and mesoderm. The mesendoderm/mesoderm then, through an unknown mechanism, promotes adhesion between neural tube cells, which is required for neural tube closure. We sequenced the transcriptome of embryos treated with a Nodal inhibitor at sphere (neural tube will be open) or 30% epiboly (neural tube will be closed) stages and froze these embryos at three time points important for neurulation: shield (6 hpf, neurectoderm induction), tailbud (10 hpf, neural plate forms), and 7 somites (12 hpf, forebrain neural rod is closed). This screen identified many mRNAs involved in Wnt, FGF, and BMP signaling, suggesting these pathways might be involved in the communication between the mesoderm/mesendoderm and the neuroectoderm. mRNAs involved in the tight junction and adherens junction pathways were also differentially expressed, suggesting these pathways might be involved in adhesion between neural tube cells. Further, we found that severe knockdown of expression of Wnt effector gene *dkk1b* or inhibition of FGF-receptors can result in an open neural tube phenotype. Overall, this study identified many transcripts with potential roles in

anterior neurulation, and showed roles for the FGF and the canonical Wnt signaling pathways in neurulation for the first time.

Introduction

Neural tube defects (NTDs) are the second most common birth defect in humans, occurring in approximately 1/1000 births (Detrait et al., 2005). The most common NTDs are anencephaly and spina bifida. Anencephaly occurs when the anterior neural tube fails to close and is characterized by partial or complete absence of the cranial vault and cerebral hemisphere (Detrait et al., 2005). Spina bifida occurs when there is defective closure of the neural tube in the spinal column (Detrait et al., 2005).

In many cases, NTDs have been linked to underlying genetic factors in humans. Studies in model organisms such as mice, chicks, zebrafish, and frogs have been used in attempt to identify some of these genetic factors. For instance, in mice, there are over 250 different models with NTDs and over 200 genes that are known to cause NTDs with missexpression (Copp et al., 2013; Harris and Juriloff, 2010). These genes have begun to be tested for relationships in human NTDs, but in most cases, this link has not been found (Copp et al., 2013). A major exception to this is the Planar Cell Polarity/Wnt signaling pathway. Disruptions of this pathway have been shown to cause NTDs in mice, frogs, chick, zebrafish, as well as in humans (Cai and Shi, 2014; Ciruna et al., 2006; Wallingford and Harland, 2002).

Nutritional factors such as folic acid have been shown to be involved in NTDs in humans and to interact with genetic factors (1991; Au et al., 2010; Correa et al., 2008; Czeizel and Dudás, 1992; Moretti et al., 2005). For instance, *Shmt* knockout mice only have NTDs when the mother is folate deficient (Beaudin et al., 2011). In other cases, such as in *Folbp1, RFC1, Cart1,* and *Cd* knockout mice, NTD rates were reduced with maternal folic acid supplementation even though *Cart1* and *Cd* are not related to folate metabolism. This suggests that NTDs are multifactorial with folic acid playing a partial role (Blom et al., 2006). Similarly, folic acid has a partial and complex role in NTDs in humans. A 10%-80% decrease in NTDs was shown after folic acid food fortification in many countries with the most obvious decreases seen in areas or ethnic groups with the highest incidence (De Wals et al., 2007; Imbard et al., 2013; Williams et al., 2005). Therefore, more research is needed to fully understand the genetic and nutritional interactions resulting in NTDs.

Mechanisms of neurulation vary between anterior and posterior regions of the embryo. Primary neurulation forms the anterior portion of the neural tube up to the sacral region and secondary neurulation forms the posterior portion of the neural tube (Smith and Schoenwolf, 1997). Only disruptions in primary neurulation result in open NTDs (Copp et al., 2003a). Basic morphological events of primary neurulation are similar across species, beginning with formation of the neural plate from columnarization of ectodermal cells. Next, neural folds form from the thickening edges of the neural plate. The neural plate

then goes through convergent extension and other movements, which assist with bending, extension, and closure to form a neural tube (Lowery and Sive, 2004; Schoenwolf and Colas, 2001).

Primary neurulation occurs slightly different by axial levels of the same embryo. For instance, in mice, spinal neurulation occurs in the cervical/hindbrain boundary with bending only at one hinge point while more caudally, spinal neurulation occurs with bending on multiple hinge points (Shum and Copp, 1996; Ybot-Gonzalez et al., 2007). These differences are also reflected by genetics. In mice, knockout of some genes results in anencephaly, while loss of others result in spina bifida or even craniorachisis, where the primary neurulation fails along the whole length of the embryo (Copp et al., 2003a). Therefore, study of genetics involved at each axial level is necessary to completely understand the mechanisms of neurulation.

Previous work in our laboratory found that zebrafish with decreased Nodal signaling display a phenotype analogous to that of humans with anencephaly (Aquilina-Beck et al., 2007; Ciruna et al., 2006). This phenotype is characterized by an open anterior neural tube, a lack of anterior mesendodermal/mesodermal tissue, decreased membrane localization of the cell adhesion protein N-cadherin in the mesoderm, and disrupted order of the cells within the neural tube (Aquilina-Beck et al., 2007; Schier and Shen, 2000). Our initial characterization of these mutants enabled us to propose a three step model of the role of Nodal in anterior nerulation. In the first step, Nodal signals induce the head

mesendoderm/mesoderm in early- to mid- blastula stages. Second, the mesendoderm/mesoderm then signals the overlying neurectoderm probably between shield and tailbud stages (6-10 hpf) as neuroepithelium is abnormal by neural plate stages in Nodal mutants (Aquilina-Beck et al., 2007). Third, this mesendodermal/mesodermal signal promotes adhesion among neural cells, resulting in proper closure of the anterior neural tube (Aquilina-Beck et al., 2007). Consistent with this model, an open neural tube phenotype is seen only when Nodal signaling is inhibited before late-blastula stages, the same time Nodal is inducing mesodermal/mesendodermal tissues and before the formation of neuroepithelium (Araya et al., 2014; Gonsar et al.).

This study used RNA-sequencing to identify genetic factors involved in neurulation in zebrafish downstream of Nodal. We compared the transcriptomes of embryos that would have open to those that would have closed neural tubes at three developmental time-points important for neurulation: shield stage (6.0 hpf) for the onset of neurectoderm induction, bud stage (8.0 hpf) when a formed neural plate begins to thicken and sink to become the neural keel, and 7 somite stage (around 12.0 hpf) for when the closed neural rod is formed in the forebrain (Grinblat et al., 1998; Kimmel et al., 1995b). This screen identified over 3,000 differentially expressed transcripts. We found genes potentially involved in (1) mesendoderm/mesoderm induction, including members of the Activin/Nodal and FGF signaling pathways, (2) mesendodermal/mesodermal signaling to the neuroectoderm, including members of the Wnt and FGF signaling pathways, and

(3) adhesion between neural tube cells, including genes involved in tight junctions and adherens junctions. We were specifically interested in identifying candidates for the mesendodermal/mesodermal signal to neural epithelium acting in step two of our model because it is the next step after Nodal. Thus, the best candidates were genes involved in generating a signal originating in the mesoderm/mesendoderm that could affect the neural plate. We also anticipated candidate genes to be more highly expressed in embryos with closed neural tubes than those with open neural tubes. Two candidates that fit these criteria were analyzed in loss of function experiments. Both *dickkopf 1b (dkk1b)* of the canonical Wnt signaling pathway and Fibroblast Growth Factor signaling were found to be involved in neurulation.

Methods

Animal Care

Zebrafish were kept in a fish facility with circulating water at 28.5 ^{o}C and a light:dark cycle of 14:10 (Westerfield, 2000b). For this project, we used the wild-type strain Zebrafish *Danio rerio* (ZDR, Aquatica Tropical, Plant City, FL) and Tg (flh:EGFP)^{C161} fish (Gamse et al., 2003). Embryos were obtained by natural spawning groups of adult fish. Embryonic stages were defined by morphology (Kimmel et al., 1995b).

Pronase Treatment

Embryos were pronase treated to remove their chorions before treatment with SB505124 or before snap freezing. Concentrated stock of pronase (15 mg/mL, Roche) was activated by incubation at 37 ^{o}C for at least 30 minutes. Next, the pronase was diluted in embryo media (5mM NaCl, 0.17 mM KCl, 0.33mM $MgSO_4$, 1 X 10^{-5}% methylene blue in fish water) to a concentration of 2 mg/mL to make a total of 15 mL. Water was poured off and then the pronase solution was added in a 100 mm x 20 mm Petri dish. Embryos were incubated at 28.5 ^{o}C. After 4 minutes, embryos were swirled with a plastic pipet. The embryos were placed back into the 28.5 ^{o}C incubator and swirled every 30 seconds until approximately 75% of the embryos were out of the chorions.

To stop the pronase reaction, the embryos were pipetted into a 1 L fish tank containing embryo media and lined with 2% agar. Embryos were transferred using a plastic pipet to 100 mm x 20 mm Petri dishes containing at least 20 mL embryo media. Embryos with intact chorions were gently agitated with forceps until the chorion disassociated. Embryos that were completely intact after this treatment were maintained at 28.5 ^{o}C until they were at the appropriate stage for SB505124 treatment or snap freezing. Glass sigma cote (Sigma-Aldrich) coated pipets were used to transfer dechorionated embryos into 2.0 mL Eppendorf tubes for snap freezing and plastic pipets were used for transferring embryos in earlier steps.

SB505124 Treatment

For the RNA-sequencing portion of this project, 2-(5-benzo [1,3] dioxol-5-yl-2-terbutyl-3H-imidazol-4-yl)-6-methylpyridine hydrochloride hydrate (SB505124) from Sigma-Aldrich was used at a concentration of 100 μM in a total of 12 mL embryo media in a 15 mm x 60 mm Petri dish (DaCosta Byfield et al., 2004; Hagos and Dougan, 2007). For RT-PCR and whole mount in-situ hybridization, SB505124 from Tocris was used at a concentration of 20 μM in a total of 30 mL in a 100 mm x 20 mm petri dish. For both drugs, DMSO (Dimethyl Sulfoxide) was used to dissolve SB505124 and comprised 1% of the final treatment volume. Drug mix (12 mL for Sigma-Aldrich and 30 mL for Tocris) was added to pooled groups of ZDR embryos at either sphere (4.0 hpf) or 30% epiboly (4.7 hpf) stages and left on until the embryos were snap frozen in liquid nitrogen or fixed in 4% paraformaldehyde. As controls, some embryos were treated with only 1% DMSO in embryo media and raised to 24 hpf. In addition, at least 20 embryos from each treatment group were left in drug until 24 hpf to ensure that the embryos had open or closed neural tube phenotypes as predicted from their time of treatment. Phenotypes at 24 hpf between the two drugs were similar at the concentrations used.

RNA Preparation

Whole embryos treated with SB505124 at sphere or 30% epiboly stages were frozen with liquid nitrogen at shield, tailbud, and 7 somite stages. Three

samples for each treatment group at each stage were collected for a total of 18 samples for sequencing. 30-60 embryos were frozen per sample with the most embryos in samples with earlier developmental stages and those treated at sphere stage. Samples were stored at -80 ^{o}C until RNA was isolated using the Qiagen RNeasy Mini Kit. Samples were quantified using a nanodrop to ensure at least 1µg was present and were sent on dry ice to the University of Minnesota Biomedical Genomics Center (St. Paul, MN) for Illumina HiSeq 2500 sequencing.

RNA Sequencing

A fluorimetric RiboGreen assay was used to quantify the isolated RNA once received by the UMGC. For each sample, an RNA integrity number (RIN) was generated by capillary electrophoresis via the Agilent BioAnalyzer 2100. Only samples that had a RIN of 8 or more and a mass of greater than 1 microgram were considered high quality and made into Illumina sequencing libraries through Illumina's Truseq RNA Preparation v2 kit (RS-122-2001). Briefly, 1 µg of RNA went through two rounds of purification for the polyA containing mRNA by using oligo-dT attached magnetic beads and was fragmented and primed with random hexamers. RNA fragments were then reverse transcribed into first strand cDNA. Next, RNA template was removed, a replacement strand was synthesized to make ds cDNA, and AMPure XP beads were used to separate the ds cDNA from the reaction mix. Ends of the cDNA were blunt ended and repaired. A single adenylate was added to the 3' ends

and multiple RNA adaptor indexes were ligated. DNA fragments with adapter indexes were PCR amplified. All libraries were validated, normalized, pooled, and size selected to approximately 200bp using Caliper's XT instrument before they were sequenced.

Libraries were clustered on the HiSeq2500 at 10 pM through hybridization to a paired end flow cell. Next, the flow cell was sequenced using Illumina's Rapid Run SBS chemistry. When read 1 was completed, a 7 base pair index read was performed. In order to produce the template for paired end read 2, library fragments were resynthesized in the reverse direction and sequenced from the opposite end of the read 1 fragment.

For each cycle of sequencing, a base call (.bcl) file was generated by Illumina Real Time Analysis (RTA) software. These base call files and run folders were exported to Minnesota Supercomputing Institute (MSI) servers. Primary analysis and de-multiplexing were performed using Illumina's CASAVA software 1.8.2 which resulted in de-multiplexed FASTQ files. FASTQ files were released to our account for bioinformatic analysis.

Bioinformatics and Statistical Analysis

Reads from each sample were mapped to NCBI's RefSeq database of mRNA for *Danio rerio* using NCBI's megablast. After genes were identified, they were quantified resulting in counts. Counts for each gene were upper quartile

normalized to obtain accurate expression levels. Normalized counts were fitted to a negative binomial distribution using DESeq v1.6.1(Anders and Huber, 2013).

Pairwise comparisons between genes in embryos that would have a closed neural tube to those that would have an open neural tube were performed using DESeq (command: nbinomGLMTest) as described in Anders and Huber (Anders and Huber, 2010; Anders and Huber, 2013). P-values were independently filtered to restrict for genes with a 50% or greater change in expression and at least 100 or more mean reads in either sample. The Benjamini-Hochberg method was used to control the false discovery rate to 0.05 (Benjamini et al., 2001). Only mRNAs meeting all of these criteria were further analyzed.

Functional Analysis

Differentially expressed transcripts were further analyzed using DAVID, KEGG, and literature searches. Transcript lists were put into DAVID for analysis to get tissue expression as well as functional groups and pathways represented (Huang et al., 2009a, b). The Kyoto encyclopedia of genes and genomes (KEGG) pathways were accessed through our DAVID analysis to visualize pathways represented and then through the KEGG pathways website to visualize specific genes in our data in pathways of interest (Ogata et al., 1999).

Relative Reverse Transcription PCR

RNA-sequencing results were confirmed by relative reverse transcription polymerase chain reaction (RT-PCR). RNA was isolated from SB505124 treated embryos as previously described. Isolated RNA was reverse transcribed into cDNA through Qiagen's omniscript Reverse Transcription Kit. Briefly, 1-1.5 µg of RNA was incubated in a mix which included dNTPs, random nonamers, and RNase inhibitor for 60 minutes at 37 ^{o}C. Resulting cDNA was then diluted 1:10 and added to a mixture containing 2x Rotor-Green SYBR Green PCR Master Mix and forward and reverse primers. All tubes were put in the RotorGene3000 with an inactivation step of 5 minutes at 95 ^{o}C followed by 40 2-step cycles of denaturation for 5 seconds at 95 ^{o}C and annealing/extension for 15 seconds at 60 ^{o}C and lastly a melting curve analysis starting at 60 ^{o}C to 95 ^{o}C. Expressed repeat elements *hatn10* and *loopern4* were used as controls (Vanhauwaert et al., 2014).

Whole Mount In-Situ Hybridization (WISH)

Expression of *orthodenticle homobox 5* (*otx5*) in the developing pineal organ, was assayed through established WISH techniques (Gamse et al., 2002; Thisse and Thisse, 2014). Briefly, whole embryos were incubated with digoxygenin (DIG) antisense RNA probes in hybridization mix (50% formamide) at 70 ^{o}C overnight. DIG was detected by an anti-DIG antibody covalently linked

to Alkaline Phosphatase (AP) enzyme. Cells expressing *otx5* mRNA were visualized after the addition of the AP substrates 4-nitro blue tetrazonium (NBT) and 5-bromo-4-chloro-3-indolyl-phosphate (BCIP) which turn into a purple product after incubation with AP (Chitramuthu and Bennett, 2013; Thisse et al., 2004b; Thisse and Thisse, 2014).

Morpholino Injections

dkk1b morpholino was obtained from gene tools and was originally created for the Flowers et al. 2012 paper published in Development 139(13): 2416-2425 with sequence: 5'-AGAGAGCATGGCGATGTGCATCATG-3'. A morpholino standard control oligo made to a mutant allele of the mouse beta globin gene (5'-CCTCTTACCTCAGTTACAATTTATA-3') and *dkk1b* morpholinos were dissolved in distilled water and diluted to a final concentration of 8 mg/mL with phenol red diluted to 0.4% in the final mixture and 1x Danieau buffer (Flowers et al., 2012). Tg (flh:EGFP)^{C161} embryos were injected at 1-cell stage with approximately 10 nL of the mixture resulting in 80 ng total of the morpholino injected.

FGF Inhibitor Treatment

The FGF receptor inhibitor 2-[(1,2-Dihydro-2-oxo-3*H*-indol-3-ylidene)methyl]-4-methyl-1*H*-pyrrole-3-propanoic acid (SU5402) was initially dissolved in 100% DMSO to make a stock solution. The stock solution was

diluted with embryo media and DMSO to obtain a concentration of 33.75 μM or 67.5 μM and 2% DMSO working solution. 12 mL working solution was placed on pooled groups of Tg (flh:EGFP)^{C161} embryos in a 15 mm x 60 mm Petri dish at high stage (3.3 hpf) or 30% epiboly stage (4.7 hpf). Embryos were then raised to 24 hpf in this treatment and subjected to WISH for *otx5*.

Results

Identifying transcripts downstream of Nodal as candidates for involvement in neurulation

This study compared the transcriptome of developing zebrafish embryos that would have a closed neural tube to the transcriptome of those that would have an open neural tube at three stages important for neurulation. To do this, we used the drug SB505124, which inhibits signaling by Nodal and Activin proteins by blocking function of their receptors, the Activin receptor-Like Kinases (ALKs) 4, 5, and 7 by competing for the ATP binding site (DaCosta Byfield et al., 2004; Hagos and Dougan, 2007). Previous studies in our laboratory found an open neural tube phenotype in embryos when Nodals were inhibited with SB505124 beginning at mid-blastula stages (sphere stage, 4.0 hpf. Early Inhibitor Treatment/EIT) and a closed neural tube phenotype in embryos when Nodals were inhibited with SB505124 at late-blastula stages (30% epiboly stage, 4.7 hpf, Late Inhibitor Treatment/LIT) (Figure 1). Pineal phenotype has been shown to indicate an open or closed neural tube phenotype (Aquilina-Beck et al., 2007). A

round pineal phenotype indicates a closed neural tube, while an elongated or divided pineal phenotype indicates an open neural tube phenotype. These phenotypes can be seen after WISH with *otx5.* EIT embryos displayed either an elongated or divided pineal phenotypes while LIT embryos displayed oval pineal phenotypes. These pineal phenotypes are equivalent to *lefty1* mRNA injected and Nodal mutant embryos ensuring SB505124 has the same effects as our previous results (Aquilina-Beck et al., 2007; Gonsar et al.).

In order to identify transcripts potentially involved in many steps of neurulation, EIT and LIT embryos were snap frozen at three stages important for neurulation. These stages included shield (6.0 hpf) for onset of neurectoderm induction, bud stage (8.0 hpf) when a formed neural plate starts to become the neural tube, and 7 somite stage (around 12.0 hpf) for when the neural rod is formed in the forebrain (Grinblat et al., 1998; Kimmel et al., 1995b). Signaling from the mesendoderm/mesoderm could start as early as shield stage since neuroepithelium is already abnormal by neural plate stages in Nodal mutants (Aquilina-Beck et al., 2007). This mesendodermal/mesodermal signal, if initially signaling at shield stage, could persist for the entirety of neurulation in the forebrain (ending when the neural tube is closed around 7 somites stage), or only signal for a short time. It is also possible the signal is not present until after shield stage. Therefore, we sequenced time points spanning the time in which the mesendoderm/mesoderm could be signaling overlying neurectoderm to promote adhesion between neural cells.

To identify all differentially expressed genes, raw reads were mapped to NCBI's RefSeq *Danio rerio* mRNA sequences and differential expression of mRNA's between EIT embryos and LIT embryos were analyzed at each of the three stages, for a total of six experimental samples (EIT frozen at 6, 10, and 12 hpf and LIT frozen at 6, 10, and 12 hpf). Three repeats for each experimental sample were also sequenced for a total of 18 samples overall. Average counts of the three repeats for each of the six samples were used to determine differential expression levels.

We applied several criteria to reduce the number of false positives. Only mRNAs differing in expression by 50% or more and had at least 100 total counts in one collection point with a false discovery rate of <0.05 were considered significantly different between EIT and LIT samples. After genes not meeting this criteria removed, there were a total of 3,187 transcripts that were significantly differentially expressed in our data (Table 1). Expression differences on this list were viewed as ratios of counts in LIT embryos divided by counts in EIT embryos. Ratios of >1 indicated higher expression in LIT embryos, which would have closed neural tubes, while ratios of <1 indicated higher expression in EIT embryos, which would have open neural tubes.

Many candidate genes for involvement in neurulation were identified in our screen

One way we confirmed our RNA sequencing screen was effective at identifying genes downstream of Nodal was to look at differential expression

ratios of transcripts known to be affected by Nodal. Cyclops and Squint, two of the three zebrafish Nodal ligands, promote the expression of *mixl1* and *sox32* which then promotes the expression of a transcription factor, *sox17,* which leads to the differentiation of the endoderm (Alexander and Stainier, 1999). Since Nodals promote *mixl1* and *sox17* expression, we expected them to have higher expression in EIT embryos than in LIT embryos and we found both had ratios of >1 on the candidate list just as we would expect. The presence of these and other Nodal target genes (Table 1) suggested that our RNA sequencing screen was effective at identifying transcripts downstream of Nodal (Table 2).

Our data also contained genes known to cause NTDs in mice and humans in our data suggesting our study was successful at identifying candidates for involvement in neurulation (Table 3). Four genes with loss-of-function mutations in human babies with anencephaly were identified in a recent study (Lemay et al., 2015). Three of these four genes were differentially expressed in our data. Also, missexpression of many genes in mice have been identified as causing NTDs and have been recently reviewed (Copp et al., 2013). Multiple of these genes were differentially expressed in our screen.

In order to verify our RNA-sequencing results, relative, reverse transcriptase polymerase chain reaction (RT-PCR) was used on six genes and two reference genes. Transcripts chosen for RT-PCR were of specific interest to us as candidates as potential candidates in our model and covered genes found in each of the three time points. Each time point had a transcript with a ratio of

>1 and a transcript with a ratio of <1. We determined average expression of the transcripts relative to our two reference genes over three replicates with a 95% confidence interval. These averages were used to form the same LIT:EIT ratio of expression that was used in our RNA-sequencing data.

Ratios were only used to determine direction of higher expression (ration >1 or <1). All RNA-sequencing differential expression ratio directions were the same as determined by our RT-PCR except for *fgf8a* at shield stage (Table 3). *fgf8a* had a ratio of <1 in our RNA-sequencing data at shield stage, but in multiple trials of RT-PCR, each with 3 replicates, the LIT:EIT ratio for *fgf8a* expression was >1. Although PCR has been used in other publications for confirmation of RNA-sequencing data, we found our PCR results differed in fold and direction of change in expression between repeats and occasionally between replicates (Aanes et al., 2011; Palstra et al., 2013).

Two tools were used to identify the subset of the differentially expressed genes that were the best potential candidates for involvement in neurulation. DAVID along with literature searches gave an overall picture of functional groups and tissues represented in the data (Huang et al., 2009a, b). KEGG was used to determine specific pathways with genes that were differentially expressed in our screen (Ogata et al., 1999).

Transcripts from many pathways and functional groups were differentially expressed and there were candidate genes for all three steps of our neurulation model for Nodals. Candidates for the first step of mesendoderm/mesoderm

induction include genes that encode components of the Nodal signaling, BMP, and FGF signaling pathways (Figures 2 and 3).

BMP signaling works in a dorsoventral gradient to specify mesodermal territories. Where BMPs are highly expressed, a ventral fate is specified for the mesoderm, and where BMPs antagonists, such as Chordin, are highly expressed, a dorsal fate is specified (Dale and Jones, 1999). These BMP antagonists are expressed in the prospective neurectoderm while the future dorsal endoderm secretes Nodal-related mesoderm-inducing factors (De Robertis and Kuroda, 2004). Previous studies in our laboratory show that Nodals are required for neurulation. Therefore, we would suspect BMP antagonists and Nodals to have higher expression in embryos that would have a closed neural tube and transcripts promoting BMPs and antagonists of Nodals to have higher expression in embryos that would have an open neural tube. This expression pattern was found for all transcripts in these pathways except for *foxh1* which we would expect to have higher expression in embryos with a closed neural tube, but in our data the opposite was true. However, a previous study shows *foxh1* isn't required for induction of Nodal-dependent cell fates in zebrafish, and instead is a part of an autoregulatory feedback loop that modulates and enhances morphogenic Nodals which could help explain the expression patters in our data (Pogoda et al., 2000). Also, since SB505124 has only been shown to block the binding of Nodal ligands to ALKs, we did not expect to see differential expression of the transcripts encoding these ALKs in the two groups of embryos treated with

this inhibitor. Differential expression of the *acvr1l* transcript which is part of the ALK receptor complex suggest SB505124 has transcription level effects (Figure 2).

FGF signaling has been shown to play an essential role in morphogenesis and patterning of the mesoderm (Ciruna and Rossant, 2001). For example, FGFs have roles in regulating convergent extension movements of gastrulating mesoderm (Ciruna and Rossant, 2001; Isaacs, 1997). FGF signaling is very complex and publications have shown FGF signaling has roles upstream and downstream of Nodals. Although we would expect FGFs to have higher expression in embryos that would have a closed neural tube based on FGFs roles in the mesoderm, the complexity of the FGF singaling pathway was represented in our data as transcripts encoding members of the pathway that should have the same or similar functions have higher expression in both embryos that would have an open neural tube and those that would have a closed neural tube (Figure 3).

Signals potentially involved in the second step of our model, mesendodermal/mesodermal signaling to the overlying neurectoderm, included members of the Wnt (Figure 4), FGF (Figure 3), and BMP (Figure 2). There are three separate Wnt signaling pathways which have different functions, but involve ligands from the same protein family. The canonical Wnt pathway has been shown to be involved in cell fate determination during embryogenesis and accumulation and translocation of β-catenin into the nucleus (Komiya and Habas,

2008). In a previous study, knockdown of a canonical Wnt antagonist, Dkk1b, and overexpressions of a Wnt ligand, Wnt8a, resulted in abnormal head phenotypes in zebrafish suggesting inhibition of the canonical Wnt signaling pathway promotes proper neural development (Seiliez et al., 2006). Therefore, we would expect Canonical Wnt signaling transcripts to be more highly expressed in embryos that would have an open neural tube, while Canonical Wnt signaling antagonists should have higher expression in embryos that would have a closed neural tube. Differential expression of transcripts in our data fit with these expression patterns (Figure 4). The PCP pathway has been implicated in NTDs in other organisms and has been shown to be involved in directed migration and polarized organization of cells (Komiya and Habas, 2008). We would expect the PCP portion of the the Wnt signaling pathway to have higher expression in embryos with a closed neural tube which we found in our data (Figure 4).

Lastly, candidates for mediating adhesion between cells in the neural tube included members of the adherens junction (Supplemental Figure 1) and tight junction pathways (Supplemental Figure 2). Adherens junction pathway is very complex with many overlapping interactions within itself as well as with other pathways including the tight junction pathway. Expression patterns from our data reflect this complexity. Since cadherins are thought to initiate cell-cell adhesion and are from the start of the adherens junction pathway, this pathway could be involved in the beginning of neurulation (Schepis and Nelson, 2012). The tight

junction pathway is also complex and many components of this pathway were represented in our RNA-sequencing data. Tight junctions are involved in cell to cell contact in between polarized cells such as those in endothelium and epithelium (Krause et al., 2009). Because Nodal-deficient embryos are known to have abnormal cell adhesion and organization, we would expect transcripts encoding adhesion proteins involved in neurulation to have higher expression in LIT embryos than in EIT embryos which have an open anterior neural tube. Multiple transcripts encoding portions of the tight junction pathway seemed to have differential expression patterns in our RNA-sequencing data that fit with our model for neurulation involving Nodal signaling.

Inhibition of FGF receptor function can cause an open neural tube phenotype

To determine if we found new genes involved in anterior neurulation, we chose two candidates to analyze through loss of function experiments. We chose FGFs because FGFs are known to have many roles in development including some roles in neural development, such as induction and survival of the telencephalon in mice and roles in brain formation in zebrafish (Ota et al., 2009; Paek et al., 2009). Also, some FGFs, including *fgf8a,* are expressed in the mesoderm/mesendoderm and the forebrain neural rod and neural tube in zebrafish (Reifers et al., 1998; Shimizu et al., 2006; Warga et al., 2013). Two fibroblast growth factors (FGFs) ligands were more highly expressed in embryos that would have a closed neural tube than in those that would have an open

neural tube in at least one time point: *fgf8a* and *fgf17b*. *fgf8a* was 0.297 times more expressed at shield stage (6.0 hpf) and 1.801 times more expressed at tailbud stage (Figure 3). *fgf17b* was 2.405 times more expressed at shield stage (6.0 hpf) (Figure 3).

In order to further analyze the roles of FGFs in neurulation, Tg(flh:EGFP)^{C161} embryos, which express EGFP in the developing pineal, were treated starting at high stage (3.3 hpf) with a low (33.8 μM) or starting at dome to 30% epiboly stage (4.3 to 4.7 hpf) with high (67.5 μM) concentrations of SU5402. Treatments were left on embryos until 24 hpf. SU5402 inhibits tyrosine kinase activity of vascular endothelial growth factor receptors and fibroblast growth factor receptors (Mohammadi et al., 1997; Sun et al., 1999).

When raised to 24 hpf, wildtype and three other phenotypic classes of differing severities were present in embryos treated with the low concentration. Class I embryos looked similarly to 25 μM SU5402 treated embryos in Kwon et al. 2010 and were characterized by having a truncated, but functional tail and could have disrupted eye development, but they still seem to form somites normally and show little to no cell death (Figure 5)(Kwon et al., 2010). Class II embryos looked similar to 50 μM SU5402 treated embryos in Liedtke et al. 2008 and were characterized by having a severely truncated, non-functional tail showing regions of black which usually indicates apoptosis (Figure 5)(Liedtke and Winkler, 2008). Black regions were also noticeable in the head and usually eyes have abnormal formation. These embryos occasionally had a few somites,

but usually they are misshapen or absent. Class III embryos looked similar to membrane-bound dominant-negative FGFR injected embryos in Shimada et al. 2008 and were characterized by a tail barely being present if at all with black regions in head and tail. These embryos usually did not have eyes or showed major eye malformations and it was difficult to determine the head from tail (Figure 5). There was some overlap between class II and class III as some embryos fit part of the criteria for one class as well as the other.

Embryos treated with the lower concentration of SU5402 all had a closed neural tube at 24 hpf, while approximately 70% of embryos treated with the higher concentration of SU5402 had an open neural tube at 24 hpf (Figure 5). Low concentrations of SU5402 produced embryos in all three classes, but even in the class III embryos, which were the most severely affected, nearly all had a closed neural tube phenotype. In contrast, almost all embryos treated with a high concentration at high stage (3.3 hpf) and raised to 24 hpf showed arrested development in the gastrulation stages and did not have a pineal phenotype. Those embryos that did not have arrested development had only class II and class III phenotypes and nearly all had an open neural tube. In order to get fewer embryos with arrested development in the gastrulation stages, we treated at dome to 30% epiboly stages (4.3-4.7 hpf) using the same protocols. Approximately 70% of these embryos had open neural tubes when raised to 24 hpf. Although Tg (flh:EGFP)^{C161} appeared to indicate the pineal and corresponding neural tube phenotype accurately when viewed under

flourescence, all neural tube phenotypes were confirmed through WISH with *otx5*.

Knock down of dickkopf1b expression can cause an open neural tube phenotype

The second choice for further analysis was *dickkopf1b* (*dkk1b*). *dkk1b* was more highly expressed in LIT embryos than in EIT embryos at both shield (4.7 ratio) and tailbud (3.2 ratio) stages (Figure 4). Previous studies indicate *dkk1b* acts in neural development as a 'head inducer' in mice and *Xenopus* which was one reason this transcript was a good potential candidate (Glinka et al., 1998; Mukhopadhyay et al., 2001). Also, *dkk1b* acts on the neural ectoderm to support forebrain formation in vertebrates (Caneparo et al., 2007). In *Xenopus*, inhibition of DKK1 protein function through anti-Dkk1 antibodies causes microcephaly (Glinka et al., 1998). We and others have found this phenotype upon dkk1b knockdown in zebrafish using morpholinos (Caneparo et al., 2007; Flowers et al., 2012). Lastly, *dkk1b* is expressed in the presumptive mesendoderm in zebrafish, is an inhibitor of the canonical Wnt pathway and functions upstream of FGF-signaling, another potential candidate for involvement in neurulation (De Robertis et al., 2000; Shinya et al., 2000; Shu et al., 2005)

To determine if *dkk1b* has a role in neurulation, we knocked-down Dkk1b protein using a previously published morpholino (Flowers et al., 2012). Injection of embryos with approximately 80 ng of morpholino at resulted in a range of phenotypes at 24 hpf (Figure 6). We categorized the severity of knockdown of

Dkk1 by the eye phenotype, which ranged from eyes of normal size to lack of eyes. Embryos with normal eye size had closed neural tube phenotypes, some embryos with small eyes had closed neural tube phenotypes and some had open neural tube phenotypes, and embryos lacking eyes displayed an open neural tube phenotype (Figure 6). To ensure effects we saw were not due to volume of injection or injection trauma, a standard control morpholino was injected into sibling embryos at the same concentration as the *dkk1b* morpholino. Most embryos injected with the control morpholino were wildtype at 24 hpf. A few embryos injected with the control morpholino displayed abnormal phenotypes such as truncated tails and apoptosis in head and tails, but never displayed an open neural tube phenotype.

Discussion

Although NTDs are the second most common human birth defect, genetic interactions involved in model organisms and how these mechanisms translate to humans are poorly understood. Zebrafish provide a useful model of study for these mechanisms in humans because neurulation is similar between zebrafish and mammals and 70% of human genes coding for proteins have zebrafish orthologs (Clark and Pazdernik, 2016). In this study, we identified over 3,000 candidate genes in zebrafish that could have a role in neurulation by comparing the transcriptome of embryos that would have a closed neural tube to that would have an open neural tube. New candidates for inducing the

mesendoderm/mesoderm, signaling from the mesoderm to the neurectoderm, and functioning in proper adhesion between neural tube cells in our model of neurulation were present in our data, supporting our model. Two of these candidates, *dkk1b* and FGF signaling, were further analyzed and were shown to have a role in neurulation.

RNA-sequencing was a useful technique for identifying candidates for involvement in our model for neurulation

Our screen supported our model for neurulation by identifying new transcripts in pathways for each of the three steps. This data provided new insights into parts of our model where our understanding is incomplete. For example, although N-cadherin localization is disrupted in Nodal mutants, N-cadherin mutants have a less severe phenotype than Nodal mutants (Aquilina-Beck et al., 2007). Many transcripts encoding adhesion proteins were differentially expressed in our screen suggesting many adhesion proteins are involved in neurulation downstream of Nodal. Because *dkk1b*, a member of the Canonical Wnt signaling pathway, and FGF signaling were involved in neurulation, we also know that multiple pathways are involved in the first portion of our model.

PCR has been used in previous publications for validating RNA-sequencing results, however, results from our PCR highly varied between runs of PCR with the same samples as well as between replicates within the same run.

This non-reproducibility could be due to a number of factors including, but not limited to degradation of RNA, pipetting errors, variability of mRNA expression between embryos, and variability of mRNA expression between embryos at slightly different stages of development. Although Illumina sequencing technology is reliable, we will further confirm our results by semi-quantitative analysis of WISH.

RNA-sequencing was a very useful approach for identifying candidates involved in neurulation downstream of Nodal. Since few embryos are needed for sequencing, this technique is very accessible. 30-60 embryos per sample in our study, and around 100 in other recent studies contained over 1 µg of high quality mRNA (Harvey et al., 2013; Vesterlund et al., 2011). Also, the cost of RNA-sequencing has decreased over the last few years, making sequencing of multiple samples more cost effective. Therefore, RNA-sequencing has become a much more accessible technique and will be very useful for a variety of future forward genetic studies.

Potential roles for FGFs in anterior neurulation

Our study suggests FGF signaling is involved in neurulation. Other studies have implicated roles for FGFs in neurulation and one study has shown mice with deletion of FGFR1 defectively close the caudal neural folds (Deng et al., 1997)(Deng et al., 1997)(Deng et al., 1997). Two FGFs, *fgf8a* and *fgf1,* were more highly expressed in embryos that would have a closed neural tube than

those that would have an open neural tube in at least one of the time points we sequenced. *fgf8a* is expressed in mesoderm/mesendoderm from bud to 9 somite stages, the forebrain neural rod around 5-9 somites, and later in the neural tube and *fgf17* is expressed in the presumptive dorsal mesoderm at sphere stage and in the presumptive telencephalon from 1-13 somite stages in zebrafish (Reifers et al., 1998; Shimizu et al., 2006; Thisse and Thisse, 2004; Warga et al., 2013) These expression patterns suggest *fgf8a* and *fgf17* are temporally expressed when anterior neurulation is occuring in tissues important for proper neurulation.

We found treating embryos with a high level of SU5402 results in an open neural tube phenotype approximately 70% of embryos, indicating FGF signaling is required for neurulation (Mohammadi et al., 1997; Shimada et al., 2008). SU5402 was originally found as a specific inhibitor of FGFR1, but acts on a well conserved region that is present in FGFR1-4 so it probably acts on all 4 receptors in zebrafish (Johnson and Williams, 1993; Mohammadi et al., 1997). Other publications using SU5402 also claim SU5402 inhibits nearly all FGFRs (Bouzaffour et al., 2009; Shimada et al., 2008; Shinya et al., 2001). Since such a high concentration of SU5402 was used to cause the open neural tube phenotype, we know FGFs must be highly inhibited for disruption of neurulation.

The expression patterns of the FGF receptors fit with FGF signaling acting the second step of our model: mesoderm/mesendoderm signaling the overlying neurectoderm. Both FGF8a and FGF17 bind to FGFR1c, FGFR2c, FGFR3c, and FGFR4 in chicks (Olsen et al., 2006). In zebrafish, FGFR3c also binds members

of the FGF8 subfamily (which includes FGF17) and FGF8 has been shown to bind to FGFR1 and FGFR4 (Ota et al., 2009; Ries et al., 2009). *fgfr3* is expressed in the axial mesoderm and neural plate at 6 and 10 hpf, in the anterior hindbrain at 11 hpf, and in the hindbrain neural rod and otic placode at 5-9 somites (Esterberg and Fritz, 2009; Sleptsova-Friedrich et al., 2001). *fgfr4* expression is first detected prior to gastrulation in the prechordal plate mesoderm and while later it is expressed in the forebrain, anterior hindbrain, and caudal hindbrain as well as in the dorsal-most portion of the rostral spinal cord (Thisse et al., 1995). *fgfr1* is expressed in the whole zebrafish embryo until 5-13 somites stages where expression is restricted to the forebrain, hindbrain and midbrain hindbrain boundary of the neural rod, the segmental plate, and somites (Rohner et al., 2009).

One possible reason the inhibitor is only effective at high doses is that multiple FGFs could have overlapping functions in neurulation. FGFs have been shown to function together in other parts of development (Fletcher et al., 2006; Klingseisen et al., 2009). For example, FGF17b and FGF18 have been shown to mimic FGF8a and promote midbrain development (Liu et al., 2003). If FGFs have overlapping functions in neurulation, only a small amount of each of the FGFs functioning in neurulation would need to be present to result in a closed neural tube.

Another possibility is only small amounts of FGFs are necessary to form a functional neural tube. Since FGFs are typically acting in a morphogen gradient

in vertebrates, it is possible that cells involved in neurulation require only a small amount of FGF signaling to function properly (Bökel and Brand, 2013; Wolpert, 1969). This is supported by work published in Ota et al. 2009. They found the forebrain was still formed in zebrafish even when the highest dose of dominant-negative FGFR3c was injected and more posterior structures were severely affected (Ota et al., 2009).

Another reason only high doses of inhibitor were effective could be that FGFs and Nodals could be working together to properly form a neural tube. In this instance, only a small amount of FGFs could be necessary with Nodal to induce the mesoderm/mesendoderm or after induction. If this is the case, both Nodals and FGFs would have to be knocked down to consistently cause the open neural tube phenotype. Like Nodals, FGFs have been shown to have important roles in mesoderm formation (Ciruna and Rossant, 2001; Kimelman, 2006). This suggests that FGF signals could be working with Nodals to induce the mesendoderm/mesoderm in the first step of our model of neurulation or after Nodals to signal the neurectoderm as the expression patterns of the FGFs from our screen suggest.

Potential roles for dkk1b/Wnt signaling in anterior neurulation

Our study also suggests *dkk1b*, an inhibitor of the canonical Wnt signaling pathway, is involved in neurulation. In our RNA-sequencing data, *dkk1b* had a differential expression ratio of 4.704 at shield and 3.167 at tailbud stage,

indicated dkk1b is more highly expressed in embryos that would have a closed neural tube than those that would have an open neural tube. *dkk1b* is expressed in the presumptive mesendoderm in zebrafish. In *Xenopus laevis*, signals from the endomesoderm to the overlying neuroepithelium (De Robertis et al., 2000; Monaghan et al., 1999; Shinya et al., 2000). If this is also the case in zebrafish, *dkk1b* would fit in our model for neurulation as the mesendodermal/mesodermal signal to the neurectoderm, the second step in our model, which promotes adhesion between neural tube cells in step three of our model.

Canonical Wnt signaling has not previously been implicated in neurulation. In our study, severe knockdown of *dkk1b* results in an open neural tube phenotype, but we do not know how or where *dkk1b* is acting in neurulation. One possibility is that *dkk1b* is acting to regulate the Wnt pathway by inhibiting multiple Wnt signals in order to promote proper neurulation. Seiliez, Thisse, and Thisse 2006 show abnormal anterior head morphology when *dkk1b* is knocked down or *wnt8a* is upregulated. Injection of *dkk1b* more often rescued the headless, truncated anterior head, or cyclopic phenotype caused by *foxa3* and *gsc* morpholino injection than injection of *wnt8a* morpholino injection. Therefore, *dkk1b* could be affecting multiple Wnt signals involved in this process. *dkk1b* could be playing a similar role in neurulation by knocking down wnt8a along with other Wnt signals. Our data supports this role for *dkk1b* as *wnt8a*'s expression ratio was 0.54 at shield stage.

It is also possible that *dkk1b* and FGF signaling are working together in our model. Previous studies in zebrafish suggest FGF and Wnt signaling pathways regulate each other and do not have a simple relationship (Stulberg et al., 2012). One study shows *dkk1b* expression depends on FGF signaling in zebrafish primordium (Aman and Piotrowski, 2008). If FGFs are working in the first step of our model, *dkk1b* expression and possible function in step two of our model, could also depend on FGF in neurulation

Conclusion: Our study identified over 3,000 candidates for potential involvement in neurulation downstream of Nodal. Within these candidates were transcripts from pathways that could be involved in inducing the mesendoderm/mesoderm, signaling from the mesendoderm/mesoderm to the overlying neurectoderm promoting adhesion, or adhesion between neural tube cells. Both FGFRs/FGF signaling and *dkk1b*/canonical Wnt signaling were on our candidate list and were shown to be involved in anterior neurulation for the first time.

Table 1: RNA-sequencing of Nodal inhibited embryos provided candidates for involvement in neurulation

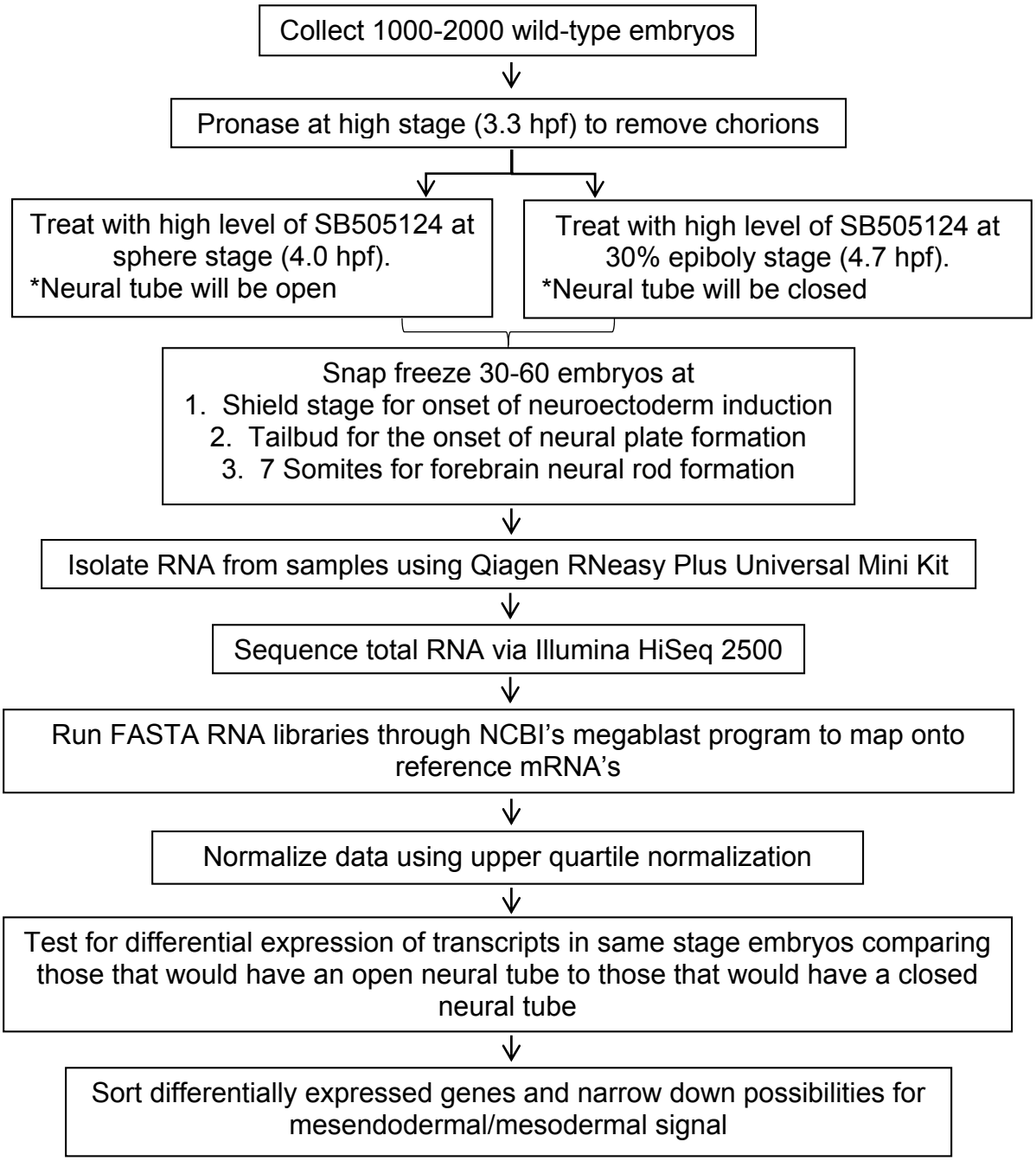

Table 2: Many transcripts were significantly differentially expressed in our RNA-sequencing data

		Shield (6.0 hpf)	Tailbud (10.0 hpf)	7 somites (12.0 hpf)	All 3 stages
Number of Transcripts	**Total significantly differentially expressed**	2,553	423	634	3,186
	Higher expression in embryos that would have a closed vs. open neural tube	1,427	288	290	1,792

*Genes with significant differential expression had to have at least 100 average counts in at least one treatment group, had to differ in expression by at least 50%, and have a false discovery rate of <0.05.

Table 3: Genes known to be affected by Nodal were differentially expressed in our RNA-sequencing data

	Ratio of Expression Closed:Open Neural Tube			
Gene	Shield (6.0 hpf)	Tailbud (10.0 hpf)	7 Somites (12 hpf)	Reference
sox17	8.63	-	-	(Alexander and Stainier, 1999; David and Rosa, 2001)
mixl1	3.23	-	-	(Alexander and Stainier, 1999; Kikuchi et al., 2000)
gsc	6.12	2.04	-	(Agius et al., 2000)
nog1	5.09	6.12	1.58	(Ragland and Raible, 2004; Szeto and Kimelman, 2006)
fsta	-	36.57	2.94	(Ragland and Raible, 2004; Szeto and Kimelman, 2006)
pitx2	-	-	2.27	(Liang et al., 2000)

Table 4: Genes known to cause NTDs in other vertebrates when missexpressed were differentially expressed in our RNA-sequencing data.

	Expression Ratio Closed:Open Neural Tube			
	In Animals with NTDs			
Zebrafish Gene Symbol	**Zebrafish** Found in Our RNA-Seq Analysis	**Mouse**	**Humans**	**Citation**
plld	>1	>1	-	(Luo et al., 2005)
vcla	>1	>1	-	(Xu et al., 1998)
shroom3	<1	>1	>1	(Hildebrand and Soriano, 1999; Lemay et al., 2015)
brd2a	>1	>1	-	(Shang et al., 2009)
nf1b	>1	>1	-	(Lakkis et al., 1999)
casp9	>1	>1	-	(Hakem et al., 1998; Kuida et al., 1998)
cited2	>1	>1	-	(Bamforth et al., 2001; Yin et al., 2002)
crebbpa	<1	>1	-	(Tanaka et al., 2000)
gli2a	<1	>1	-	(Pan et al., 2009)
prkacab	>1	>1	-	(Huang et al., 2002)
ptch1	<1	>1	-	(Goodrich et al., 1997; Milenkovic et al., 1999)
cyp26a1	<1	>1	-	(Niederreither et al., 2002)
grhl3	>1	-	>1	(Lemay et al., 2015)
ptprsa	>1	-	>1	(Lemay et al., 2015)

Table 5: Relative, RT-PCR confirmed the direction of higher expression from our RNA-sequencing data

	Shield Stage Ratio Closed:Open		Bud Stage Ratio Closed:Open		7 Somites Stage Ratio Closed:Open	
Gene Name	**RNA-seq**	**Relative-PCR**	**RNA-seq**	**Relative-PCR**	**RNA-seq**	**Relative-PCR**
t-box 1 (tbx1)	10.12	4.21	114	2.66	20	1.41
protocadherin 10b (pcdh10b)	1.69	1.52	2.49	0.745	-	-
fibroblast growth factor 8a (fgf8a)	0.30	4.89	1.80	1.88	-	-
dickkopf 1b (dkk1b)	4.70	0.73	3.17	1.64	-	-
cadherin 11 (cdh11)	-	-	7.63	10.42	2.68	1.27
protocadherin 8 (pcdh8)	2.35	36.79	9.20	11.46	-	
sizzled (szl)	0.32	0.36	0.44	0.47	0.35	.731
Average Amplification		1.47+ or - 0.25		1.49 + or - 0.26		1.48 + or - 0.21

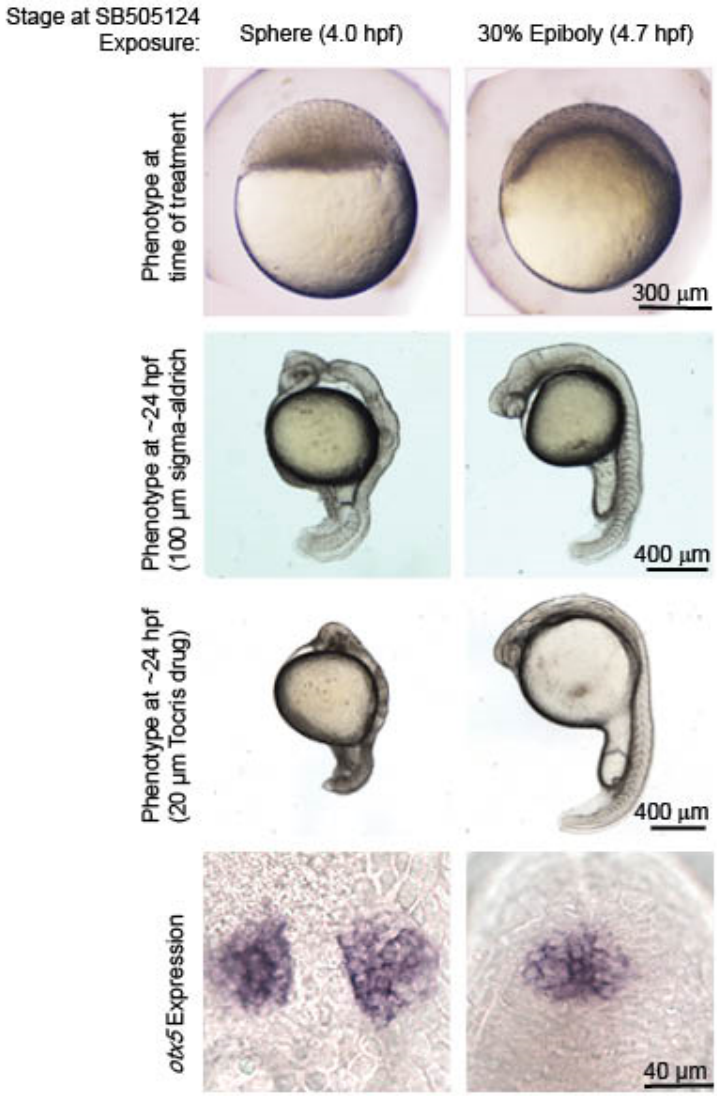

Figure 1: EIT and LIT cause open and closed neural tube phenotypes, respectively.
Treatment with SB505124 at sphere stage (4.0 hpf) always results in an open neural tube phenotype. Treatment with SB505124 at 30% epiboly stage always results in a closed neural tube phenotype. Due to variability in the effectiveness of SB505124 from Sigma-Aldrich, SB505124 from Tocris was used for the relative, RT-PCR portion of this study. 100 µM treatment with inhibitor from Sigma-Aldrich caused the same pineal phenotypes at 24 hpf as 20 µM treatment with inhibitor from Tocris. Also, overall phenotypes at 24 hpf were similar with somites only forming in the tail region in sphere treated embryos and forming in the trunk and tail region in 30% epiboly treated embryos. Top row: Lateral views, animal pole to top. 2nd and 3rd rows: Lateral views, anterior towards top. Bottom row: Dorsal view, anterior towards top.

A

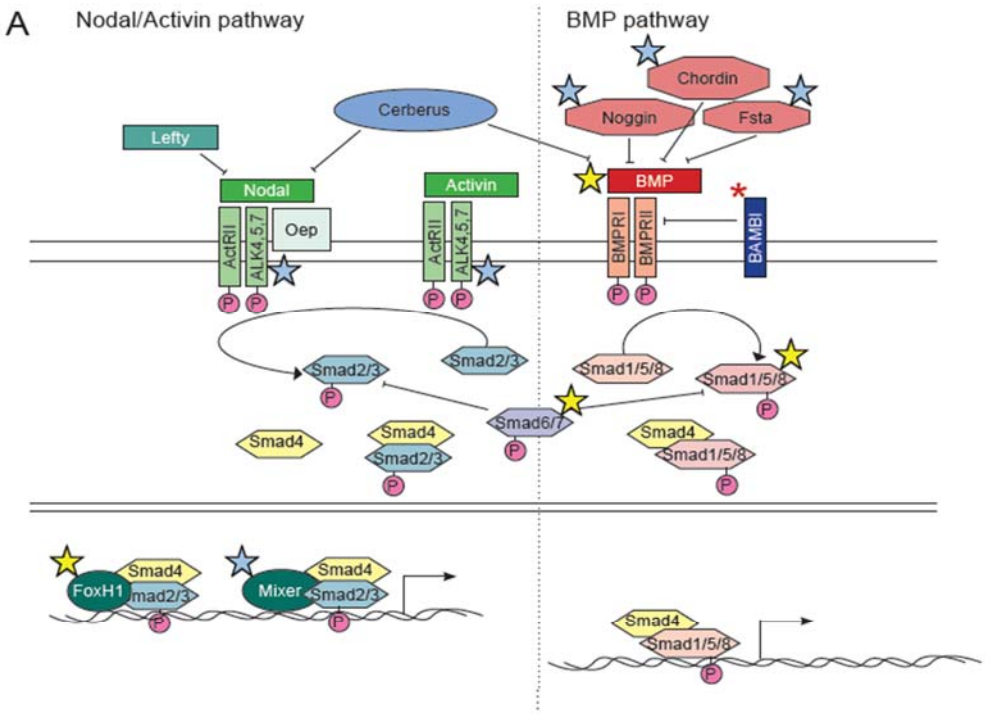

B

	Differential Expression Ratio LIT (closed NT) / EIT (open NT)		
Gene Name	**Shield Stage**	**Tailbud Stage**	**7 Somite Stage**
activin receptor type 1 like (acvr1l)	1.872	-	-
forkhead box H1 (foxh1)	-	0.644	-
mix paired like homeobox (mixl1)	3.227	-	-
bmp and activin membrane bound inhibitor (bambia)	-	0.644	-
bone morphogenetic protein 7a (bmp7a)	-	0.602	0.626
bone morphogenetic protein 2b (bmp2b)	-	0.653	-
chordin (chd)	1.874	-	-
follistatin a (fsta)	-	36.571	2.942
inhibitor of DNA binding 4 (id4)	0.456	-	-
noggin 1 (nog1)	5.089	6.115	1.576
mad homolog 1 (smad1)	0.469	-	-
smad family member 6a (smad6a)	0.626	-	-

Figure 2: Differential expression of transcripts encoding components of the BMP and Nodal signaling pathways.
A) Nodal/Activin and BMP signaling pathways for *Danio rerio* based on KEGG (Ogata et al., 1999). Genes indicated with a star are genes that were significantly differentially expressed in our data. A blue star indicates genes with higher expression in LIT embryos than EIT embryos while a yellow star indicates genes with lower expression in LIT embryos than EIT embryos. B) Table of differentially expressed genes represented in the pathway and corresponding expression ratios from our RNA-sequencing data analysis.

A

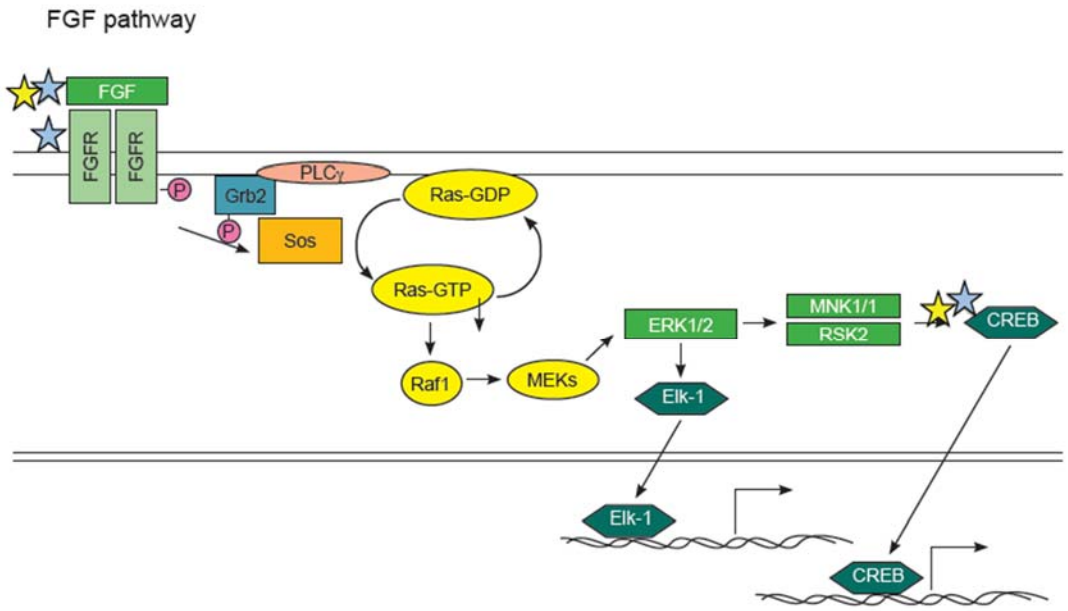

B

	Differential Expression Ratio LIT (closed NT) / EIT (open NT)		
Gene Name	**Shield Stage**	**Tailbud Stage**	**7 Somite Stage**
cAMP responsive element binding protein 3-like 3 like (creb3l3l)	0.401	-	0.623
cAMP responsive element binding protein 3-like 1 (creb3l1)	-	1.91	-
fibroblast growth factor 8a (fgf8a)	0.297	1.801	-
fibroblast growth factor 17 (fgf17)	2.405	-	-
fibroblast growth factor 24 (fgf24)	0.488	-	-
fibroblast growth factor receptor-like 1b (fgfrl1b)	-	-	5.537
fibroblast growth factor receptor-like 1a (fgfrl1a)	-	-	1.629

Figure 3: Differential expression of transcripts encoding portions of the FGF signaling pathway.
A) FGF signaling pathway for *Danio rerio* based on KEGG (Ogata et al., 1999). Genes indicated with a star are genes that were significantly differentially expressed in our data. A blue star indicates genes with higher expression in LIT embryos than EIT embryos while a yellow star indicates genes with lower expression in LIT embryos than EIT embryos. B) Table of differentially expressed genes represented in the pathway and corresponding expression ratios from our RNA-sequencing data analysis.

A

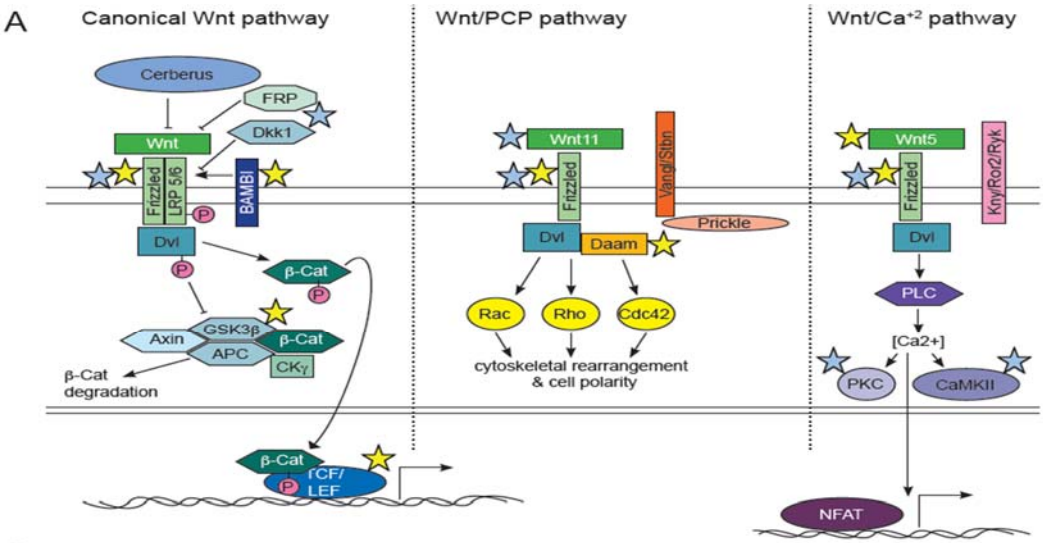

B

Gene Name	Differential Expression Ratio LIT (closed NT) / EIT (open NT)		
	Shield Stage	Tailbud Stage	7 Somite Stage
bmp and activin membrane-bound inhibitor homolog a (bambia)	-	0.644	-
calcium/calmodulin-dependent protein kinase (CaM kinase) II gamma 1(camk2g1)	1.527	-	-
calcium/calmodulin-dependent protein kinase II beta 1 (camk2b1)	1.955	-	-
dishevelled associated activator of morphogenesis 1b (daam1b)	0.462	-	-
dickkopf WNT signaling pathway inhibitor 1b (dkk1b)	4.704	3.167	-
frizzled class receptor 8b (fzd8b)	3.842	4.083	2.339
frizzled class receptor 10 (fzd10)	1.551	1.874	-
frizzled class receptor 7a (fzd7a)	0.540	-	-
frizzled class receptor 3a (fzd3a)	0.534	-	-
glycogen synthase kinase 3 beta *(gsk3b)*	0.506	-	-
lymphoid enhancer-binding factor 1 (lef1)	0.655	-	-
protein kinase, cAMP-dependent, catalytic, alpha, genome duplicate a (prkacaa)	1.583	-	-
protein kinase, cAMP-dependent, catalytic, alpha, genome duplicate b (prkacab)	-	1.638	-
protein kinase, cAMP-dependent, catalytic, beta b (prkcbb)	2.051	-	-
transcription factor 7-like 2 (tcf7l2)	0.421	-	-
transcription factor 7-like 1a (tcf7l1a)	0.658	0.572	-
wingless-type MMTV integration site family, member 11, related (wnt11r)	-	-	1.771
wingless-type MMTV integration site family, member 5b (wnt5b)	0.666	-	-

Figure 4: Differential expression of transcripts encoding portions of the Wnt signaling pathway.
A) Wnt signaling pathway for *Danio rerio* based on KEGG (Ogata et al., 1999). Genes indicated with a star are genes that were significantly differentially expressed in our data. A blue star indicates genes with higher expression in LIT embryos than EIT embryos while a yellow star indicates genes with lower expression in LIT embryos than EIT embryos. B) Table of differentially expressed genes represented in the pathway and corresponding expression ratios from our RNA-sequencing data analysis.

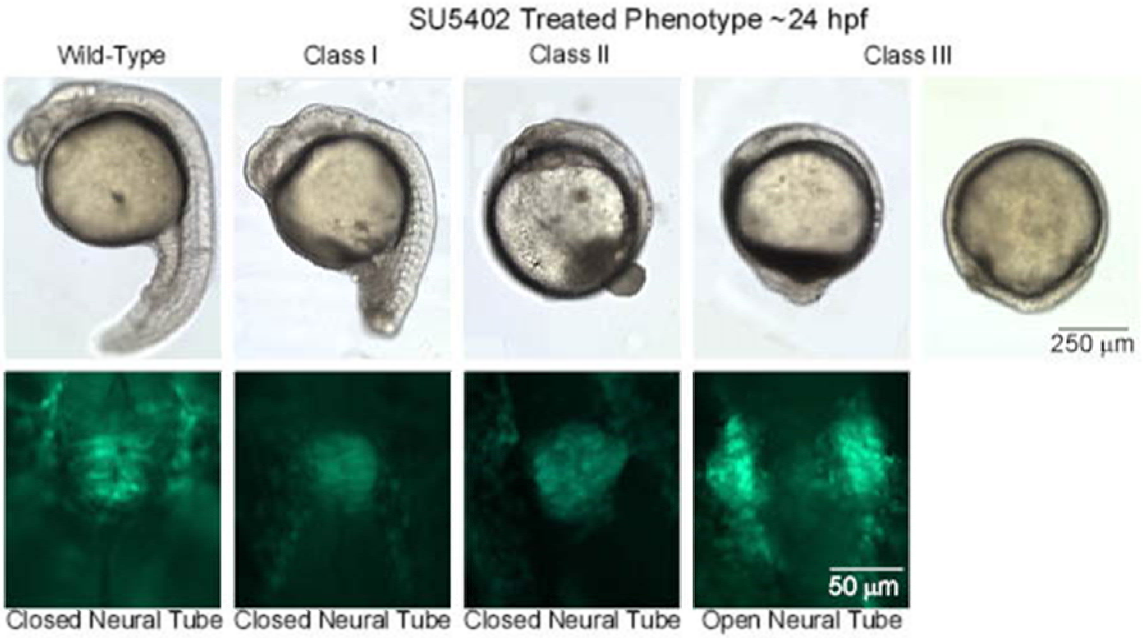

SU5402 Treatment Concentration	Class I	
	Closed Neural Tube	Open Neural Tube
33.7 µM	333	0
67.4 µM	0	0

SU5402 Treatment Concentration	Class II and Class III	
	Closed Neural Tube	Open Neural Tube
33.7 µM	385	16
67.4 µM	60	142

Figure 5: Inhibition of FGF signaling causes an open neural tube phenotype

Wildtype embryos and embryos from all three phenotypic classes were present in 33.7 µM treatments while only class II and class III embryos were present in 67.4 µM treatments. Embryos from class II and class III were difficult to distinguish from each other after in-situ hybridization and results from these two classes are combined. Overall there were 266 control embryos treated with corresponding concentrations of DMSO. All of these control embryos were wildtype and had closed neural tubes. 22 wildtype embryos were also present overall in the 33.7 µM treatments, all which had a closed neural tube. Some class III embryos in the higher treatment groups remained in gastrulation stages at 24 hpf and therefore did not have pineal phenotypes. Top row: Lateral views, anterior to left. Bottom row: Dorsal view, anterior to the top.

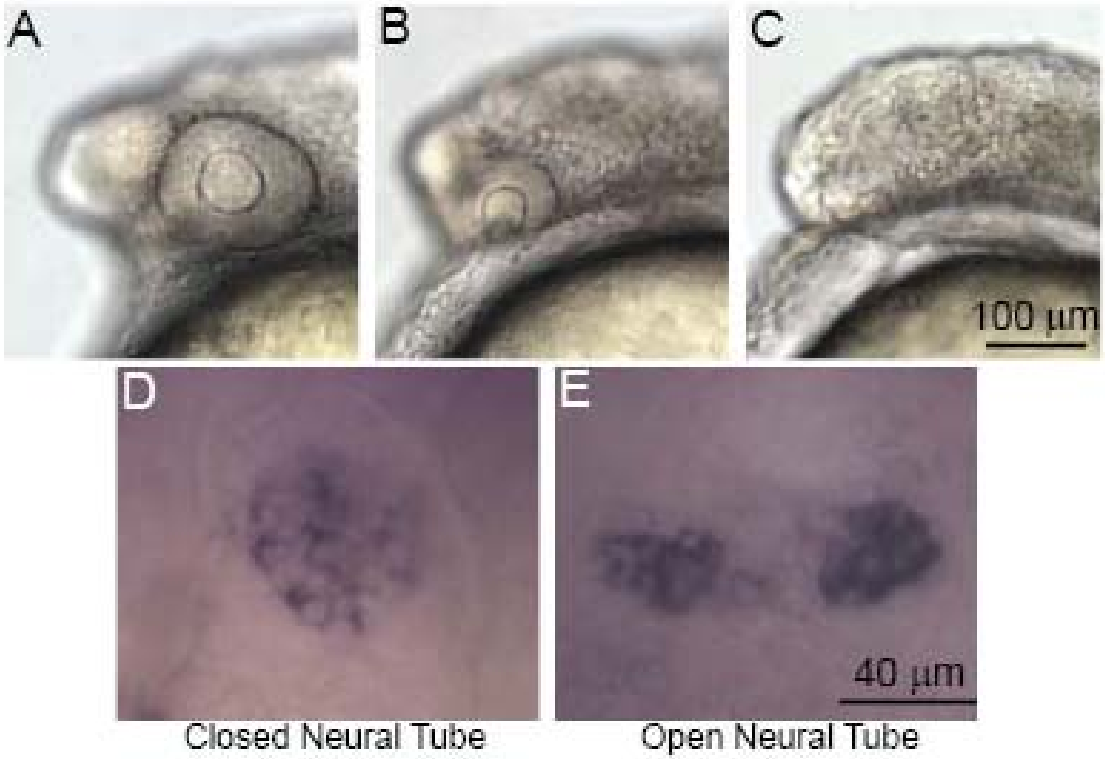

Figure 6: Knock-down of DKK1b by morpholino injection causes an open neural tube phenotype
Embryos were injected with a DKK1b morpholino at the 1- to 2-cell stage. The severity of the phenotype was scored by eye phenotype at 24 hpf. Three eye phenotypes resulted: A) Normal eye size (n= 14/73 embryos), B) Small eye phenotype (52/73 embryos) and C) No eyes (7/73 embryos). D) All embryos with normal eye size (n=14/14) and a subset of embryos with a small eye phenotype (32/52) had a round pineal anlage, indicating a closed neural tube. E) The remaining embryos with 20/52 small eyes (20/52) and all embryos lacking eyes (7/7) had divided pineal anlage and an open neural tube. 22 sibling embryos were injected with a standard control morpholino and all had closed neural tube phenotypes (22/22). Top row: Lateral views, anterior to left. Bottom row: Dorsal view, anterior to the top.

A

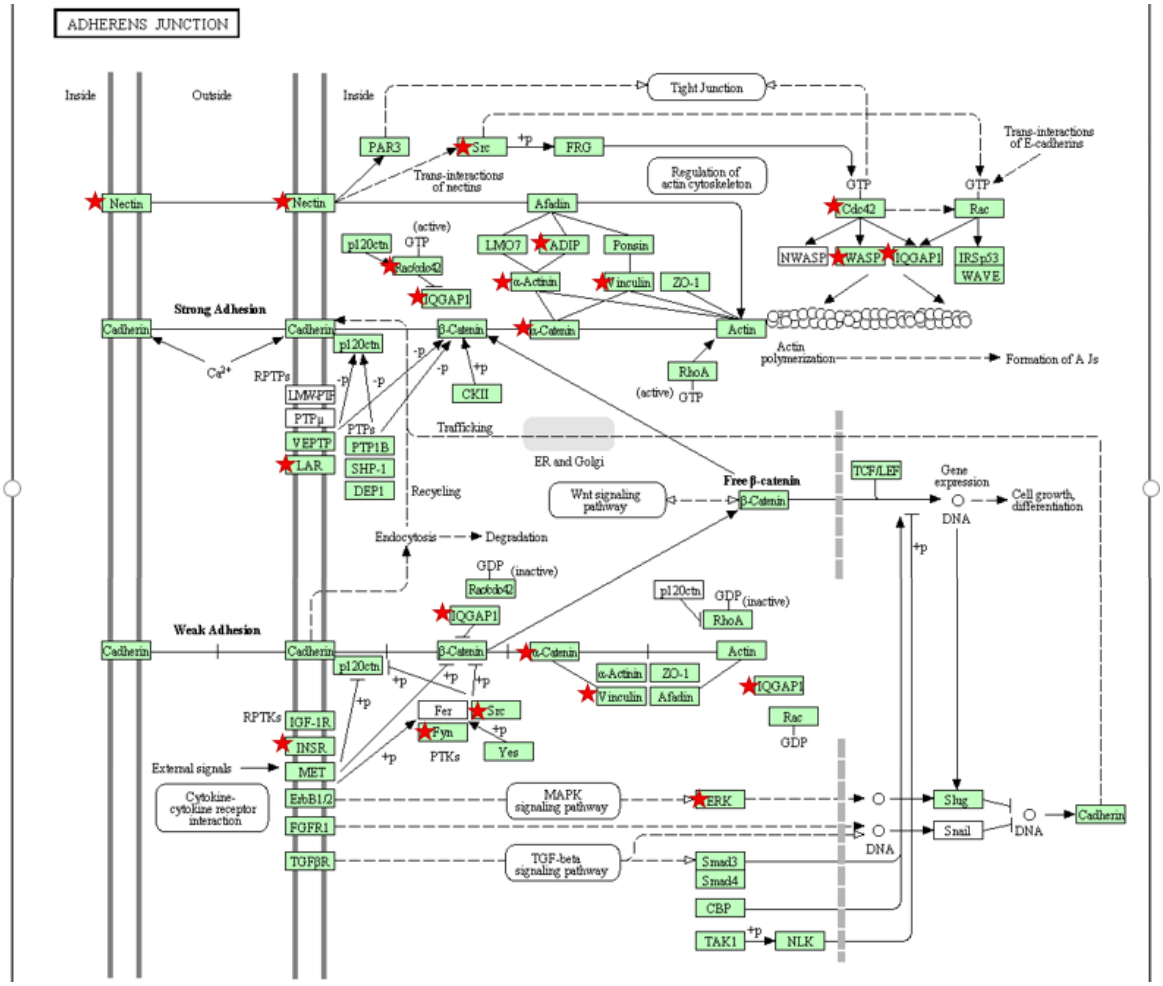

B

	Differential Expression Ratio From Embryos that Would Have a Closed Neural Tube to Those that Would have an Open Neural Tube (if significant)		
Gene Name	**Shield Stage**	**Tailbud Stage**	**7 Somites Stage**
pvrl3b	1.535	-	-
pvrl1b	.495	-	-
LOC560816	-	1.532	-
ptprfb	.524	-	-
insrb	-	-	.562
cdc42	1.508	-	-
Iqgap1	1.758	-	.633
fyna	3.163	-	-
src	1.767	-	-

ssx2ip	2.09	-	-
actn3b	.432	-	-
actn1	-	-	.602
ctnna2	2.802	-	-
LOC100002756	-	-	2.581
vcla	3.036	-	-
mapk1	1.584	-	-
crebbpa	.658	-	-
cdc42	1.508	-	-
wasla	.589	-	-
baiap2a	2.576	-	-
tcf7l2	.421	-	-
tcf7l1a	.658	.527	-
lef1	.655	-	-
snai2	1.698	-	-

Supplemental figure 1: Differential expression of transcripts encoding portions of the Adherens Junction pathway.
A) Adherens junction pathway for *Danio rerio* from KEGG (Ogata et al., 1999). Genes indicated with a star are genes that were significantly differentially expressed in our data. We recognize the limitations of KEGG and that there may be errors in the pathways generated. B) Table of differentially expressed genes represented in the pathway and corresponding expression ratios from our RNA-sequencing data analysis.

A

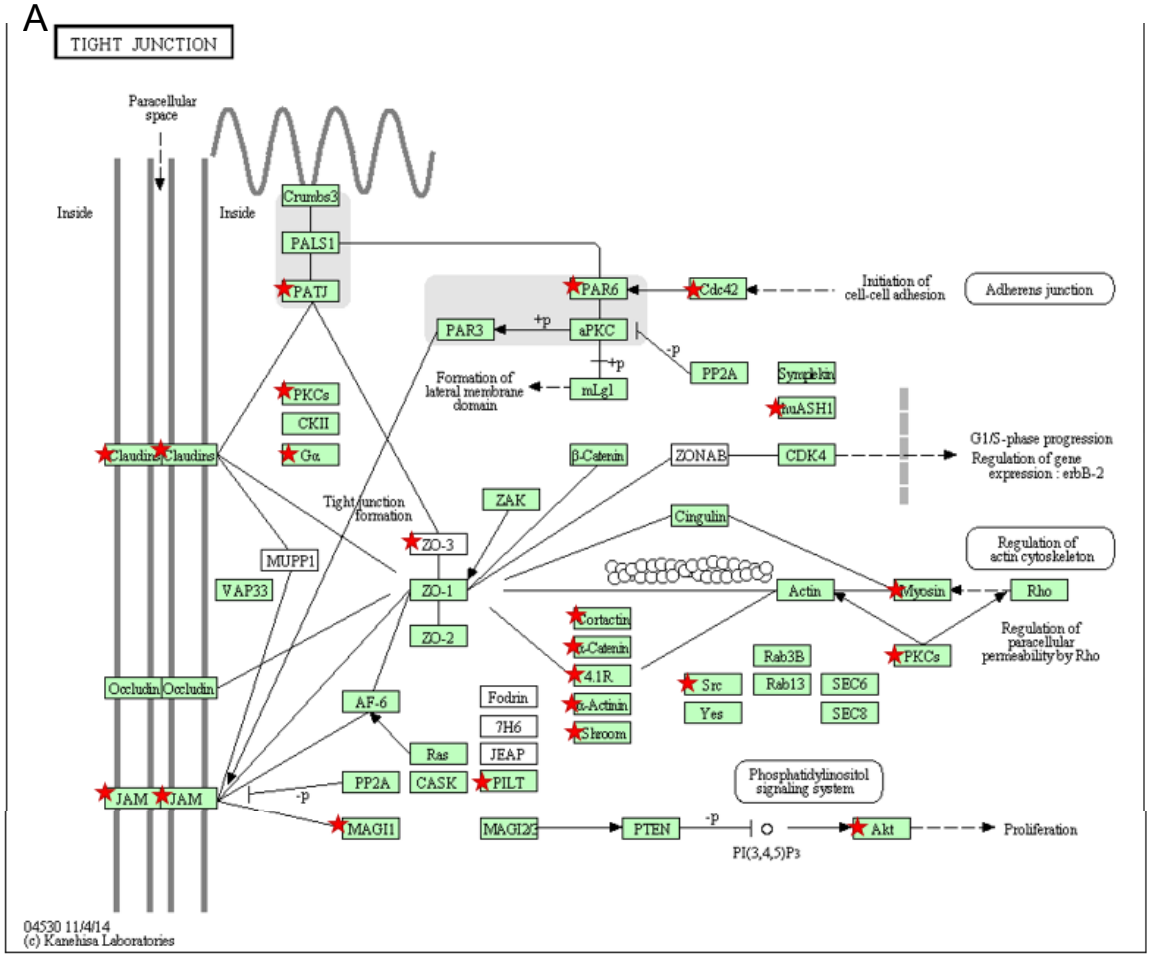

B

	Differential Expression Ratio From Embryos that Would Have a Closed Neural Tube to Those that Would have an Open Neural Tube (if significant)		
Gene Name	**Shield Stage**	**Tailbud Stage**	**7 Somites Stage**
cldnd	2.891	-	-
Cldng	2.629	-	-
Cldn7b	1.546	-	-
Cldn5a	.444	-	-
Jam3b	.631	-	-
Jam2a	1.605	-	-
Inadl	-	-	.633
prkcbb	2.051	-	-
Prkcea	.572	-	-
Prkcda	3.312	-	-
Gnai2b	1.684	-	-

Magi3	1.617	-	-
Tjp3	1.521	-	-
LOC566060	1.674	-	-
Magi3	1.617	-	-
Pard6b	.628	-	-
Hcls1	1.782	-	-
Ctnna2	2.802	-	-
Epb41l3b	-	-	.62
Epb41l3a	.639	-	-
Actn1	-	-	.602
Actn3b	.432	-	-
Shroom4	2.028	-	-
Shroom3	.584	-	-
Cdc42	1.508	-	-
Src	1.767	-	-
Ash1l	.655	-	-
Akt3	1.84	-	-
Akt2l	1.766	-	-
Myh9a	-	-	.62
Smyhc1	-	-	7.425
Myhz2	.37	-	-
prkacaa	1.583	-	-
prkacab	-	1.638	-
prkcbb	2.051	-	-

Supplemental figure 2: Differential expression of transcripts encoding portions of the Tight Junction pathway.
A) Tight junction pathway for *Danio rerio* from KEGG (Ogata et al., 1999). Genes indicated with a star are genes that were significantly differentially expressed in our data. We recognize the limitations of KEGG and that there may be errors in the pathways generated. B) Table of differentially expressed genes represented in the pathway and corresponding expression ratios from our RNA-sequencing data analysis.

Chapter III: Temporal and spatial requirements for Nodal-induced anterior mesendoderm and mesoderm in anterior neurulation.

Ngawang Gonsar, Alicia Coughlin, Jessica A. Clay-Wright, Bethanie R. Borg, Lexy M. Kindt, Jennifer O. Liang

Zebrafish with defective Nodal signaling have a phenotype analogous to the fatal birth defect anencephaly, which is caused by an open anterior neural tube. Previous work in our laboratory found that open neural tube defects in Nodal signaling mutants were corrected by rescue of mesendodermal/mesodermal tissue and that defects in these mutants start at neural plate stage, before the neuroepithelium starts to fold into a tube. In this study, we found that the requirement for Nodal signaling maps to mid-late blastula stages. This timing is consistent with prechordal plate mesendoderm and anterior mesoderm acting to promote neurulation. To further identify the tissues involved in promoting neurulation, we used *sqt* and *lefty1*-overexpressing embryos, which have variable phenotypes. Statistical analysis indicated a strong, positive correlation for a closed neural tube and the presence of several tissues derived from mesendoderm and mesoderm (hatching glands, cephalic paraxial mesoderm, notochord, and head muscles). However, none of these tissues were necessary or sufficient for neurulation, suggesting no single mesendodermal/mesodermal tissue was required. Instead, we propose a model in which a critical amount of mesendoderm/mesodermal precursors are required during gastrulation to promote formation of the neural plate and its subsequent closure into a neural tube.

Introduction

NTD are among the most common human birth defects, occurring in approximately 1 in every 1000 pregnancies (Copp et al., 2013). NTD are caused by failure in closure of the neural tube, a structure that runs along the entire anterior-posterior axis of the developing embryo. One of the most severe NTD is anencephaly in which the anterior neural tube fails to close, causing complete or partial absence of the developing cranial vault and cerebral hemisphere (Detrait et al., 2005).

NTD are a result of failures in primary neurulation, which forms the entire brain and the majority of the trunk spinal cord. The morphological events of primary neurulation are well conserved across many vertebrate species. Primary neurulation initiates with the columnarization of ectodermal epithelial cells forming the neural plate (Colas and Schoenwolf, 2001; Lowery and Sive, 2004). This is followed by the thickening and elevation of the neural plate borders to form the neural folds, which fuse at the dorsal midline forming the neural tube (Colas and Schoenwolf, 2001; Lowery and Sive, 2004). In zebrafish, there is a slight variation in this process (Colas and Schoenwolf, 2001; Kimmel et al., 1995a; Lowery and Sive, 2004; Schmitz and Campos-Ortega, 1994). The neural tube first forms a neural rod, in which cells of the right and left sides of the neural tube are in contact. A lumen later forms in the center of the rod to transform it into a tube.

Many human NTD are thought to have a genetic component, although these are not fully understood (Au et al., 2010; Harris and Juriloff, 2010; Juriloff and

Harris, 2000). Work in genetic model organisms has the potential to identify candidate genes as well as increase understanding of the complex process of neurulation. Zebrafish mutants that have defective Nodal signaling exhibit NTD analogous to the human birth defect anencephaly (Aquilina-Beck et al., 2007; Lu et al., 2013). Zebrafish have three Nodal ligands, Cyclops (Cyc), Squint (Sqt) and Southpaw (Schier, 2003). These ligands all signal through a receptor complex containing the One Eyed Pinhead (Oep) protein (Schier, 2003). *oep*, *sqt* and *cyc*;*sqt* double mutants all exhibit open anterior neural tubes, as do embryos overexpressing the Nodal signaling inhibitor Lefty1 (Aquilina-Beck et al., 2007; Lu et al., 2013). In contrast, the posterior region of the neural tube is closed (Ciruna et al., 2006). One of the primary defects in these embryos appears to be lack of cell adhesion during the earliest steps of neurulation. The cells of the developing neural tube are disorganized from the neural plate stage onwards (Aquilina-Beck et al., 2007). This disorganization is likely in part caused by decreased expression of the cell adhesion protein N-cadherin, which is required for closure of the zebrafish neural tube (Aquilina-Beck et al., 2007; Lele et al., 2002)

Our previous research suggested the role for Nodal signaling is not directly in the neuroepithelium, but rather in the induction of the mesendoderm and mesoderm (Aquilina-Beck et al., 2007). Embryos that completely lack Nodal signaling have no anterior mesendoderm or mesoderm and always have an open neural tube (Aquilina-Beck et al., 2007). In these embryos, activation of the Nodal signaling pathway cell autonomously rescued the formation of

mesendoderm/mesodermal tissue and corrected the neural tube defect (Aquilina-Beck et al., 2007). This suggested that the Nodal signaling pathway need not be activated in the neural tube cells, but instead has an indirect role within the mesendoderm/mesoderm. Consistent with this model, a recent study added a Nodal signaling inhibitor at 70% epiboly, after the induction of mesendoderm/mesoderm is complete, and found that there was no effect on anterior neurulation (Araya et al., 2014).

Similar to the role of the anterior mesendoderm and mesoderm in zebrafish, the head mesenchyme in mice, which is composed of mesodermal and neural crest cells, plays an essential role in neurulation (Chen and Behringer, 1995). In rodents, the elevation of the cranial neural folds is preceded by the expansion of the underlying head mesenchyme (Morriss and Solursh, 1978; Solursh and Morriss, 1977; Tuckett and Morriss-Kay, 1986). Additionally, loss of function of various genes expressed in the head mesenchyme results in lethal NTD, including anencephaly (Chen and Behringer, 1995). For example, the *twist* and *cart1* genes are both expressed in the mesenchyme. Knockout of either of these genes affects the expansion of the cranial mesenchyme and results in NTD (Chen and Behringer, 1995; Zhao et al., 1996). This has led to the hypothesis that expansion of head mesenchyme helps drive the convergence of the left and right folds resulting in the fusion of the dorsal midline and closure of the neural tube. However, more characterization is needed to determine whether the anterior

mesendoderm/mesoderm in zebrafish and head mesenchyme in mice have overlapping functions.

Our goal was to identify the temporal requirement for Nodal signaling in neurulation and define the areas of the mesendoderm/mesoderm that have a role in neural tube closure. Consistent with the fact that the morphology of the neuroepithelium is already abnormal by neural plate stages (Aquilina-Beck et al., 2007), we found that the requirement for Nodal signaling in anterior neurulation occurs up to late blastula stages (dome stage, 4.3 hpf). This temporal requirement falls within the time when Nodal is inducing mesendoderm and mesoderm, and is before the onset of neuroepithelium formation. We found a strong statistical correlation between the presence of derivatives of prechordal plate mesendoderm and head mesoderm derivatives and a closed neural tube. However, none of the tissues assayed (hatching gland, anterior notochord, cephalic paraxial mesoderm, and head muscles) were always present when the neural tube was closed. Together, these data suggest a model whereby Nodal signaling induces prechordal plate mesendodermal and anterior mesodermal tissues during blastula stages (Aquilina-Beck et al., 2007). During gastrulation, a wide range of these tissues then communicates with the overlying neuroectoderm, which becomes competent to undergo closure.

Results

Temporal overlap in Nodal signaling's role in neural tube closure and mesendoderm/mesoderm induction

Our previous work suggested that Nodal signaling's role in neurulation is through the induction of mesendoderm/mesoderm or a signal produced by these tissues (Aquilina-Beck et al., 2007). If this hypothesis is correct, then Nodal's temporal requirement in neurulation should occur at the same time as Nodal induction of mesendoderm/mesoderm, which occurs between 3 hpf (1000 cell stage, early blastula) and 6 hpf (shield stage, early gastrulation) (Hagos and Dougan, 2007). We found that Nodal signaling is required for neural tube closure during a subset of this time, suggesting a subset of Nodal-dependent mesendodermal/mesodermal tissues are involved in neurulation.

To determine the temporal requirement for Nodal signaling in neurulation, we used the Nodal inhibitor SB505124, a small molecule that blocks the activity of ALK 4, 5 and 7 Nodal specific receptors (DaCosta Byfield et al., 2004). In zebrafish, SB505124 causes phenotypes similar to those in mutants with reduced Nodal signaling as well as a decrease in the expression of Nodal-regulated genes (Hagos and Dougan, 2007; Hagos et al., 2007). Because of unexpected complexities with using the inhibitor, we used two experimental designs to determine the timing of the Nodal signaling requirements. Results from both designs suggest that the requirement for Nodal signaling occurs between 3 hpf (1000 cell stage, mid blastula) and 4.3 hpf (dome stage, late blastula).

In our first experiments, embryos were exposed to a 75 or 100 μM dose of SB505124 for 20 minutes, and then the embryos were moved to a new Petri dish containing 10-12 ml embryo media, resulting in an approximately 1:10 dilution of SB505124. The fish were raised until ~24 hpf and then assayed for pineal morphology, which is a sensitive indicator of anterior neural tube closure (Aquilina-Beck et al., 2007). An oval shaped pineal anlage indicated a closed anterior neural tube, while an elongated or divided pineal indicated an open neural tube (Fig. 1) (Aquilina-Beck et al., 2007). The majority of embryos treated with the inhibitor starting at 3.8 hpf (oblong stage, mid blastula) and 4.0 hpf (sphere stage, mid blastula) had an open neural tube phenotype (Fig. 1, Table 1). Treatment starting at 4.3 hpf (dome stage, late blastula), treated embryos resulted in embryos with both open and closed neural tubes. Initiating treatment at 4.7 hpf (30% epiboly, late blastula) consistently resulted in closed neural tubes (Fig. 1; Table 1). This suggests that 4.3 hpf is very close to the boundary between when Nodal signal is required and when it is not. The same inhibitor treatments that caused open neural tube phenotypes caused defects in mesendoderm and mesoderm formation, including complete absence of dorsal mesendoderm-derived prechordal plate, decreased numbers of dorsal mesoderm-derived notochord cells, and loss of intermediate mesoderm-derived pronephric mesoderm (Fig. 2).

As part of control experiments, we found SB505124 inhibitor activity was persisting after post-treatment washing. Increased washing decreased the severity of the phenotype, but some activity persisted even when the inhibitor

concentrations were reduced by a 1:2000 dilution (Supplemental Fig. 1). Because these difficulties made it difficult to identify when the inhibitor was acting, we repeated the time course using a different experimental design. In these experiments, inhibitor was again added at different time points in development, but it was left on until the time the embryos were fixed at 24 hpf. In these new experiments, the supplier of SB505124 was switched from Sigma to Tocris.

A concentration curve indicated that there was a strong dose dependent effect of the Tocris SB505124. Embryos were treated starting at 3.8 hpf (high oblong, mid blastula stage) through 24 hpf with concentrations ranging from 0.1 to 100 μM. The penetrance of the open neural tube phenotype increased with increasing inhibitor concentration, with complete penetrance at doses of 10 μM and higher (Fig. 3; Table 2). Similarly, the number of mesoderm-derived somites decreased with increasing inhibitor concentrations (Fig. 3) Embryos developed cyclopia starting at 5 μM (Fig. 3).

Embryos treated with 10 and 20 μM of Tocris SB505124 had similar phenotypes to MZ*oep* mutants, which lack all Nodal signaling (Fig. 3) (Gritsman et al., 1999). Phenotypes at higher doses of SB505124 were more severe than MZ*oep* mutants (Fig. 3). This suggests that at these high concentrations, we may have also been blocking activity of other Activin-like proteins, which signal through the same receptors as Nodal but do not require Oep (Sun et al., 2006).

We chose to use our highest concentration, 100 μM Tocris SB505124, in our subsequent experiments to ensure effective inhibition of Nodal signaling.

Despite the change in treatment time from 20 minutes to over 20 hours and the change in supplier of the inhibitor, the timing of effect on neural tube closure remained the same (Fig. 4, Table 3). There was also an almost exact match between open neural tubes defects in the expression of mesendodermal/mesodermal markers (Supplemental Fig. 2, Supplemental Table 1). For instance, all embryos treated with SB505124 starting at 3.8 hpf (high-oblong stage, mid blastula) or 4.0 hpf (sphere stage, mid blastula) had open neural tubes as expected and lacked all or almost all expression of mesendodermal/mesodermal markers (Supplemental Fig. 2, Supplemental Table 1). Treatment starting at 4.3 hpf (dome stage, late blastula) caused mixed neural tube and mesendodermal/mesodermal phenotypes while treatment at or after 4.7 hpf (30% epiboly, late blastula) resulted in closed neural tube phenotypes and substantial recovery of mesendodermal/mesodermal tissues.

Absence of head mesendodermal/mesodermal tissues correlates with open neural tube phenotype

With the goal of identifying specific regions of the head mesendoderm and anterior mesoderm required for neural tube closure, we used *sqt* mutants and *lefty1* overexpressing embryos in a correlative approach. These embryos have variable mesendoderm/mesoderm and neural tube phenotypes (Aquilina-Beck et al., 2007; Thisse et al., 2000). Four tissues were assayed, including the prechordal plate mesendoderm derived hatching glands, mesoderm derived anterior notochord,

cephalic paraxial mesoderm, and mesendoderm and mesoderm derived head muscles (Fig. 5). If the precursors to an anterior mesendodermal/mesodermal tissue was required for neurulation, then it would always be present when the neural tube was closed and always absent when the neural tube was open. We found there was a strong correlation between the presence of each head mesendodermal/mesodermal tissue and a closed neural tube phenotype, but no tissue was absolutely required.

The hatching glands are derived from the anterior most prechordal plate, which is the first mesendodermal tissue to involute during gastrulation (Thisse et al., 1994; Vogel and Gerster, 1997). The prechordal plate underlies the presumptive anterior neuroectoderm during gastrulation, when specification of the neuroectoderm is initiated (Schmidt et al., 2013). Hence, precursors to the hatching glands were strong candidates to be influencing neurulation. Embryos were categorized into four groups based on whether the hatching gland tissue was present or absent and whether the neural tube was open or closed (Fig. 6, Supplemental Fig. 3). To assess the correlation, we calculated the φ coefficient. φ=1 indicated an absolute positive correlation between a closed neural tube and hatching gland presence, and φ=-1 indicated an absolute negative correlation. Fisher's exact test was used to determine whether a correlation was statistically significant. This analysis indicated a positive correlation between neural tube closure and hatching gland presence that reached significance only in the Lefty1 overexpressing embryos (*sqt*: φ=0.2566, *sqt*: P=0.26; *lefty1* injected: φ=0.61; P=0.000086).

Notochord precursors are also in close proximity to the anterior neuroepithelium during early development, suggesting they could also influence closure of the anterior neural tube (Kimmel et al., 1990; Solnica-Krezel and Sepich, 2012). Consistent with this, there was a statistically significant positive correlation between presence of anterior notochord and a closed neural tube (*sqt* φ=0.39; P=5.4 X 10^{-4}; *lefty1* mRNA injected φ=0.49; P=4.6x10^{-9}) (Fig. 6; Supplemental Fig. 4).

The cephalic paraxial mesoderm (cpm) serves as the primary precursor to all cranial skeletal muscles and the pharyngeal arches. Mouse *twist* mutants with an altered cpm display open cranial neural tubes, suggesting a potential role for cpm in vertebrate neurulation (Chen and Behringer, 1995). As with the other tissues tested, cpm presence had a strong positive correlation with a closed neural tube (*sqt* φ=0.42, P=8.1 X 10^{-4}; *lefty1* mRNA injected φ=0.67, P=2.5 X 10-6)(Fig. 7; Supplemental Fig. 5).

Anterior mesendodermal/mesodermal-derived head muscles had the lowest correlation with neural tube closure of the tissues assayed (Fig. 8; Supplemental Table 2). Developing head muscles become apparent at approximately 50 hpf, during the hatching period, and give rise to the eye, jaw and gill arch muscles in the adult (Kimmel et al., 1990)(Kimmel et al., 1990). We found a strong relationship between head muscles in *lefty1* mRNA injected embryos (φ=0.40, P=0.024), but only a weak correlation in *sqt* (P=0.52; φ=0.10).

Despite the positive correlation of each mesendodermal/mesodermal tissue tested, none had an absolute correlation with successful anterior neurulation. For each tissue, there were a subset of Nodal deficient embryos that completely lacked the tissue and had a closed anterior neural tube, and others that had the tissue but an open anterior neural tube (Fig. 6-8, Supplemental Fig. 3-5, Supplemental Table 2). This suggests that the precursors of these tissues are not essential for driving the process of neurulation.

As a final test, we assayed the same mesendodermal/mesodermal tissues in *cyc* mutants, which lack one of the zebrafish Nodal ligands, and *casanova* (*cas)* mutants, which lack a transcription factor required for endoderm development. Both mutants always have a closed neural tube (Fig. 9) (Aquilina-Beck et al., 2007; Liang et al., 2000). Consistent with their normal anterior neurulation, both mutants also had hatching gland, notochord, and cpm tissues that were indistinguishable from WT siblings (Fig. 9).

Discussion

In this study, we established the temporal requirement for Nodal signaling and mapped regions of mesendoderm and mesoderm important for anterior neurulation. Treatment of embryos with an inhibitor of Nodal signaling starting before or at late blastula stage (4.3 hpf) produced an open neural tube phenotype in the forebrain. Correlation studies using Nodal deficient embryos with variable mesendodermal/mesodermal phenotypes found that there was a strong

correlation between the presence of the prechordal plate derived hatching glands, axial mesoderm derived notochord, paraxial cephalic mesoderm, and mesendoderm and mesendoderm derived head muscles and a closed neural tube. However, no single mesendodermal/mesodermal-derivative was always present when the neural tube was closed or always absent when the neural tube was open. Since the neural tube in Nodal deficient embryos is defective even at neural plate stages (Aquilina-Beck et al., 2007; Araya et al., 2014), we propose a model in which multiple Nodal-induced mesendoderm/mesoderm tissues act during gastrulation to make the developing anterior neuroectoderm competent to undergo the process of neurulation. When cumulative amount of these tissues in an embryo drops below a required threshold, the process of anterior neural tube closure fails.

Nodal acts during blastula stages to induce the mesendodermal/mesodermal tissues required for neural tube closure

We found Nodal signaling was required for anterior neurulation up to late blastula stages (up to 4.3 hpf). Treatment with even very high levels of Nodal inhibitor after this time period did not cause NTD, although the inhibitor was still effective as embryos treated until early gastrula stage (5.3 hpf, 50% epiboly stage) had cyclopia. This timing falls within the time period when mesoderm, endoderm, and mesendoderm are being induced. However, we can rule out a role for endoderm, as *cas* mutants, which completely lack endoderm, always have a closed neural tube (Figure 9) (Liang et al., 2000).

Nodal signals also have direct roles in patterning the neural tube. For instance, in zebrafish, Nodal is required for the development of the ventral neural tube (ventral brain in the anterior and floor plate in the spinal cord) (Hatta et al., 1991; Rebagliati et al., 1998; Sampath et al., 1998). In some cases, the ventral neural tube acts as a hinge point that bends the neural tube so that it can close. We can rule out an essential role for ventral neural tube in zebrafish neurulation, as *cyc* mutants, which have no ventral brain or spinal cord, have a closed neural tube (Figure 9) (Liang et al., 2000). It is also unlikely that the neural tube is open due to a lack of another neural tissue. The SB505124 sensitive period is over before neural induction has begun. In addition, treatment with a related Nodal signaling inhibitor (SB431542) at 70% epiboly, when the anterior neural tube is beginning to close, did not cause NTD (Araya et al., 2014).

The period in which SB505124 causes open neural tubes is also consistent with studies of Zygotic *oep* (*Zoep*) mutants, which can have either closed or open neural tubes (Aquilina-Beck et al., 2007; Lu et al., 2013). The onset of zygotic transcription in zebrafish falls at the 1000 cell stage, or around 2.75 hpf, within the period when SB505124 caused NTD. The onset of zygotic transcription can vary slightly from one embryo to another (Tadros and Lipshitz, 2009). Thus, a likely explanation of the incomplete penetrance of the NTD is that some *Zoep* embryos might have persistence of maternally-derived Oep or a slightly earlier onset of zygotic transcription, resulting in sufficient Oep protein during the period when Nodal is required for neurulation.

We used two different experimental designs to determine the temporal requirement for Nodal signaling in anterior neural tube closure. Even though the first exposed embryos to high doses of Nodal signaling inhibitor for 20 minutes and the second to high doses for ~20 hours, they both identified the same temporal requirement. Nodal signals act in a positive feedback loop that positively regulates the transcription of their own genes. We know from our washing experiments that a small amount of inhibitor persisted in the embryos treated for only 20 minutes. Thus, one possible explanation is that after a short treatment at high concentrations, only a minimal amount of SB505124 was needed to inhibit the small amount of remaining Nodal signaling. Another possibility is that the embryos sequestered SB505124 so that high concentrations persisted within the embryo even after washing.

Broad region of mesendoderm and mesoderm is important for anterior neural tube closure

Our data strongly suggests that a large region of anterior mesendoderm/mesoderm interacts with the overlying neuroectoderm to promote neural tube closure. Our favorite model is that a critical amount of anterior mesendoderm/mesoderm tissue required for anterior neurulation. When the amount drops below this threshold, the embryo develops NTD. However, we cannot rule out the possibility that a specific region of mesendoderm/mesoderm that we did not test is required for neural tube closure. The precursors to the tissues

analyzed in this study were the most likely to be involved in neurulation due to their spatial proximity or length of contact with the presumptive anterior neural tube. It is possible that the analyzed tissues correlated with a closed neural tube not because they were involved, but because they were co-induced by Nodal along with such a specific, required tissue. The presence of such a tissue is improbable, as we tested tissues that spanned the range of anterior mesendoderm/mesoderm derivatives.

We do not yet know the mechanisms by which mesendodermal/mesodermal tissues promote anterior neurulation. One possibility is that there is a biochemical signal that is secreted by a large range of mesendodermal/mesodermal tissues. If adequate numbers of mesendodermal/mesodermal cells s were present, then enough of this signal was produced to drive neural tube closure. Consistent with this possibility, a large region of the head mesendoderm/mesoderm is in close proximity to the overlying anterior neuroectoderm (Kimmel et al., 1990; Solnica-Krezel and Sepich, 2012). At the start of gastrulation, the mesendodermal cells move inward through the blastopore, forming a lining beneath the future neuroectodermal cells and the yolk cell below (Solnica-Krezel and Sepich, 2012). Contact between the germ layers persists until they undergo further specification around the end of gastrulation. Thus, the head mesendoderm/mesoderm is within a few cell diameters of the overlying neuroectoderm prior to and during anterior neurulation.

There are other examples of neural patterning events where a wide range of mesendodermal/mesodermal tissues are involved. For instance, Engrailed (En) proteins have a prominent role in midbrain and anterior hindbrain development (Joyner, 1996). In *Xenopus* explants, anterior notochord tissue acted a strong inducer of En-2 in ectodermal tissue, demonstrating that had been induced to form an anterior neural fate. However, the presumptive head mesoderm and anterior somites could induce En-2 expression, although not as efficiently (Hemmati-Brivanlou *et al.*, 1990). A similar redundant system could explain why absence of any one tissue was not sufficient to cause anterior NTD in zebrafish embryos.

In mice, the head mesenchyme, which is composed of anterior mesoderm and neural crest cells, is required for anterior neurulation. It has been proposed that proliferation and expansion of the underlying head mesenchyme drives the lateral edges of the neural plate toward each other (Chen and Behringer, 1995; Harris and Juriloff, 2007, 2010). However, it is improbable that head mesendoderm/mesoderm proliferation drives neural tube closure in zebrafish. In contrast to other vertebrates, primary neurulation in zebrafish results from the thickening and then ‘sinking’ of the neural plate (Lowery and Sive, 2004). It is hard to reconcile proliferation of the underlying mesenchyme/mesendoderm causing this ‘sinking’ morphological event in zebrafish as it is unlikely to be driven by an external force.

Consistent with our model that the interaction between mesendoderm/mesoderm with anterior neuroectoderm is driven by a secreted

protein, there is growing evidence for signals that mediate communication between anterior neuroectoderm and underlying mesoderm-related tissue. Disruptions of approximately 70 genes in mice result in either spina bifida or exencephaly (Harris and Juriloff, 2007, 2010). Many of these genes encode secretory proteins that have functions including involvement in biochemical cell-cell signaling pathways, apoptosis and cell adhesion (ex. Sonic Hedgehog, Fibroblast Growth Factors, and Wingless Integrated) (Harris and Juriloff, 2007, 2010; Londin et al., 2005; Yamamoto et al., 2003; Ybot-Gonzalez et al., 2002). Additionally, many of these secreted proteins are highly expressed before and during anterior neurulation in the neuroepithelium and in adjacent tissues such as the head mesenchyme (Harris and Juriloff, 2007, 2010). These signals are potential candidates for mediating a biochemical interaction between the anterior mesendoderm/mesoderm and the anterior neural tube.

Methods

All protocols using animals were approved by the U of MN Institutional Animal Care and Use Committee.

Zebrafish stocks

Zebrafish were maintained as per standard protocols at a constant temperature of 28.5 °C in a 14:10 light:dark cycle (Westerfield, 2000a). The stocks used were WT strain Zebrafish *Danio rerio* (ZDR) (Aquatica Tropical, Plant City,

FL), and fish carrying the *sqt* ^{cz35} (Feldman et al., 1998), *cyc* ^{m294} (Schier et al., 1996), or *casanova* ^{ta56} (*cas*) (Chen et al., 1996) mutations. WT, *cyc*, and *cas* embryos were incubated at 28.5 °C and *sqt* embryos were incubated at 34 °C to increase the penetrance of the open neural tube phenotype (Hagos and Dougan, 2007; Lu et al., 2013). All embryonic stages were defined morphologically (Kimmel et al., 1995a).

SB505124 treatment

For the short term treatment experiments, 3 hpf (1000-cell stage) ZDR embryos were dechorionated with 2mg/ml Pronase (Roche) using established methods (Link et al., 2006; Westerfield, 2000a). Embryos not fully dechorionated by the Pronase solution were dechorionated through gentle agitation with forceps. Post pronase treatment, embryos were always transferred using Sigma Cote (Sigma Aldrich) coated glass pipettes to prevent damage. At the desired morphological stage, embryos were exposed to 50, 75, or 100 μM of 2-(5-benzo [1,3] dioxol-5-yl-2-terbutyl-3H-imidazol-4-yl)-6-methylpyridine hydrochloride hydrate (SB505124) (Sigma Aldrich) at room temperature (Hagos and Dougan, 2007; Hagos et al., 2007). After 20 minutes of SB505124 treatment, embryos were transferred to a Petri dish with ~10 ml of new embryo media. Post SB505124 exposure, embryos were incubated at 28.5 °C until the desired stage, then fixed and assayed.

ZDR embryos were treated at specific morphological stages with 100 μM of SB505124 (Tocris) until fixation at approximately 24 hpf. We found no difference in SB505124 effectiveness between experiments where the chorions were on or off. Therefore, some experimental trials used dechorionated embryos and others used embryos still in their chorions. The dechorionated embryos were produced by treatment with 2 mg/ml Pronase at the 64 cell stage for ~7 minutes at 28.5 °C.

Whole mount RNA in situ hybridization (WISH)

Embryos were assayed by RNA whole mount in situ hybridization using established methods (Thisse and Thisse, 2014). Digoxygenin antisense RNA probes included *orthodenticle homobox 5* (*otx5*) (Gamse et al., 2002), *cathepsin L 1b* (*ctsl1b*) (Vogel and Gerster, 1997), *paired box gene 2.1* (*pax 2.1*) (Pfeffer et al., 1998), *floating head* (*flh*) (Talbot et al., 1995), *goosecoid* (*gsc*) (Stachel et al., 1993), *collagen type IX alpha 2* (*col9a2*) (Thisse et al., 2001), *collagen type 2 alpha-1a* (*col2a1*) (Yan et al., 1995), *sonic hedgehog* (*shh*) (Krauss et al., 1993) and *smooth muscle myosin heavy chain 2* (*smyhc2*) (Elworthy et al., 2008).

PCR genotyping

sqt heterozygotes were identified by natural breeding or by Polymerase Chain Reaction (PCR) using *sqt*^{cz35} specific primers on DNA extracted from fin clips. The shared forward primer was 5'-GAGCTTTATTTCAATAACTGCGTG-3'.

The reverse primer to detect the insertion in the *sqt* mutants was 5'-ATATAAAATCAGTACAACCGCCCG-3', and the reverse primer to detect the WT allele was 5'-GCCAGCTGCTCGCATTTTATTCC-3' (Feldman et al., 1998).

Photography

Bright field images were taken with a SPOT Insight Fire Wire camera mounted on a Nikon Eclipse 80i microscope. All images were processed using Adobe InDesign 6.0 (Adobe Systems Inc).

mRNA injections

One to two celled stage ZDR embryos were pressure injected with 0.38-2.5 pg of *lefty1* mRNA using Harvard Apparatus PL190-nitrogen driven pico-injector. Embryos were maintained at 28.5 °C and then fixed and assayed by light microscopy and WISH. Uninjected or GFP mRNA injected sibling embryos served as controls.

Data analyses

Homozygous *sqt*, *cyc*, *cas*, and *lefty1* mRNA injected embryos were assayed by WISH for the presence of mesendodermal and mesodermal tissues and pineal morphology. The embryos were categorized into 4 groups: mesendodermal/mesodermal tissue present and elongated or divided pineal (open NT), mesendodermal/mesodermal tissue absent and open NT,

mesendodermal/mesodermal tissue present and closed NT and mesendodermal/mesodermal tissue absent and closed NT. Tissue was counted as present if there was either partial or full expression of the mesendodermal/mesodermal marker. These groups corresponded to the four quadrants within a 2 X 2 contingency table of a one-tailed Fisher's exact test. If a statistically significant relationship was observed ($P<0.05$), the strength of the correlation between neural tube closure and mesendodermal/mesodermal tissue presence was determined through the Phi Coefficient (φ). One-tailed Fisher's exact tests were conducted using R version 3.1.2 software.

Table 1: Treatment of embryos with Sigma SB505124 for 20 minutes at or before 4.3 hpf causes failure in neural tube closure.

Stage of SB 505124 Exposure	SB50514 Dose	Closed NT	Open NT		Total
		Oval Pineal	Elongated Pineal	Divided Pineal	
Oblong (3.8 hpf)	75 µM	0 (0%)	0 (0%)	6 (100%)	6
Oblong (3.8 hpf)	100 µM	0 (0%)	5 (20%)	20 (80%)	25
Sphere (4.0 hpf)	75 µM	0 (0%)	2 (9%)	21 (91%)	23
Sphere (4.0 hpf)	100 µM	8 (11%)	20 (27%)	46 (62%)	74
Dome (4.3 hpf)	75 µM	8 (73%)	0 (0%)	3 (27%)	11
30% Epiboly (4.7 hpf)	75 µM	12 (100%)	0 (0%)	0 (0%)	12
30% Epiboly (4.7 hpf)	100 µM	6 (100%)	0 (0%)	0 (0%)	6

Table 2: Increasing penetrance of NTD with increasing dose of Tocris SB505124.

SB505124 Dose	Closed NT	Open NT		Total
	Oval Pineal	Elongated Pineal	Divided Pineal	
0 μM	74 (100%)	0 (0%)	0 (0%)	74
0.1 μM	73 (100%)	0 (0%)	0 (0%)	73
1 μM	61 (100%)	0 (0%)	0 (0%)	61
5 μM	36 (55%)	10 (16%)	19 (29%)	65
10 μM	1 (1%)	8 (11%)	63 (88%)	72
20 μM	0 (0%)	53 (93%)	4 (7%)	57
50 μM	0 (0%)	1 (1%)	83 (99%)	84
100 μM	0 (0%)	1 (2%)	51 (98%)	52

Table 3: Initiating treatment of embryos with 100 uM Tocris SB505124 at or before 4.3 hpf causes open neural tubes.

Stage of Drug Exposure	Closed NT	Open NT		Total
	Oval Pineal	Elongated Pineal	Divided Pineal	
High Oblong (3.8 hpf)	0 (0%)	32 (14%)	199 (86%)	231
Sphere (4.0 hpf)	9 (2%)	85 (18%)	380 (80%)	474
Dome (4.3 hpf)	209 (90%)	17 (8%)	5 (2%)	231
30% Epiboly (4.7 hpf)	452 (98%)	6 (1%)*	5 (1%)*	463
50% Epiboly (5.3 hpf)	178 (99%)	1 (0.05%)	1 (0.05%)	180

* The small number of embryos with open neural tubes in the 30% epiboly time point were likely slightly younger embryos that contaminated those samples.

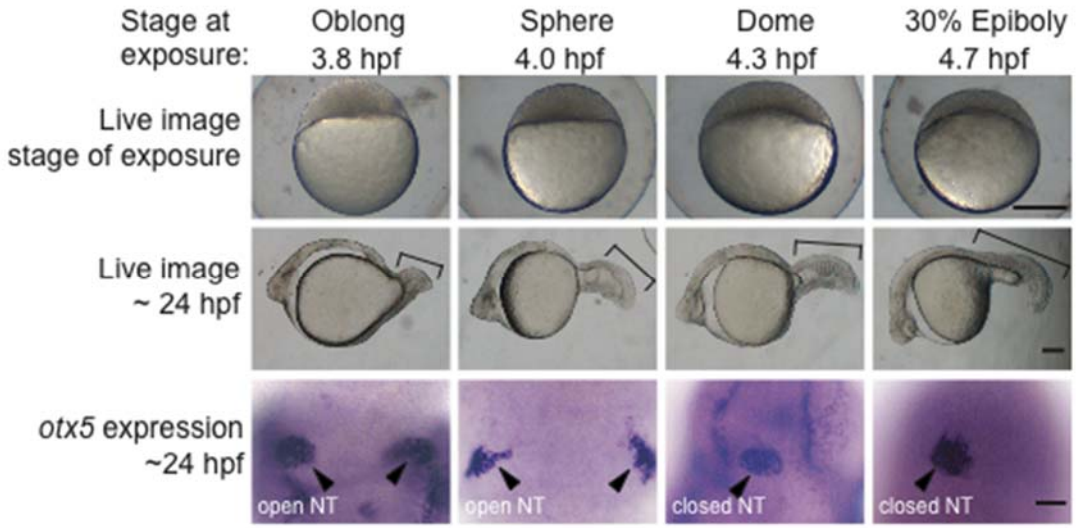

Figure 1: Failure of neural tube closure in embryos treated with the Nodal inhibitor SB505124 for 20 minutes before the late blastula stage (4.3 hpf). Embryos treated with 75 uM SB505124 at all four stages of development have cyclopic eyes. The severity of the defects in mesendodermal/mesodermal derivatives, such as somites (brackets) decreases as the treatments initiate later in development. Embryos treated for 20 minutes at 3.8 and 4.0 hpf have open neural tubes (open NT), as evidenced by the two domains of pineal precursors (arrowheads). In contrast, embryos treated at 4.3 and 4.7 hpf have oval shaped pineal anlage (arrowheads) indicating a closed anterior neural tube (closed NT). Top row: Lateral views, animal pole to the top, scale bar: 250 μm. Second row: Lateral views anterior to the left, scale bar: 50 μm. Third row: Dorsal views anterior to the top. Scale bar: 50 μm. Refer to Table 1 for quantitative data.

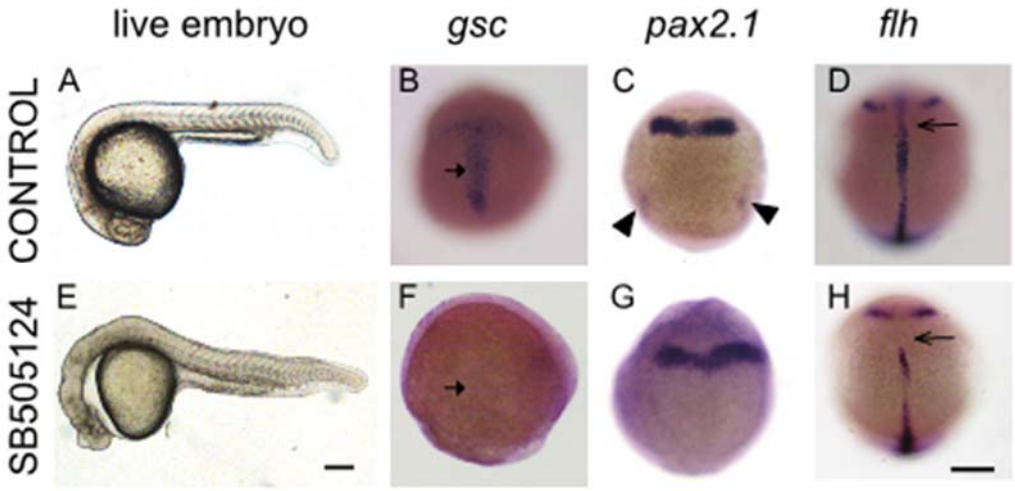

Figure 2: Exposure to Nodal inhibitor SB505124 at 3.8 hpf causes loss of mesendodermal and mesodermal derivatives.
(A-D) Control WT embryos exposed to DMSO and (E-H) WT embryos exposed to 50 μM SB505124. (A) WT embryo at 1 dpf has a normal smooth and round head, a straight body axis, and complete somite formation, while (E) inhibitor treated embryo displays cyclopia and abnormal morphology. (B) Normal *gsc* expression in the prechordal plate of a 9 hpf embryo (90% epiboly) displays a T-shaped expression domain (arrow) that (F) is absent in an inhibitor treated embryo. (C) Normal *pax2.1* expression is present along the midbrain-hindbrain border and in the posterior region in the pronephric mesoderm (arrowheads) in 10 hpf (tailbud stage) embryos. (G) In Nodal deficient embryos, *pax2.1* mRNA is present in the midbrain-hindbrain border (arrowheads) but absent in the pronephric mesoderm. (D) At 12 hpf (6 somite stage), *flh* is expressed in the developing notochord (arrow). (H) SB505124 treated embryos have partial reduction of notochord tissue. Scale bars: 250 μm.

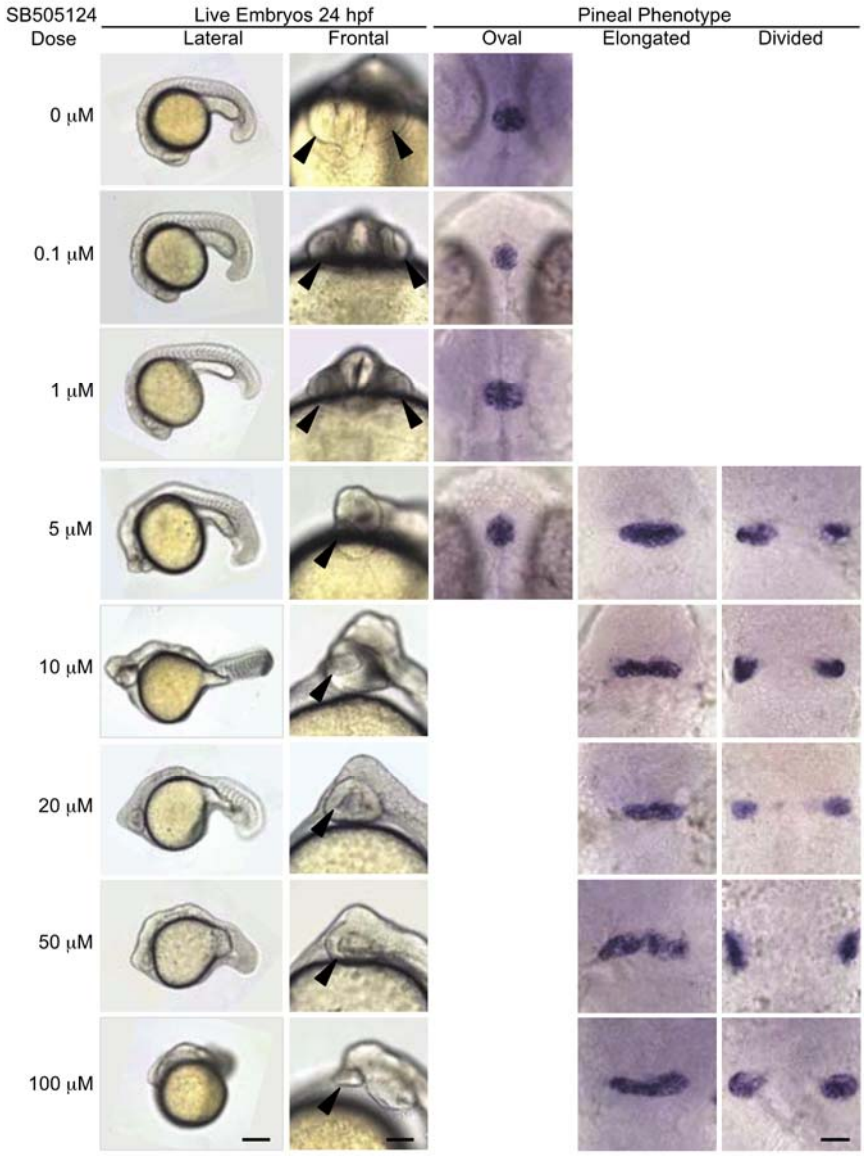

Figure 3: Open neural tube phenotype is fully penetrant upon treatment with Tocris SB505124 at concentrations of 10 μM and higher. All embryos were treated with the indicated concentration of SB505124 at 3.8 hpf (high oblong stage). First column: Anterior to the left and dorsal to the top. Scale bar: 250 μM. Second column: Anterior to the top. Scale bar: 100 μM. Arrowheads point to the eye. Third-fifth columns: Embryos were assayed for *otx5* expression in the pineal. Dorsal views, anterior to the top. Scale bar: 50 μM. Refer to Table 2 for quantitative data.

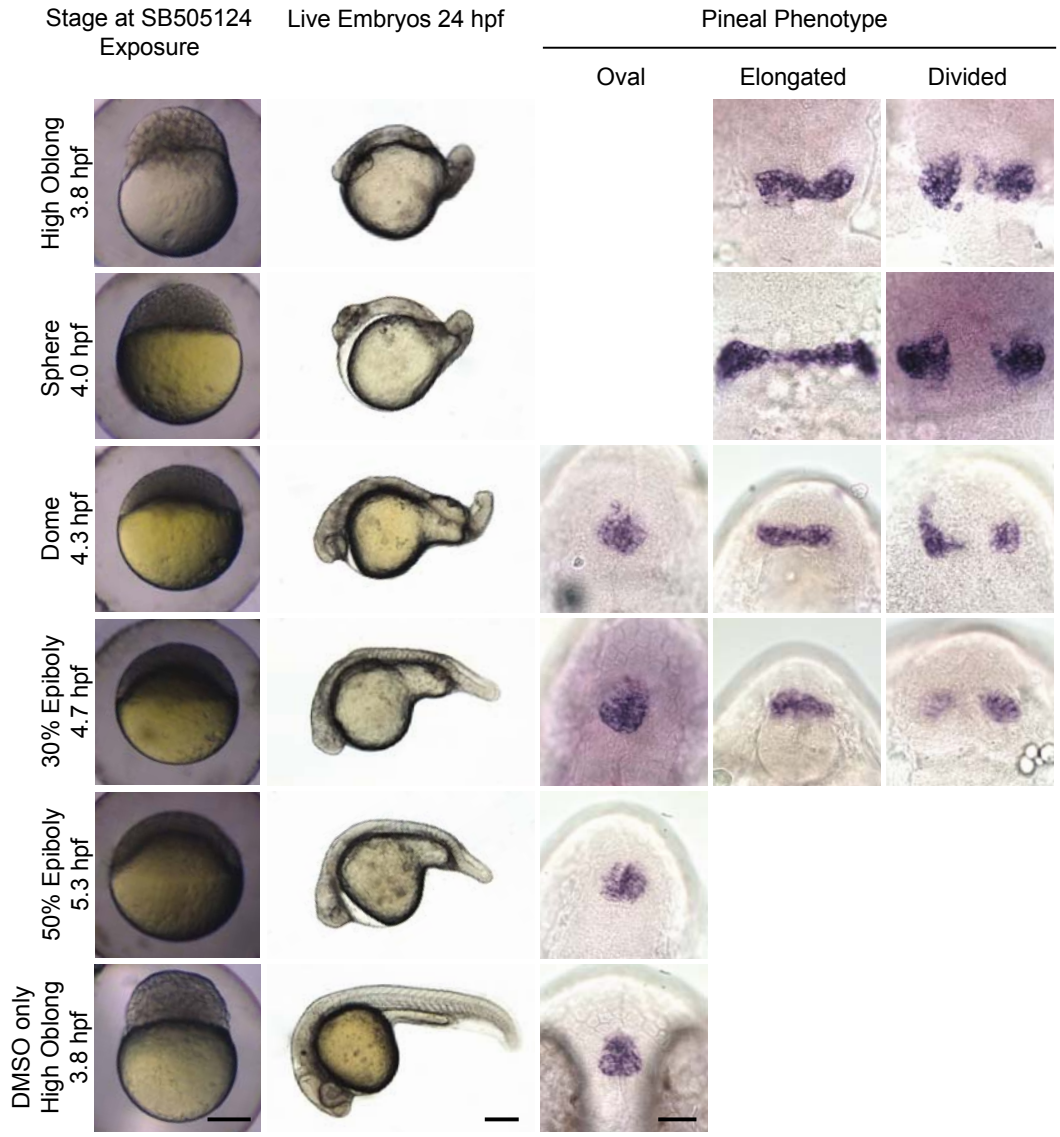

Figure 4: Initiating SB505124 treatment during mid blastula stages blocks neural tube closure. First column: developmental stage and images of live embryos at the onset of inhibitor exposure. Lateral views with animal pole to the top. Scale bar: 250 μM. Second column: Lateral views of whole embryos with anterior to the left and dorsal to the top. Scale bar: 250 μM. Third column: Lateral views of whole embryos with anterior to the left and dorsal to the top. Scale bar: 250 μM. Third through fifth column: Embryos were assayed for *otx5* expression in the pineal gland. Dorsal views, anterior to the top. Scale bar: 50 μM. Refer to Table 3 for quantitative data.

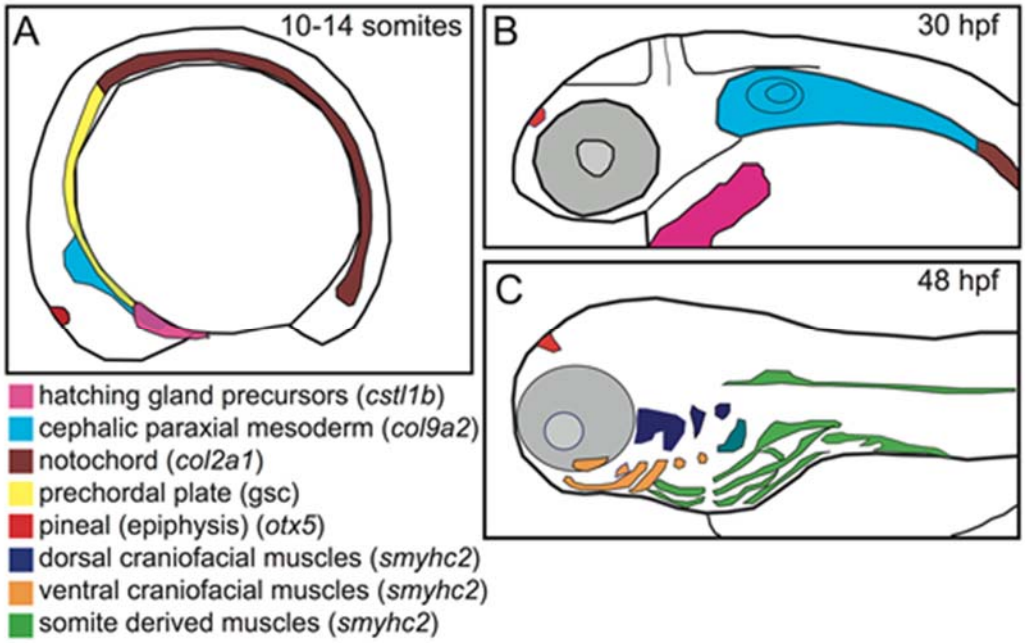

Figure 5: Regions of the head mesendoderm were assayed using a panel of markers.
Schematic representation of expression patterns of mesendodermal and mesodermal tissues along the anterior-posterior axis during (A) the early somite stage, (B) the mid pharyngula period, and (C) the onset of the hatching period. Lateral views, dorsal to the top. Schematics based on published gene expression data (Elworthy et al., 2008; Murakami et al., 2006; Thisse et al., 2001).

A

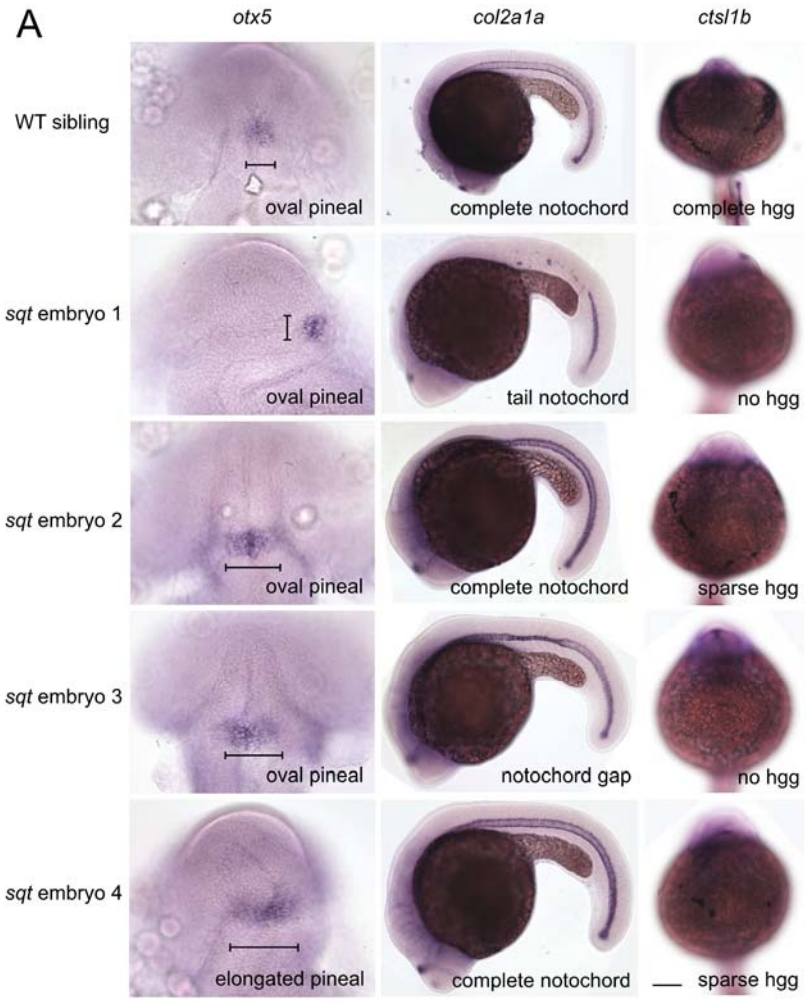

B

	Pineal Morphology			
	Closed	Open		Total
	Oval	Elongated	Divided	
anterior nc Present	10	1	0	11
anterior nc Absent	4	6	10	20
Total	14	7	10	31

C

	Pineal Morphology			
	Closed	Open		Total
	Oval	Elongated	Divided	
hgg Present	3	1	0	4
hgg Absent	5	5	10	20
Total	8	6	10	24

Figure 6: Positive correlation between a closed neural tube and the presence of prechordal plate-derived hatching glands and axial mesoderm derived notochord.

Embryos were raised to ~1 dpf and processed in tandem for *otx5* in the pineal anlage, *col2a1* in the notochord, and *cstl1b* in the hatching gland cells (hgg). (A) In WT embryos, the pineal organ is oval indicating a closed neural tube, the notochord spans the complete anterior-posterior extent of the trunk, and the hatching glands make a “necklace” around the anterior of the head. *sqt* embryos have a range of neural tube, notochord, and hgg defects as indicated. Note that, at this stage, *col2a1* is expressed in three adjacent lines of cells, the floor plate (dorsal to the notochord), the hypochord (ventral to the notochord), and the notochord. The gaps in staining in *sqt* embryo 1 correspond to loss of all three tissues. The narrow region of staining in *sqt* embryo 3 just above the hind yolk corresponds to a place where the floor plate and hypochord cells persist, but the wider notochord cells are missing. The neural tube was scored as open if the pineal organ was at least twice as wide along its left-right axis (brackets) compared to its anterior-posterior axis. (B, C) Complete set of quantitative data. Images in the same row are different views of the same embryo. First column: Dorsal views with anterior to the top. Second column: Lateral views with anterior.

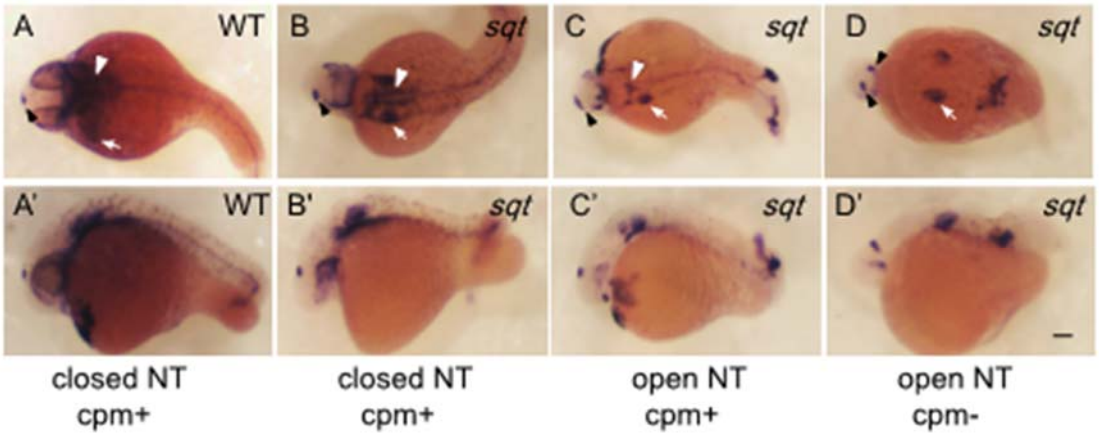

E

	Pineal Morphology			
	Closed	Open		Total
	Oval	Elongated	Divided	
cpm Present	2	3	6	11
cpm Absent	2	1	7	10
Total	4	4	13	21

Figure 7: Correlation between cephalic paraxial mesoderm and neural tube closure. (A, A') In WT embryos, *col9a2* is expressed in the cpm (white arrowheads) and the ears (white arrow) and the *otx5* expressing pineal anlage (black arrowheads) is oval shaped indicating a closed neural tube. (B-D') *sqt* embryos with different combinations of cpm deficiencies and neural tube phenotypes. (A-D) Dorsal views with anterior to the left and (A'-D') lateral views with anterior to the left and dorsal to the top. Images with the same letter are of the same embryo. Scale bar: 100 μm.

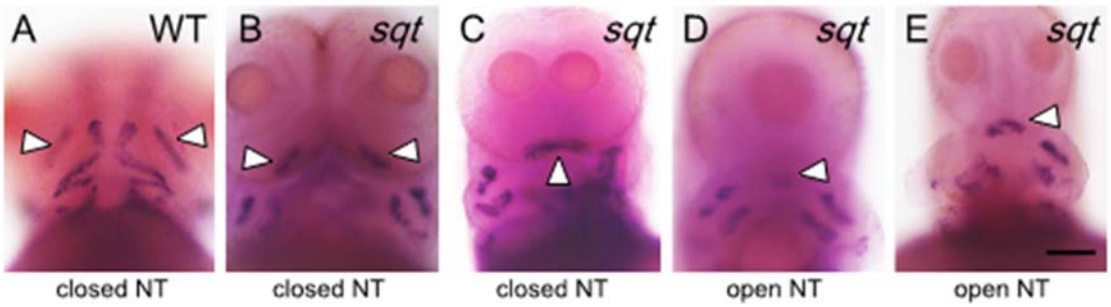

F

	Pineal Morphology			
	Closed	Open		Total
	Oval	Elongated	Divided	
hm Present	12	1	6	19
hm Absent	2	0	2	4
Total	14	1	8	23

Figure 8: Correlation between presence of head muscles and neural tube closure in *sqt* mutants. (A-E) WT and *sqt* embryos were raised to 3 dpf and processed in tandem for *smyhc2*, in the head muscles (hm) and *otx5,* in the pineal anlage. The adductor mandibulae (am; white arrowheads) are the first muscles to develop in the head region and were used as an indicator for head muscle presence. (A) In WT embryos, am precursors are in two clusters just anterior to the yolk sac and other jaw muscles. The pineal organ is oval indicating a closed neural tube. (B-E) *sqt* embryos with an (B, C) oval pineal with the am present and (D, E) divided pineal with the am present. (F) Complete set of quantitative data. All images are frontal views with anterior to the top. Scale bar: 100 μm (A-E).

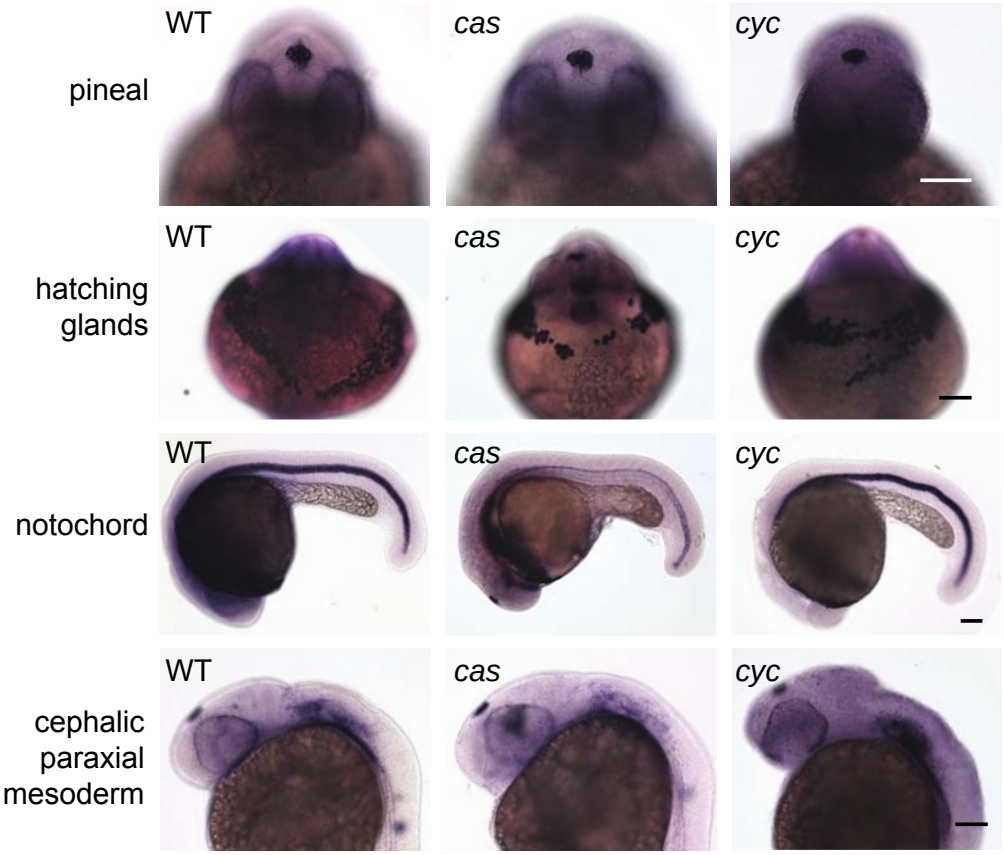

Figure 9: Closed neural tubes and normal mesendoderm/mesoderm development in *cyc* and *cas* mutants. Embryos were co-assayed for *otx5* expression in the pineal precursors and a combination of the following mesendodermal/mesodermal markers: *ctsl1b* in the hatching glands, *pax 2.1*, *col9a2* in cephalic paraxial mesoderm, and *shh* (for *cas* mutant) or *col2a1* in the notochord (WT embryo and *cyc* mutant). Embryos in the first three rows are at ~26 somite stage and those in the last two rows are 30 hpf. Images in the same column and of the same age are different views of the same embryo. Scale bars: 100 μm.

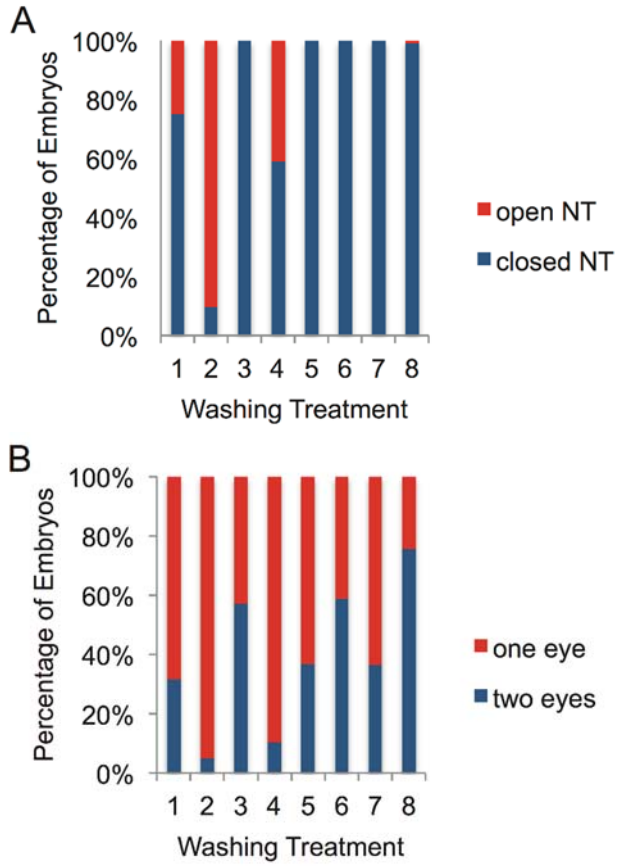

Supplemental Figure 1: SB505124 activity persists after extensive washing. All embryos were treated with 100 µM Tocris SB505124 for 20 minutes starting at 3.8 hpf (high-oblong stage). Eight different washing methods were attempted to remove SB505124 activity. Following the washes, embryos were raised at 28.5° C, fixed at 24 hpf, and processed for WISH with a probe for *otx5*. Embryos were scored for (A) neural tube and (B) eye phenotype. Embryos were either transferred from wash to wash with a Pasteur pipet along with minimal liquid or the Petri dish was tilted and most of the liquid removed and replaced with fresh embryo media. Treatment 1: Embryos transferred with minimal liquid to 12 ml and then 40 ml of embryo media. Treatment 2: Embryos washed 3 times in 40 ml of embryo media. Treatment 3: Embryos washed twice in 40 ml of embryo media followed by replacement with 40 ml new embryo media. Treatment 4: Embryos transferred to 40 ml embryo media followed by replacement three times with 40 ml embryo media. Treatment 5: Embryos transferred to 400 ml of embryo media. Treatment 6: Embryos transferred to a 400 ml embryo media + 1% DMSO followed by replacement of 400 ml embryo media four times. Treatment 7: Embryos were transferred to 400 ml embryo media followed by replacement of 400 ml embryo media four times. Treatment 8: Embryos were transferred to a 400 ml DMSO and embryo media solution followed by replacement with 400 ml embryo media + 1% DMSO four times.

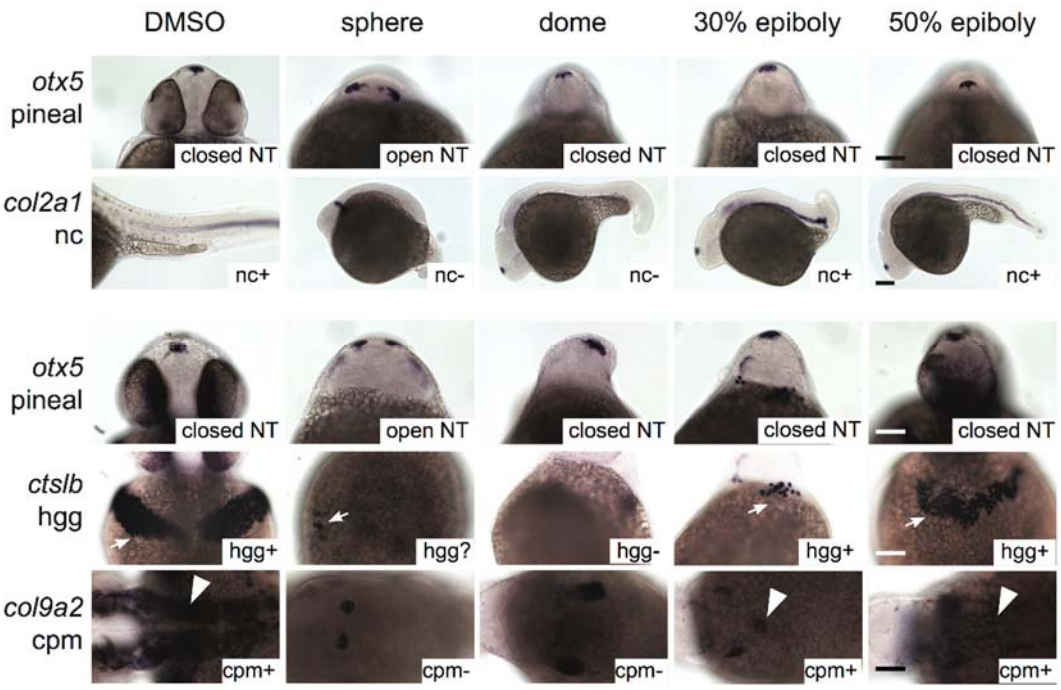

Supplemental Figure 2: Loss of mesendodermal and mesodermal derivatives in embryos treated with SB505124.
Each column represents the developmental stage at SB505124 addition. Embryos were raised in DMSO or 100 µM Tocris SB505124 SB505124 treatment at 28.5 °C until fixation at 22 hpf (26 somites stage) (rows 1, 2) or 30 hpf (rows 3, 4, 5). Rows 1, 3, 4: Frontal views, anterior to the top. Row 2: Lateral views, anterior to the left. Row 5: Dorsal views: anterior to the left. The bilateral *col9a2* staining present in all embryos is in the otic vesicles. White arrows point to hatching gland cells, white arrowheads to cephalic paraxial mesoderm. Nc, hgg, and cpm presence (+) or absence (-) is noted. Scale bars: 100 µm.

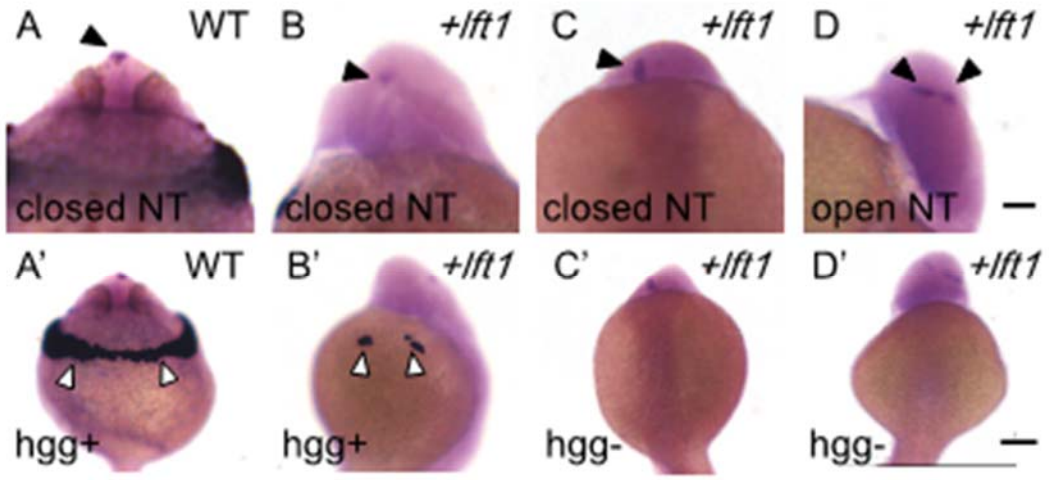

E

	Pineal Morphology			
	Closed	Open		Total
	Oval	Elongated	Divided	
hgg Present	9	0	1	10
hgg Absent	7	1	28	36
Total	16	1	29	46

Supplemental Figure 3: Correlation between hatching gland presence and closed neural tube in Lefty1 overexpressing embryos.
Embryos were (A, A') left uninjected or (B-D') injected with *lefty1* mRNA (+*lft1*), raised to 1 dpf and processed in tandem for expression of *cstl1b* in the hatching gland cells (hg, white arrowheads) and *otx5* in the pineal anlage (black arrowheads). (A, A') In uninjected embryos, the hatching glands make a "necklace" around the anterior of the head. The pineal organ is oval indicating a closed neural tube. (B-D') *lefty1* injected embryos with an (B, B') oval pineal and the hatching glands present, (C, C') oval pineal and complete absence of the hatching glands, (D, D') elongated pineal with complete absence of the hatching glands. (E) Complete set of quantitative data. Frontal views with dorsal to the top. Panels with the same letter are different views of the same embryo. Scale bar: 100 μm.

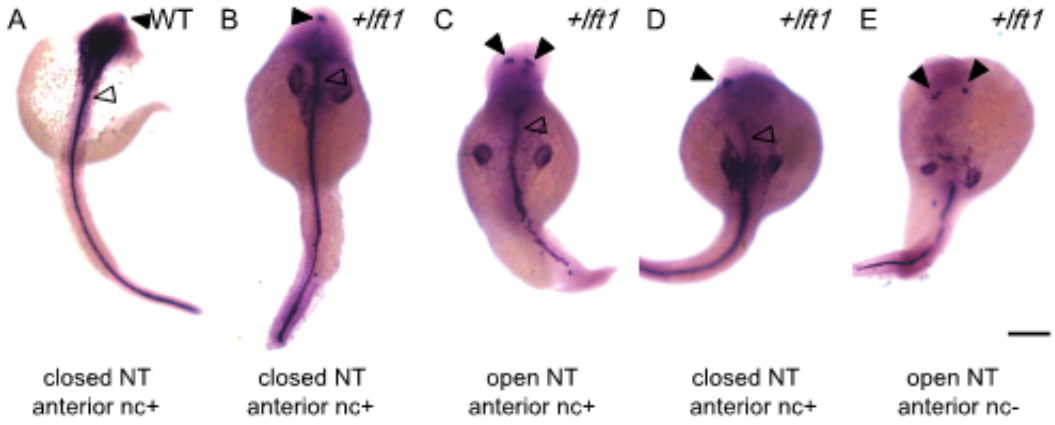

F

	Pineal Morphology			
	Closed	Open		Total
	Oval	Elongated	Divided	
anterior nc Present	50	4	14	68
anterior nc Absent	18	9	46	73
Total	68	13	60	141

Supplemental Figure 4: Presence of anterior notochord correlated with a closed neural tube in Lefty1 overexpressing embryos.
Embryos were (A) left uninjected or (B-E) injected with *lefty1* mRNA (*+lft1*) at the 1-2 cell stage, raised to 1 dpf and processed in tandem for expression of *col2al* in the notochord (anterior nc, open arrowheads), and *otx5* in the pineal anlage (closed arrowheads). Whether an embryo is positive (+) or negative (-) for anterior nc staining is indicated. The otic capsules, precursors to the ears were used as the division point for the anterior and posterior notochord. (A) In WT, uninjected embryos, the notochord runs the length of the anterior-posterior axis. The pineal organ is oval indicating a closed neural tube. (B-D) *lefty1* mRNA injected embryos with an (B) oval pineal and anterior notochord present, (C) divided pineal and anterior notochord present, (D) oval pineal and absence of anterior notochord, and (E) oval pineal and absence of anterior notochord. (F) Complete set of quantitative data. Dorsal views with anterior on the top. Scale bar: 100 μm.

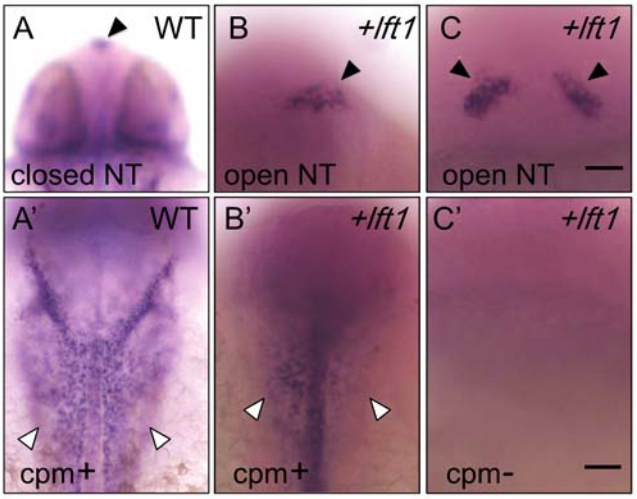

D

	Pineal Morphology			
	Closed	Open		Total
	Oval	Elongated	Divided	
CPM Present	13	1	1	15
CPM Absent	6	5	27	38
Total	19	6	28	53

Supplemental Figure 5: Cephalic paraxial mesoderm is not required for neural tube closure in *lefty1* mRNA injected embryos. Embryos were (A) left uninjected or (B-C') injected with *lefty1* mRNA (+*lft1*) at the 1-2 cell stage, raised to 1 dpf and processed in tandem for expression of *col9a2* in the cephalic paraxial mesoderm (cpm, white arrowheads) and *otx5* in the pineal anlage (black arrowheads). Whether an embryo is positive (+) or negative (-) for cpm staining is indicated. (A, A') In WT, uninjected embryos, the cephalic paraxial mesoderm is expressed in the hindbrain region, projecting laterally from the anterior notochord. The pineal organ is oval indicating a closed neural tube. (B-C') *lefty1* mRNA injected embryos with an (B, B') elongated pineal and the cephalic paraxial mesoderm present and (C, C') divided pineal and complete absence of the cephalic paraxial mesoderm. (D) Complete set of quantitative data. Dorsal views with anterior on the top. Panels with the same letter are different views of the same embryo. Scale bar: 100 μm (A-C), 200 μm (A'-C').

Supplemental Table 1: Decrease in mesendodermal and mesodermal derivatives upon treatment with 100 µM SB505124.

Stage of SB505124 Exposure	hgg*		nc		cpm*		Total
	present	absent	present	absent	present	absent	
DMSO Control							
closed NT	21	0	27	0	21	0	48 (100%)
open NT	0	0	0	0	0	0	0 (0%)
High Oblong							
closed NT	not determined		0	0	not determined		0 (0%)
open NT			0	116			116 (100%)
Sphere							
closed NT	0	0	0	0	0	0	0 (0%)
open NT	0	77	0	137	0	77	214 (100%)
Dome							
closed NT	17	13	9	82	30	0	121 (88%)
open NT	1	5	2	9	4	2	17 (12%)
30% Epiboly							
closed NT	18	8	105	5	25	1	136 (100%)
open NT	0	0	0	0	0	0	0 (0%)
50% Epiboly							
closed NT	23	0	69	0	23	0	92 (100%)
open NT	0	0	0	0	0	0	0 (0%)

Supplemental Table 2: Correlation between presence of head muscles and neural tube closure in Lefty1 overexpressing embryos.

	Pineal Morphology			
	Closed	Open		Total
	Oval	Elongated	Divided	
hm Present	40	2	0	42
hm Absent	5	0	3	8
Total	45	2	3	50

Chapter IV: Temperature sensitivity of neural tube defects in *Zoep* mutants

Phyo Ma, Morgan R. Swartz, Lexy M. Kindt, Ashley M. Kangas, Jennifer Ostrom Liang

Neural tube defects (NTD) occur when the flat neural plate epithelium fails to fold into the neural tube, the precursor to the brain and spinal cord. Squint (Sqt/Ndr1), a Nodal ligand, and One eyed-pinhead (Oep), a component of the Nodal receptor, are required for anterior neural tube closure in zebrafish. The NTD in *sqt* and *Zoep* mutants are incompletely penetrant. The penetrance of several defects in *sqt* mutants increases upon heat- or cold-shock. In this project, undergraduate students tested whether temperature influences the *oep* open neural tube phenotype. Single pairs of adults were spawned at 28.5 °C, the normal temperature for zebrafish, and one half of the resulting embryos were moved to 34 °C at different developmental time points. ANOVA indicated temperature and clutch/genetic background significantly contribute to the penetrance of the open neural tube phenotype. Heat-shock affected the embryos only at or before mid-blastula stage. Many factors including temperature changes in the mother, nutrition, and genetic background contribute to NTD in humans. Thus, *sqt* and *Zoep* mutants may serve as valuable models for studying the interactions between genetic and external environment during neurulation.

Introduction

NTD are one of the most common birth defects in the world. In the United States, NTD occurred in approximately 4.3 in every 10,000 live births during 2006-2008.(Parker et al., 2010) All NTD are characterized by a failure of the

developing neuroepithelium to form the closed neural tube that later gives rise to the brain and spinal cord. NTD are classified by the part of the developing neural tube that fails to close. The two most common NTD are spina bifida, which occurs when the most posterior part of the neural tube fails to close, and anencephaly, which occurs when the most anterior part of the neural tube fails to close.(Copp et al., 2013; Parker et al., 2010) Spina bifida can cause mild to severe problems with movement and feeling in the legs. Anencephaly causes severe defects in brain development and is always fatal. (Copp et al., 2003)

Human NTD are complex, with multiple genes and environmental factors playing a role.(Au et al., 2010; Copp et al., 2013; Dreier et al., 2014; Kappen, 2013; Moretti et al., 2005; Zohn, 2012) This complexity is reflected by the efforts to prevent NTD with folic acid supplementation. In controlled clinical trials, supplementation of the mother's nutrition with folic acid reduced the recurrence of NTD by up to 70%.(Imbard et al., 2013) Mandatory folic acid supplementation in the grain supply of the US and other countries have resulted in a 13-78% reduction in NTD, with some of the biggest effects occurring in areas with the highest incidence.(Imbard et al., 2013) Despite folic acid supplementation, NTDs persist likely due to many factors including failure of the folic acid to reach all pregnant women, folate-resistant NTD, roles for other nutrients, metabolic state of the mother such as the presence of diabetes or obesity, and genetic background.(Carmichael et al., 2010; Copp et al., 2013; Kappen, 2013; Zohn, 2012) Thus, a greater understanding of the interactions among genetic and

environmental factors affecting neurulation is needed to further reduce the incidence of this congenital defect and improve prenatal care and diagnosis.

The zebrafish model system may provide a simple system to start understanding the interactions between genes and the environment. Mechanisms of neural tube closure, or neurulation, are well conserved between zebrafish and mammals. Genes identified in mice are starting to be tested for relationships to human NTD. Although in most cases the match has not yet been made, mutations in genes encoding components of the Wnt/Planar Cell Polarity pathway have been shown to cause NTD in humans, frogs, mice, and zebrafish.(Cai and Shi, 2014; Ciruna et al., 2006; Copp et al., 2013; Wallingford and Harland, 2002)

Our previous findings demonstrated that Nodal signaling is required for neurulation of the anterior neural tube of zebrafish. Nodals are secreted proteins in the TGFβ super family and are required for many events during vertebrate development, including the induction of mesoderm and endoderm, the regulation of left-right asymmetry of visceral organs and the epithalamus, and formation of the ventral neural tube.(Halpern et al., 2003; Liang and Rubinstein, 2003; Schier and Shen, 2000; Schier and Talbot, 2001) Zebrafish have three secreted Nodal proteins, Squint (Sqt), Cyclops (Cyc), and Southpaw (Spaw). *sqt*, and *cyc*;*sqt* double mutants have open neural tube phenotypes while *cyc* mutants do not, suggesting that the timing or spatial pattern of *sqt* expression is important for neural tube closure.(Aquilina-Beck et al., 2007; Lu et al., 2013)

In contrast to *cyc* mutants, several aspects of the *sqt* mutant phenotype are incompletely penetrant and have variable expressivity.(Aquilina-Beck et al., 2007; Dougan et al., 2003; Hagos et al., 2007; Liang et al., 2000; Mathieu et al., 2002; Pei and Feldman, 2009; Pei et al., 2007) Both environmental factors and genetic background affect the phenotype of MZ*sqt* mutants, which lack both maternally- and zygotically-supplied *sqt* mRNA.(Pei and Feldman, 2009; Pei et al., 2007) One of the variable phenotypes is a midline bifurcation, where the left and right side of the embryo become separated.(Pei and Feldman, 2009) Penetrance of the midline bifurcation phenotype increased with heat shock (raising the embryos at 34 °C instead of 28.5 °C) and correlated with decreased non-canonical Wnt signaling, increased canonical Wnt/β-catenin signaling, and decreased Heat shock protein 90 (Hsp90) activity.(Pei and Feldman, 2009) Similarly, penetrance of the cyclopic phenotype was caused by heat shock (34 °C) and cold shock (15 °C) and correlated with residual activity from other Nodal/Activin proteins and with activity of Hsp90.(Pei et al., 2007)

All three zebrafish Nodal ligands signal through a receptor complex containing Type I and Type II TGF-β receptors and the membrane associated protein One eyed pinhead (Oep).(Halpern et al., 2003; Liang and Rubinstein, 2003; Schier and Shen, 2000; Schier and Talbot, 2001) MZ*oep* mutants always have an open neural tube while Z*oep* mutants, which lack only zygotically-transcribed *oep* mRNA, have an incompletely penetrant open neural tube phenotype.(Aquilina-Beck et al., 2007; Lu et al., 2013) As part of an independent

undergraduate research project, we tested the hypothesis that the penetrance of the NTD in *Zoep* mutants might be affected by temperature. Surprisingly, although other aspects of the *Zoep* mutant phenotype, such as cyclopia, were completely penetrant(Schier et al., 1996), the percentage of embryos with an open neural tube phenotype varied from 0-100% in clutches raised at 28.5 °C (Figures 3 and 4). Despite this variability, ANOVA indicated that temperature and genetic background both significantly contributed to the degree of penetrance of the open neural tube phenotype. The percentage of *Zoep* mutants with NTD increased when embryos were moved to 34 °C at or before 4 hours post fertilization (hpf), but not when moved at later time points. This closely matches what was found for *sqt* mutants (Pei and Feldman, 2009; Pei et al., 2007) and strongly suggests that in a subset of embryos, Sqt signaling through Oep is required during the first few hours of development to promote neural tube closure. Thus, Nodal signaling mutants serve as sensitive systems to find factors with a modulatory effect on multiple developmental defects, and to help increase our understanding of the interactions between genetics and the environment.

Methods

Zebrafish Stocks

Zebrafish were maintained at 28.5 °C in a 14:10 light:dark cycle in an aquatic facility with a recirculating water system. Embryonic stages were defined morphologically and *Zoep*^{m134} mutants were identified by their cyclopic

phenotype.(Kimmel et al., 1995a) Clutches of embryos from spawnings of single pairs of heterozygous adults were spawned in a 28.5 ºC incubator. At selected hpf, one half of each clutch was moved to a 34 ºC incubator with the same light cycle, while the other half remained in the 28.5 ºC incubator. Embryos were then fixed at approximately 24 hpf.

Whole mount in situ hybridization (WISH)

Expression of *orthodenticle homobox 5* (*otx5*) in the pineal organ was assayed by WISH using established methods.(Chitramuthu and Bennett, 2013; Thisse et al., 2004a; Thisse and Thisse, 2014) Briefly, embryos were incubated with digoxygenin-labeled antisense RNA probe overnight at 70 ºC in hybridization solution containing 50% formamide. The probe was then detected with an anti-digoxygenin antibody that was covalently linked to the enzyme Alkaline Phosphatase. The cells containing otx5 mRNA were visualized by adding the alkaline phosphatase substrates 4-nitro blue tetrazonium (NBT) and 5-bromo-4-chloro-3-indolyl-phosphate (BCIP), which were transformed into a purple substrate.

Analysis

Bright field images of the dorsal side of the embryos heads were taken with a SPOT Insight Fire Wire camera mounted on a Nikon Eclipse 80i microscope. They were then scored on whether they had the normal oval shaped pineal or an

abnormal divided or elongated pineal morphology. (Aquilina-Beck et al., 2007) ANOVA with JMP 10 software was used to determine whether there was a significant difference in the percentage of embryos with an open neural tube among embryos raised at different temperatures, embryos moved to 34 ºC at different developmental time points, and embryos from different clutches with different parents.

Results

Penetrance of open neural tube phenotype increases in Zoep embryos exposed to 34 °C

Although many aspects of the Z*oep* phenotype, such as cyclopia, are present in all mutant embryos, our previous work indicated that the open neural tube phenotype in Z*oep* embryos is incompletely penetrant (Lu et al., 2013). Even siblings from the same clutch could differ in whether they had an open neural tube and in the severity of the neural tube defect. Since environmental temperature can affect the penetrance of the mutant phenotypes in *sqt* mutants (Pei and Feldman, 2009; Pei et al., 2007), which lack one of the ligands for receptor complex containing the Oep protein, we hypothesized that temperature was also affecting the penetrance of the neural tube phenotype in Z*oep* embryos.

In our first test of this hypothesis, during the summer of 2012, progeny from single pairs of *oep*^{m134}/+ adults were divided into two halves and placed in a 28.5 °C incubator within the first few hpf. At different points in development, one

half of the progeny was moved to 34 °C, a temperature that increased the penetrance of the cyclopic phenotype in *sqt* mutants (Pei and Feldman, 2009; Pei et al., 2007). These time points included 0-2 hpf (cleavage stages), 2-4 hpf (early-mid blastula), 4-6 hpf (mid blastula to early gastrula), 6-8 hpf (early-mid gastrula), and after 8 hpf (mid-gastrula onwards). The embryos were fixed at approximately 24 hpf and processed for expression of the pineal marker *otx5*. Our previous work indicated that the morphology of the pineal organ accurately reports the extent of closure of the anterior neural tube, with an oval pineal morphology indicating a closed neural tube and an elongated or divided pineal morphology indicating an open neural tube (Figure 1)(Aquilina-Beck et al., 2007).

We found that that embryos moved to 34 °C had a significantly greater penetrance of the open neural tube phenotype than embryos raised only at 28.5 °C (Figure 2). However, the pattern of this effect was hard to match to the biology. For instance, the temperature effect was present even when the embryos were moved to the higher temperature after 8 hpf, even though this was after the anterior neural tube has already closed (Table 1; Supplemental Table 1). Further, the percentage of embryos with open neural tubes varied greatly among clutches, even when only the embryos maintained at 28.5 °C were considered (Figure 3). Thus, we were concerned that the clutches with high penetrance of NTD might have been cold-shocked during their time in the fish facility, which typically has an air temperature of 25 °C. Pei et al. (2007) reported

that the cyclopic phenotype of *sqt* mutants also increased when embryos are cold shocked (15 °C).

Because of this concern, we changed our experimental design. In our new design, adults were spawned in the 28.5 °C incubator instead of the fish facility, ensuring that the embryos would be at 28.5 °C from the time of fertilization. The large variation in the penetrance of NTD persisted in the embryos raised at 28.5 °C even in this experimental design (Figure 3; Supplemental Table 1). Consistent with the results of others, the cyclopic phenotype was completely penetrant, however there was variation in the shape of the head and in the placement and morphology of the eye (Figure 4).

To determine the influences on open neural tube penetrance, the data from this new experimental design were analyzed by three way ANOVA, with temperature, the stage embryos were split between 28.5 °C and 34 °C, and clutch number/parentage as the variables, and with the 28.5 °C and 34 °C data from the same clutch paired. This model accounted for a large portion of the variation in the penetrance in the neural tube phenotype, as $R^2 = 0.78$, meaning 78% of the variation in penetrance of the open neural tube phenotype is explained by considering the three variables. Consideration of the three variables within the model indicated that temperature (P=0.016) and clutch number (P= 0.0081) had significant contributions to the penetrance of the open neural tube phenotype. There was no significant interaction between temperature and stage of treatment when all of the data were considered together (P=0.5274). However,

this interaction approached significance for the two earliest developmental periods tested when embryos were split between 28.5 and 34 °C between 0-2 and 2-4 hpf (Figure 5, Table 2; Supplemental Table 1). The results were very different when the data from summer 2012 were included, suggesting the colder fish facility temperatures affected these embryos (Supplemental Table 2). Together, these data suggest that the temperature effect largely or completely occurred during the first four hours of development, corresponding to cleavage stages to mid-blastula stages.

Discussion

In this study, a team of undergraduate students used classical genetics and statistics to parse out individual factors contributing to the penetrance of defects in the complex process of neurulation. Three-way ANOVA indicated that genetic background/clutch number and environmental temperature had significant contributions to the penetrance of NTD. Like *Zoep*, the penetrance of the cyclopic and MB in MZ*sqt* were dependent on temperature and genetic background. Further, the temperature sensitive period is very similar between the cyclopic and neural tube phenotypes, suggesting the penetrance of these phenotypes is caused by the same underlying mechanism.

Comparison of sqt and Zoep mutants.

In their studies of MZ*sqt* embryos, Pei et al. (2007, 2009) found that the penetrance of the cyclopic and MB phenotypes are temperature dependent, but the temperature sensitive period was different between these two phenotypes. The cyclopic phenotype was affected by a 0.5 hr heat shock at 34 °C before the midblastula transition, which occurs at the 1024 cell stage (3 hpf) or a 1 hr heat treatment between the 1024 cell stage and the onset of gastrulation (3-6 hpf). This is very similar to our finding that moving *Zoep* embryos to 34 °C before sphere stage (4 hpf), caused an increase in penetrance of the neural tube phenotype that approached significance (P=0.066 for movement between 0-2 hpf, and P=0.057 for movement between 2-4 hpf). This raises the possibility that the same underlying defect is responsible for both phenotypes.

The strongest possibility is that higher temperatures are affecting development of the mesoderm and endodermal tissues. First, the timing closely matches the period when Nodal signaling is acting to induce these tissue layers. Studies with small molecular inhibitors of Nodal signaling indicates that Nodal acts between mid-late gastrula stages.(Hagos and Dougan, 2007) Further, separation of the eye field to create two eyes as well as closure of the anterior neural tube have depend upon correct development of mesoderm and mesendoderm (cells that give rise to both mesodermal and endodermal derivatives). For instance, injection of a constitutively activated form of the Nodal receptor subunit Taram-A cell autonomously rescues mesoderm and

mesendoderm formation in MZ*oep* mutants while also correcting their open neural tube defect.(Aquilina-Beck et al., 2007) Similarly, anterior prechordal plate mesendoderm/mesoderm is required for separation of the single primordial eye field of vertebrates into the precursors of the two separated eyes.(Chow and Lang, 2001) Induction of prechordal plate mesendoderm requires some of the highest and longest signaling of the mesendoderm/mesodermal tissues in zebrafish.(Gritsman et al., 1999; Hagos et al., 2007; Thisse and Thisse, 1999) Since the temperature sensitive period is shorter for open neural tube phenotypes, a tissue other than prechordal plate is probably involved.

Temperature effects on human neural tube defects

There is some suggestion that temperature sensitivity is a characteristic of neurulation in many vertebrate species. Exposure to elevated temperatures during development has been associated with increased risk of NTD in humans and mammalian model systems such as mice, hamsters, and even chicks.(Buckiova and Brown, 1999; Buckiova et al., 1998; Dreier et al., 2014; Finnell et al., 1986; Seller and Perkins-Cole, 1987; Zhang et al., 2012) Recent meta-analysis of human studies indicate that maternal fever during the first trimester of pregnancy significantly increases the incidence of several birth defects, including NTD, congenital heart defects, and oral clefts.(Dreier et al., 2014; Moretti et al., 2005) These studies also provide a potential link between temperature sensitivity and Nodal signaling. Oral clefts in humans are associated

with mutations in the Nodal pathway gene TG Interacting Factor (TFIG), and are part of a larger syndrome called holoprosencephaly, which occurs when the left and right hemispheres of the brain failing to properly separate.(Gripp et al., 2000) The cyclopic phenotype in zebrafish with defects in Nodal signaling, including *Zoep* and *sqt* mutants, is also part of a holoprosencephaly disorder. Thus, many aspects of the temperature sensitive phenotype is shared between zebrafish and mammals, suggesting that zebrafish could serve as a model system for defining the interactions between genetics and environment that contribute to NTD.

The factors causing temperature sensitivity of the neural tube phenotype in humans or zebrafish have not yet been definitively identified. The studies of Pei et al. (2009) indicate that the temperature sensitive factor is unlikely to be Sqt itself, as the temperature sensitivity persists in MZ*sqt*$^{hi975/hi975}$ mutants, which lack all functional Sqt protein. However, they did find that depletion of Heat Shock Protein 90 family members caused increased penetrance of both the cyclopic phenotype (HSP90a depletion) and MB phenotype (HSP90a and HSP90b depletion) in MZ*sqt* embryos.(Pei and Feldman, 2009; Pei et al., 2007) Similarly, targeted deletion of the Hsp70 family members in mice increased the penetrance of the anterior open neural tube defect exencephaly.(Barrier et al., 2009) Heat shock proteins are upregulated dramatically in responses to stress because they act to stabilize unfolded proteins and prevent protein aggregation. This suggests there is an unknown protein or proteins involved in neural tube closure that

become unfolded or misfolded upon heat shock, and these proteins could be conserved between zebrafish and mammals.

ANOVA indicated that genetic background had a significant contribution to the incomplete penetrance of the open neural tube phenotype independently of temperature. This is also consistent with studies of MZ*sqt* mutants, which found that penetrance of the cyclopic and MB phenotypes were fairly constant upon repeated spawning of the same parental pair of parents. Defects in the Wnt signaling pathway caused increased penetrance of cyclopia (Wnt5b depletion) and the MB phenotypes (Wnt11 depletion) in MZ*sqt* embryos, suggesting that variations in the expression of Wnt pathway could influence the penentrance of these phenotypes.(Pei and Feldman, 2009) Making a potential connection in neurulation, non-cononical Wnt signaling is a key regulator of the convergent-extension movements that shape the neural plate, the precursor to the neural tube.(Gray et al., 2011) In mice and *Xenopus*, deficient Wnt signaling causes the neural plate to become widened, and consequently it fails to close.(Ueno and Greene, 2003) Mutations in a number of Wnt pathway genes have also been linked to neural tube defects in humans.(Cai and Shi, 2014) However, in zebrafish, loss of Wnt signaling causes a widening of the neural tube, but the neural tube is still able to close.(Ciruna et al., 2006; Tawk et al., 2007) Thus, an important next will be to determine if loss of Wnt signaling increases the penetrance of NTD in zebrafish Nodal signaling mutants.

Table 1: Penetrance of open neural tube phenotype increases in *Zoep* embryos that are exposed to temperatures outside of their ideal of 28.5 °C.

Temperature	Time embryos were split between 28.5 °C and 34 °C			
	0-2 hpf	2-4 hpf	4-6 hpf	8+ hpf
28.5 °C	31.3±27.5	17.4±29.6	3.6±5.0	20.7±2.9
34 °C	24.9±9.5	62.2±15.0	24.9±9.5	32.3±20.8
number of clutches	3	6	2	3

*Some of the clutches were at approximately 25 °C for the first few hpf.

Table 2: Penetrance of open neural tube phenotype increases when *Zoep* embryos are exposed to high temperatures before 4 hpf.

Temperature	Time embryos were split between 28.5 °C and 34 °C				
	0-2 hpf	2-4 hpf	4-6 hpf	6-8 hpf	8+ hpf
28.5 °C	49.7 + 42.3	31.9 + 32.9	22.9 + 32.2	14.1 + 19.3	32.0+ 32.5
34 °C	75.3 + 19.4	48.1 + 34.8	50.5 + 12.8	4.2 + 8.4	42.9 + 21.3
number of clutches	6	16	5	4	6
P value	0.066	0.057	0.1483	0.5507	0.4235

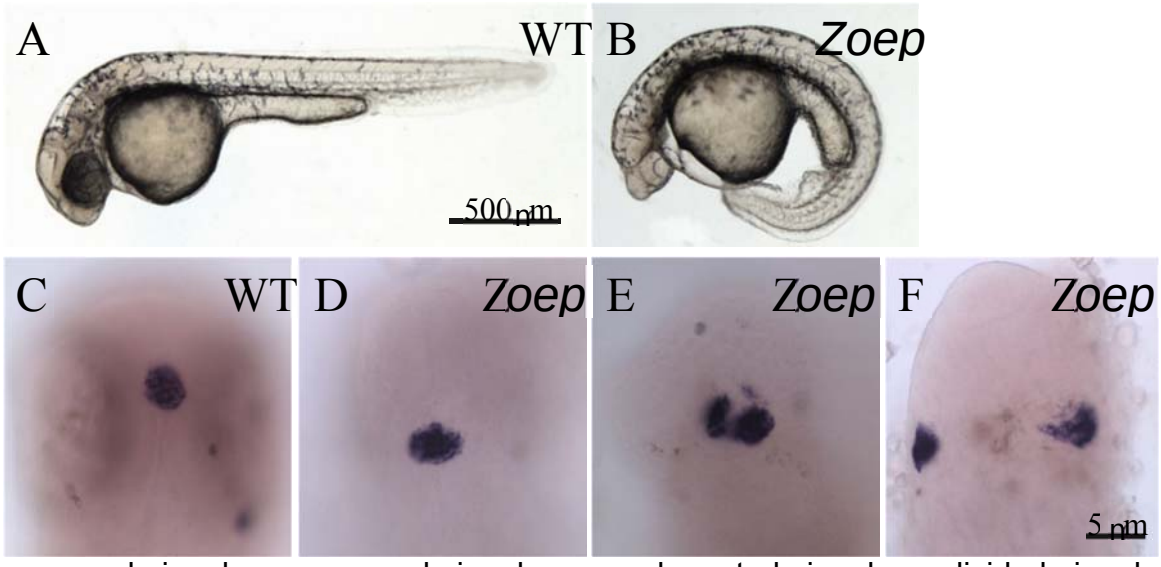

Figure 1: Pineal morphology reports anterior neural tube defect in zebrafish embryos. A. A WT zebrafish embryo has a round shaped head and a straight body axis. **B.** In contrast, an **Z***oep* mutant embryo has a pointed head and a curved body axis. **C.** In WT embryos, the pineal organ forms a single, oval-shaped domain in the center of the dorsal forebrain. **D.** In some *Zoep* mutant embryos, the pineal has an oval shape, indicating the neural tube is closed. **(E., F.)** In other *Zoep* mutants, the pineal is elongated or divided into two domains indicating the anterior neural tube is open. Dorsal views of embryos at approximately 24 hpf processed for expression of *otx5* in the pineal organ.

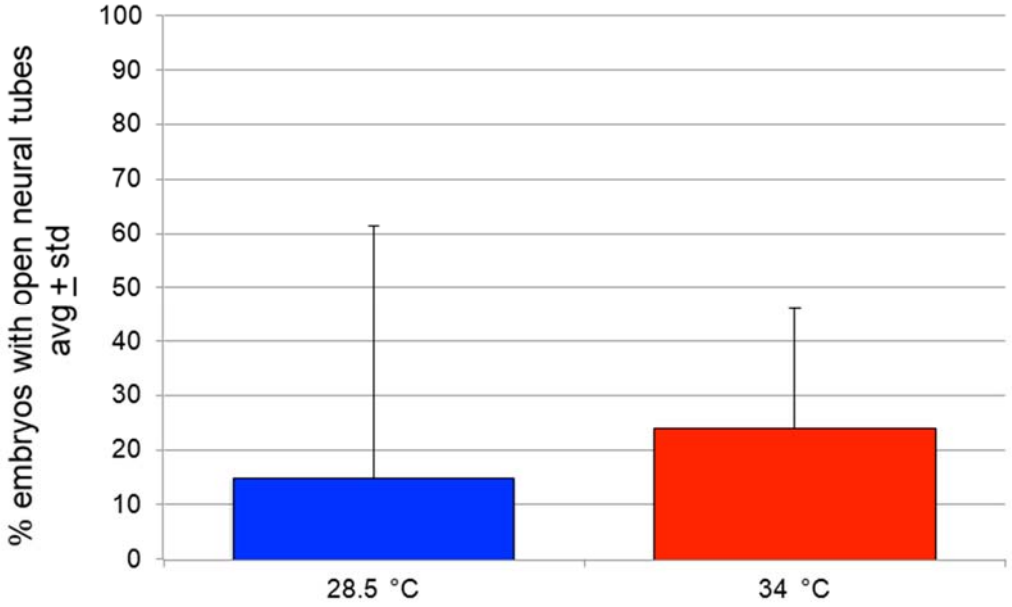

Figure 2: Penetrance of open neural tube phenotype is slightly higher in embryos born in fish facility and then raised at 34 °C. The average percentage of Z*oep* embryos in a clutch with an open neural tube phenotype was slightly higher in embryos raised at 34 °C than at 28.5 °C. However, these data, collected during the summer of 2012, may be confounded by the fact that the fish may have been cold shocked by spending the first few hours post-fertilization in the fish facility at ~25 °C.

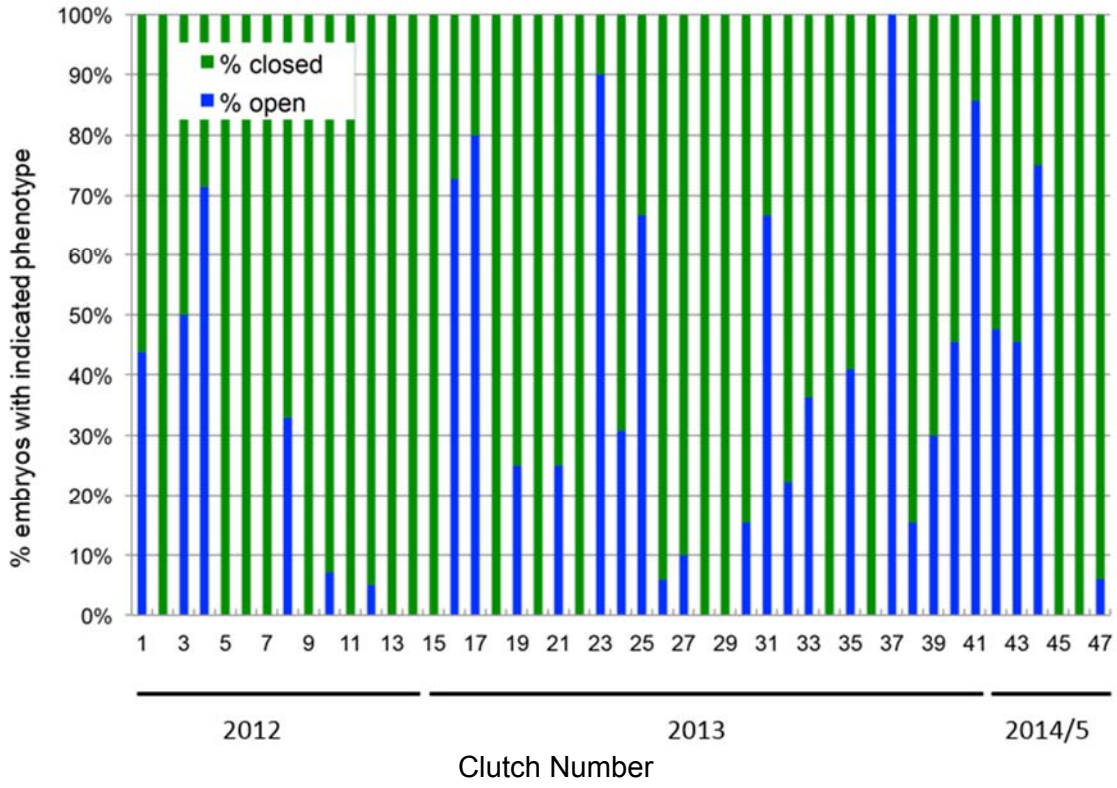

Figure 3: Variation in penetrance in open neural tube phenotype in clutches raised at 28.5 °C. The percentage of *Zoep* embryos with an open neural tube phenotype varied from 0-100% in different clutches. Note the 2012 data were obtained from fish spawned in the fish facility, and thus potentially cold-shocked during the first few hours of development, while the fish from 2013-15 were spawned in a 28.5 °C incubator. Clutches with ≤ 3 *Zoep* embryos were omitted from the graph.

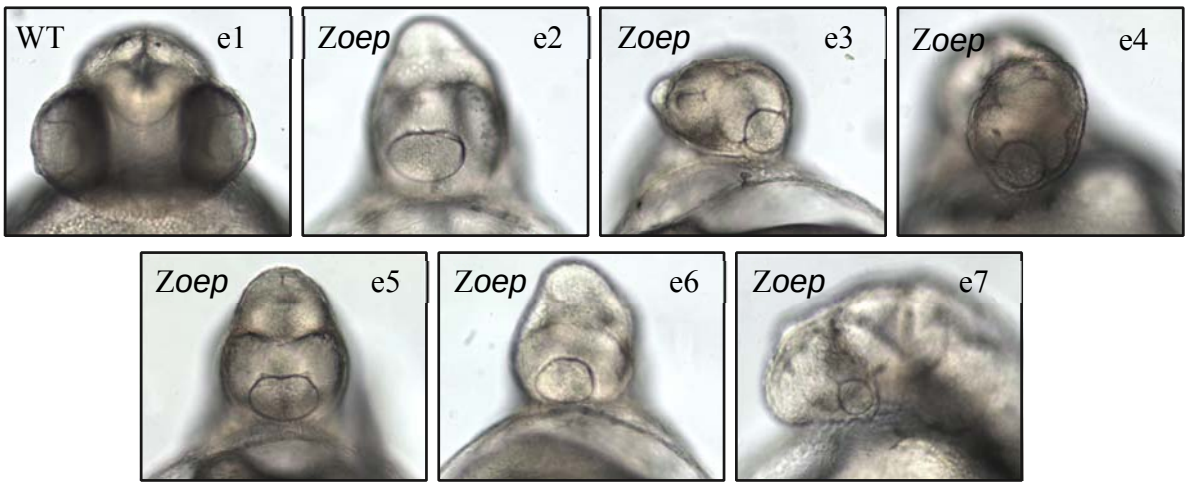

Figure 4: Variation in eye phenotype among zebrafish embryos from the same clutch. Although all of these *Zoep* sibling embryos have a one eye compared to the two eyes in their WT sibling phenotype, the morphology of the head and eye vary. For instance, while the shape of the lens in embryo 5 (e5) is slightly heart-shaped, the lens in e6 is round. The head of e2 has the typical "pin head" shape that the mutant was named for. In e3, this pinhead shape appears to be tipped on its side, similar to the twisted brain phenotype often seen in *sqt* mutants. One *Zoep* embryo from this clutch is not shown as the eye could not be located, suggesting that it was degraded or severely misplaced. Frontal views of live embryos at ~30 hpf.

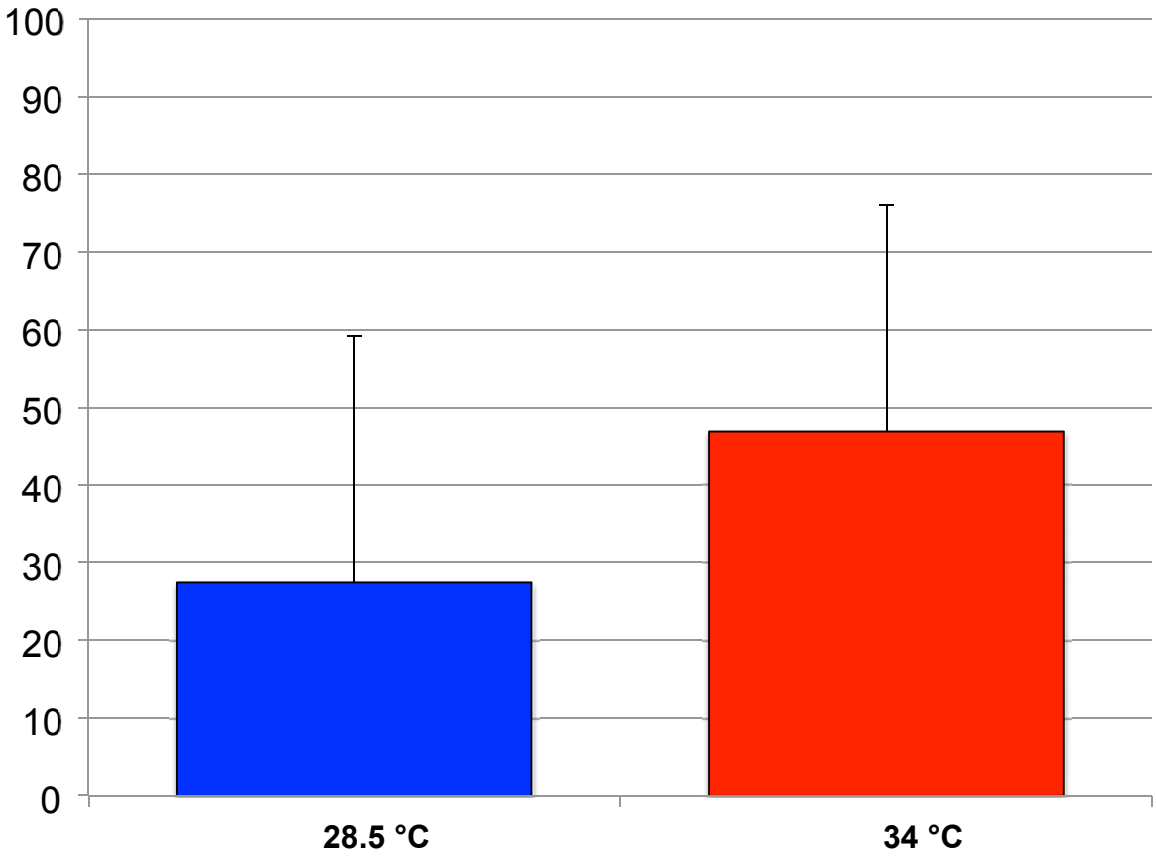

Figure 5: Significant increase in penetrance of open neural tube phenotype in *Zoep* embryos raised at 34 °C. The average percentage of *Zoep* embryos in a clutch with an open neural tube phenotype was significantly higher in embryos raised at 34 °C than at 28.5 °C. This graph includes only data collected during 2013-2015, when fish were spawned in an incubator at 28.5 °C (compare to Figure 2).

Chapter V: Discussion

From these studies, we have filled multiple knowledge gaps in the process of neurulation in zebrafish. First, we found Nodals are required for mesendodermal/mesodermal formation in neurulation up to late blastula stage (dome stage at 4.3 hpf). Previous studies have suggested Nodals work indirectly, probably by inducing mesendodermal/mesodermal tissues, to affect neurulation (Aquilina-Beck et al., 2007). We also found that high temperatures, like those of fever in humans, cause increased penetrance of NTDs in *Zoep* mutants that were exposed to these high temperatures up to mid-blastula stages (0-4 hpf). Downstream of Nodal, we identified multiple candidates for involvement in neurulation. Two of these candidates, FGF signaling and *dkk1b*, a canonical Wnt signaling inhibitor, were shown to be involved in neurulation.

Model for Nodal's role in neurulation

Our recent studies along with previous work from our lab has suggested a model for the role of Nodal in neurulation involving three steps: 1) Mesendodermal/mesodermal tissue is induced by Nodal, 2) The mesendoderm/mesoderm signals the overlying neurectoderm, and 3) This mesendodermal/mesodermal signal promotes proper adhesion between neural tube cells and the neural tube is properly formed.

Step one of our model is probably complete by late blastula stage (30% epiboly stage at 4.7 hpf). Heat sensitivity of the genes playing a role in this NTD

is probably highest before and during step one of our model. FGF signaling could be functioning similar to Nodal and acting to induce the mesendoderm/mesoderm in this step. In support of this, FGFs have been shown to have important roles in mesoderm formation in other studies (Ciruna and Rossant, 2001; Kimelman, 2006). Also, expression patterns of the FGF candidates present in our RNA-sequencing data (*fgf8a* and *fgf17b*) and their receptors could fit activity instep one of our model. *fgf8a* is expressed in mesoderm/mesendoderm and the forebrain neural rod and neural tube and *fgf17b* is expressed in the presumptive dorsal mesoderm in zebrafish (Reifers et al., 1998; Shimizu et al., 2006; Thisse and Thisse, 2004; Warga et al., 2013). In zebrafish, FGFR3c binds members of the FGF8 subfamily (which includes FGF17b) and FGF8 has been shown to bind to FGFR1 and FGFR4 (Ota et al., 2009; Ries et al., 2009). *fgfr3* is expressed in the axial mesoderm and neural plate at 6 and 10 hpf, in the anterior hindbrain at 11 hpf, and in the hindbrain neural rod and otic placode at 5-9 somites (Esterberg and Fritz, 2009; Sleptsova-Friedrich et al., 2001). *fgfr4* expression is first detected prior to gastrulation in the prechordal plate mesoderm and while later it is expressed in the forebrain, anterior hindbrain, and caudal hindbrain as well as in the dorsal-most portion of the rostral spinal cord (Thisse et al., 1995). *fgfr1* is expressed in the whole zebrafish embryo until 5-13 somites stages where expression is restricted to the forebrain, hindbrain and midbrain hindbrain boundary of the neural rod, the segmental plate, and somites (Rohner et al., 2009).

Based on these expression patterns, it is also possible that FGFs are working in the second step of our model to signal the overlying neurectoderm. This step is also likely when *dkk1b* in the canonical Wnt signaling pathway is working. *dkk1b* is expressed in the presumptive mesendoderm in zebrafish. In *Xenopus laevis*, *dkk1b* signals from the endomesoderm to the overlying neuroepithelium (De Robertis et al., 2000; Monaghan et al., 1999; Shinya et al., 2000). If *dkk1b* signals similarly in zebrafish as in *Xenopus laevis*, *dkk1b* could be a signal from the mesendoderm/mesoderm in step two of our model. In support of this, Hashimoto et al. 2000 found that *dkk1* expression was reduced and could not be detected in the embryonic shield or late in the anterior axial mesendoderm in zebrafish *sqt*^{cz35} and *oep*^{tz57} mutants (Hashimoto et al., 2000).

Our RNA-sequencing data also showed differential expression of members of the tight-junction and adherens junction pathways. Members of these pathways could be acting in proper adhesion of neural tube cells and step three of our model.

Potential future directions

In the future, we have many directions of further investigation based on our recent studies. For the *Zoep* study, we could further investigate if the genetic background of a mating pair of *Zoep* mutants does affect how much the penetrance of the NTD increases with heat shock. For the other studies, future directions overlap. One idea is to analyze the temporal requirement of

FGF and canonical Wnt signaling in neurulation. We could also determine if Wnts, Nodals, and FGFs are working together in any portion of neurulation. Analyzing knockdown or knockout of single members of the FGF signaling pathway would help us determine specific FGFs involved in neurulation. Since so many transcripts were differentially expressed in our RNA-sequencing screen, another direction of future study would be to test more of these transcripts for potential involvement in neurulation. For example, we could test *tbx1* which was one of the most highly differentially expressed transcripts with higher expression in embryos that would have a closed neural tube in all three stages that we sequenced. We could also test some of the transcripts encoding portions of the adhesion pathways. Along with investigating new candidates for involvement in neurulation, we could analyze where the differences in expression are occurring spatially in our SB505124 treated embryos. Overall, our research has suggested many ideas for further investigation.

Bibliography

1991. Prevention of neural tube defects: results of the Medical Research Council Vitamin Study. MRC Vitamin Study Research Group. Lancet 338, 131-137.
Aanes, H., Winata, C.L., Lin, C.H., Chen, J.P., Srinivasan, K.G., Lee, S.G., Lim, A.Y., Hajan, H.S., Collas, P., Bourque, G., Gong, Z., Korzh, V., Aleström, P., Mathavan, S., 2011. Zebrafish mRNA sequencing deciphers novelties in transcriptome dynamics during maternal to zygotic transition. Genome Res 21, 1328-1338.
Agius, E., Oelgeschläger, M., Wessely, O., Kemp, C., De Robertis, E.M., 2000. Endodermal Nodal-related signals and mesoderm induction in Xenopus. Development 127, 1173-1183.
Alexander, J., Stainier, D.Y., 1999. A molecular pathway leading to endoderm formation in zebrafish. Curr Biol 9, 1147-1157.
Aman, A., Piotrowski, T., 2008. Wnt/beta-catenin and Fgf signaling control collective cell migration by restricting chemokine receptor expression. Dev Cell 15, 749-761.
Anders, S., Huber, W., 2010. Differential expression analysis for sequence count data. Genome Biol 11, R106.
Anders, S., Huber, W., 2013. Differential expression of RNA-Seq data at the gene level-the DESeq package.
Aquilina-Beck, A., Ilagan, K., Liu, Q., Liang, J.O., 2007. Nodal signaling is required for closure of the anterior neural tube in zebrafish. BMC Dev Biol 7, 126.
Araya, C., Tawk, M., Girdler, G.C., Costa, M., Carmona-Fontaine, C., Clarke, J.D., 2014. Mesoderm is required for coordinated cell movements within zebrafish neural plate in vivo. Neural Dev 9, 9.
Au, K.S., Ashley-Koch, A., Northrup, H., 2010. Epidemiologic and genetic aspects of spina bifida and other neural tube defects. Dev Disabil Res Rev 16, 6-15.
Bamforth, S.D., Bragança, J., Eloranta, J.J., Murdoch, J.N., Marques, F.I., Kranc, K.R., Farza, H., Henderson, D.J., Hurst, H.C., Bhattacharya, S., 2001. Cardiac malformations, adrenal agenesis, neural crest defects and exencephaly in mice lacking Cited2, a new Tfap2 co-activator. Nat Genet 29, 469-474.
Barrier, M., Dix, D.J., Mirkes, P.E., 2009. Inducible 70 kDa heat shock proteins protect embryos from teratogen-induced exencephaly: Analysis using Hspa1a/a1b knockout mice. Birth Defects Res A Clin Mol Teratol 85, 732-740.
Beaudin, A.E., Abarinov, E.V., Noden, D.M., Perry, C.A., Chu, S., Stabler, S.P., Allen, R.H., Stover, P.J., 2011. Shmt1 and de novo thymidylate biosynthesis underlie folate-responsive neural tube defects in mice. Am J Clin Nutr 93, 789-798.
Benjamini, Y., Drai, D., Elmer, G., Kafkafi, N., Golani, I., 2001. Controlling the false discovery rate in behavior genetics research. Behav Brain Res 125, 279-284.
Blom, H.J., Shaw, G.M., den Heijer, M., Finnell, R.H., 2006. Neural tube defects and folate: case far from closed. Nat Rev Neurosci 7, 724-731.
Bökel, C., Brand, M., 2013. Generation and interpretation of FGF morphogen gradients in vertebrates. Curr Opin Genet Dev 23, 415-422.
Bouzaffour, M., Dufourcq, P., Lecaudey, V., Haas, P., Vriz, S., 2009. Fgf and Sdf-1 pathways interact during zebrafish fin regeneration. PLoS One 4, e5824.

Buckiova, D., Brown, N.A., 1999. Mechanism of hyperthermia effects on CNS development: rostral gene expression domains remain, despite severe head truncation; and the hindbrain/otocyst relationship is altered. Teratology 59, 139-147.
Buckiova, D., Kubinova, L., Soukup, A., Jelinek, R., Brown, N.A., 1998. Hyperthermia in the chick embryo: HSP and possible mechanisms of developmental defects. Int J Dev Biol 42, 737-740.
Cai, C., Shi, O., 2014. Genetic evidence in planar cell polarity signaling pathway in human neural tube defects. Front Med 8, 68-78.
Caneparo, L., Huang, Y.L., Staudt, N., Tada, M., Ahrendt, R., Kazanskaya, O., Niehrs, C., Houart, C., 2007. Dickkopf-1 regulates gastrulation movements by coordinated modulation of Wnt/beta catenin and Wnt/PCP activities, through interaction with the Dally-like homolog Knypek. Genes Dev 21, 465-480.
Carmichael, S.L., Rasmussen, S.A., Shaw, G.M., 2010. Prepregnancy obesity: a complex risk factor for selected birth defects. Birth Defects Res A Clin Mol Teratol 88, 804-810.
Chen, J.N., Haffter, P., Odenthal, J., Vogelsang, E., Brand, M., van Eeden, F.J., Furutani-Seiki, M., Granato, M., Hammerschmidt, M., Heisenberg, C.P., Jiang, Y.J., Kane, D.A., Kelsh, R.N., Mullins, M.C., Nusslein-Volhard, C., 1996. Mutations affecting the cardiovascular system and other internal organs in zebrafish. Development 123, 293-302.
Chen, Z.F., Behringer, R.R., 1995. twist is required in head mesenchyme for cranial neural tube morphogenesis. Genes Dev 9, 686-699.
Chitramuthu, B.P., Bennett, H.P., 2013. High resolution whole mount in situ hybridization within zebrafish embryos to study gene expression and function. J Vis Exp, e50644.
Chow, R.L., Lang, R.A., 2001. Early eye development in vertebrates. Annu Rev Cell Dev Biol 17, 255-296.
Chowanadisai, W., Graham, D.M., Keen, C.L., Rucker, R.B., Messerli, M.A., 2013. A zinc transporter gene required for development of the nervous system. Commun Integr Biol 6, e26207.
Ciruna, B., Jenny, A., Lee, D., Mlodzik, M., Schier, A.F., 2006. Planar cell polarity signalling couples cell division and morphogenesis during neurulation. Nature 439, 220-224.
Ciruna, B., Rossant, J., 2001. FGF signaling regulates mesoderm cell fate specification and morphogenetic movement at the primitive streak. Dev Cell 1, 37-49.
Clark, D.P., Pazdernik, N.J., 2016. Biotechnology: Applying the Genetic Revolution, 2 ed. Academic Cell Publications, Elsevier Inc.
Colas, J.F., Schoenwolf, G.C., 2001. Towards a cellular and molecular understanding of neurulation. Dev Dyn 221, 117-145.
Copp, A.J., Greene, N.D., Murdoch, J.N., 2003a. The genetic basis of mammalian neurulation. Nat Rev Genet 4, 784-793.
Copp, A.J., Greene, N.D.E., Murdoch, J.N., 2003b. The genetic basis of mammalian neurulation. Nature Reviews Genetics 4, 784-793.
Copp, A.J., Stanier, P., Greene, N.D., 2013. Neural tube defects: recent advances, unsolved questions, and controversies. Lancet Neurol 12, 799-810.

Correa, A., Gilboa, S.M., Besser, L.M., Botto, L.D., Moore, C.A., Hobbs, C.A., Cleves, M.A., Riehle-Colarusso, T.J., Waller, D.K., Reece, E.A., 2008. Diabetes mellitus and birth defects. Am J Obstet Gynecol 199, 237.e231-239.
Czeizel, A.E., Dudás, I., 1992. Prevention of the first occurrence of neural-tube defects by periconceptional vitamin supplementation. N Engl J Med 327, 1832-1835.
DaCosta Byfield, S., Major, C., Laping, N.J., Roberts, A.B., 2004. SB-505124 is a selective inhibitor of transforming growth factor-beta type I receptors ALK4, ALK5, and ALK7. Mol Pharmacol 65, 744-752.
Dale, L., Jones, C.M., 1999. BMP signalling in early Xenopus development. Bioessays 21, 751-760.
David, N.B., Rosa, F.M., 2001. Cell autonomous commitment to an endodermal fate and behaviour by activation of Nodal signalling. Development 128, 3937-3947.
Davidson, L.A., Keller, R.E., 1999. Neural tube closure in Xenopus laevis involves medial migration, directed protrusive activity, cell intercalation and convergent extension. Development 126, 4547-4556.
De Robertis, E.M., Kuroda, H., 2004. Dorsal-ventral patterning and neural induction in Xenopus embryos. Annu Rev Cell Dev Biol 20, 285-308.
De Robertis, E.M., Larraín, J., Oelgeschläger, M., Wessely, O., 2000. The establishment of Spemann's organizer and patterning of the vertebrate embryo. Nat Rev Genet 1, 171-181.
De Wals, P., Tairou, F., Van Allen, M.I., Uh, S.H., Lowry, R.B., Sibbald, B., Evans, J.A., Van den Hof, M.C., Zimmer, P., Crowley, M., Fernandez, B., Lee, N.S., Niyonsenga, T., 2007. Reduction in neural-tube defects after folic acid fortification in Canada. N Engl J Med 357, 135-142.
Deng, C., Bedford, M., Li, C., Xu, X., Yang, X., Dunmore, J., Leder, P., 1997. Fibroblast growth factor receptor-1 (FGFR-1) is essential for normal neural tube and limb development. Dev Biol 185, 42-54.
Detrait, E.R., George, T.M., Etchevers, H.C., Gilbert, J.R., Vekemans, M., Speer, M.C., 2005. Human neural tube defects: developmental biology, epidemiology, and genetics. Neurotoxicol Teratol 27, 515-524.
Dougan, S.T., Warga, R.M., Kane, D.A., Schier, A.F., Talbot, W.S., 2003. The role of the zebrafish nodal-related genes squint and cyclops in patterning of mesendoderm. Development 130, 1837-1851.
Dreier, J.W., Andersen, A.M., Berg-Beckhoff, G., 2014. Systematic review and meta-analyses: fever in pregnancy and health impacts in the offspring. Pediatrics 133, e674-688.
Elworthy, S., Hargrave, M., Knight, R., Mebus, K., Ingham, P.W., 2008. Expression of multiple slow myosin heavy chain genes reveals a diversity of zebrafish slow twitch muscle fibres with differing requirements for Hedgehog and Prdm1 activity. Development 135, 2115-2126.
Esterberg, R., Fritz, A., 2009. dlx3b/4b are required for the formation of the preplacodal region and otic placode through local modulation of BMP activity. Dev Biol 325, 189-199.

Feldman, B., Gates, M.A., Egan, E.S., Dougan, S.T., Rennebeck, G., Sirotkin, H.I., Schier, A.F., Talbot, W.S., 1998. Zebrafish organizer development and germ-layer formation require nodal-related signals. Nature 395, 181-185.
Finnell, R.H., Moon, S.P., Abbott, L.C., Golden, J.A., Chernoff, G.F., 1986. Strain differences in heat-induced neural tube defects in mice. Teratology 33, 247-252.
Fletcher, R.B., Baker, J.C., Harland, R.M., 2006. FGF8 spliceforms mediate early mesoderm and posterior neural tissue formation in Xenopus. Development 133, 1703-1714.
Flowers, G.P., Topczewska, J.M., Topczewski, J., 2012. A zebrafish Notum homolog specifically blocks the Wnt/β-catenin signaling pathway. Development 139, 2416-2425.
Gamse, J.T., Shen, Y.C., Thisse, C., Thisse, B., Raymond, P.A., Halpern, M.E., Liang, J.O., 2002. Otx5 regulates genes that show circadian expression in the zebrafish pineal complex. Nat Genet 30, 117-121.
Gamse, J.T., Thisse, C., Thisse, B., Halpern, M.E., 2003. The parapineal mediates left-right asymmetry in the zebrafish diencephalon. Development 130, 1059-1068.
Glinka, A., Wu, W., Delius, H., Monaghan, A.P., Blumenstock, C., Niehrs, C., 1998. Dickkopf-1 is a member of a new family of secreted proteins and functions in head induction. Nature 391, 357-362.
Gonsar, N., Coughlin, A., Clay-Wright, J., Borg, B., Kindt, L., Liang, J., Temporal and spatial requirements for Nodal-induced anterior mesendoderm and mesoderm in anterior neurulation.
Goodrich, L.V., Milenković, L., Higgins, K.M., Scott, M.P., 1997. Altered neural cell fates and medulloblastoma in mouse patched mutants. Science 277, 1109-1113.
Gray, R.S., Roszko, I., Solnica-Krezel, L., 2011. Planar cell polarity: coordinating morphogenetic cell behaviors with embryonic polarity. Dev Cell 21, 120-133.
Griffith, C.M., Wiley, M.J., Sanders, E.J., 1992. The vertebrate tail bud: three germ layers from one tissue. Anat Embryol (Berl) 185, 101-113.
Grinblat, Y., Gamse, J., Patel, M., Sive, H., 1998. Determination of the zebrafish forebrain: induction and patterning. Development 125, 4403-4416.
Gripp, K.W., Wotton, D., Edwards, M.C., Roessler, E., Ades, L., Meinecke, P., Richieri-Costa, A., Zackai, E.H., Massague, J., Muenke, M., Elledge, S.J., 2000. Mutations in TGIF cause holoprosencephaly and link NODAL signalling to human neural axis determination. Nat Genet 25, 205-208.
Gritsman, K., Zhang, J., Cheng, S., Heckscher, E., Talbot, W.S., Schier, A.F., 1999. The EGF-CFC protein one-eyed pinhead is essential for nodal signaling. Cell 97, 121-132.
Hagos, E.G., Dougan, S.T., 2007. Time-dependent patterning of the mesoderm and endoderm by Nodal signals in zebrafish. BMC Dev Biol 7, 22.
Hagos, E.G., Fan, X., Dougan, S.T., 2007. The role of maternal Activin-like signals in zebrafish embryos. Dev Biol 309, 245-258.
Hakem, R., Hakem, A., Duncan, G.S., Henderson, J.T., Woo, M., Soengas, M.S., Elia, A., de la Pompa, J.L., Kagi, D., Khoo, W., Potter, J., Yoshida, R., Kaufman, S.A., Lowe, S.W., Penninger, J.M., Mak, T.W., 1998. Differential requirement for caspase 9 in apoptotic pathways in vivo. Cell 94, 339-352.

Halpern, M.E., Liang, J.O., Gamse, J.T., 2003. Leaning to the left: laterality in the zebrafish forebrain. Trends Neurosci 26, 308-313.
Harris, M.J., Juriloff, D.M., 2007. Mouse mutants with neural tube closure defects and their role in understanding human neural tube defects. Birth Defects Res A Clin Mol Teratol 79, 187-210.
Harris, M.J., Juriloff, D.M., 2010. An update to the list of mouse mutants with neural tube closure defects and advances toward a complete genetic perspective of neural tube closure. Birth Defects Res A Clin Mol Teratol 88, 653-669.
Harvey, S.A., Sealy, I., Kettleborough, R., Fenyes, F., White, R., Stemple, D., Smith, J.C., 2013. Identification of the zebrafish maternal and paternal transcriptomes. Development 140, 2703-2710.
Hashimoto, H., Itoh, M., Yamanaka, Y., Yamashita, S., Shimizu, T., Solnica-Krezel, L., Hibi, M., Hirano, T., 2000. Zebrafish Dkk1 functions in forebrain specification and axial mesendoderm formation. Dev Biol 217, 138-152.
Hatta, K., Kimmel, C.B., Ho, R.K., Walker, C., 1991. The cyclops mutation blocks specification of the floor plate of the zebrafish central nervous system. Nature 350, 339-341.
Hildebrand, J.D., Soriano, P., 1999. Shroom, a PDZ domain-containing actin-binding protein, is required for neural tube morphogenesis in mice. Cell 99, 485-497.
Huang, d.W., Sherman, B.T., Lempicki, R.A., 2009a. Bioinformatics enrichment tools: paths toward the comprehensive functional analysis of large gene lists. Nucleic Acids Res 37, 1-13.
Huang, d.W., Sherman, B.T., Lempicki, R.A., 2009b. Systematic and integrative analysis of large gene lists using DAVID bioinformatics resources. Nat Protoc 4, 44-57.
Huang, Y., Roelink, H., McKnight, G.S., 2002. Protein kinase A deficiency causes axially localized neural tube defects in mice. J Biol Chem 277, 19889-19896.
Imbard, A., Benoist, J.F., Blom, H.J., 2013. Neural tube defects, folic acid and methylation. Int J Environ Res Public Health 10, 4352-4389.
Isaacs, H.V., 1997. New perspectives on the role of the fibroblast growth factor family in amphibian development. Cell Mol Life Sci 53, 350-361.
Johnson, D.E., Williams, L.T., 1993. Structural and functional diversity in the FGF receptor multigene family. Adv Cancer Res 60, 1-41.
Joyner, A.L., 1996. Engrailed, Wnt and Pax genes regulate midbrain--hindbrain development. Trends Genet 12, 15-20.
Juriloff, D.M., Harris, M.J., 2000. Mouse models for neural tube closure defects. Human molecular genetics 9, 993-1000.
Kappen, C., 2013. Modeling anterior development in mice: diet as modulator of risk for neural tube defects. American journal of medical genetics. Part C, Seminars in medical genetics 163C, 333-356.
Kikuchi, Y., Trinh, L.A., Reiter, J.F., Alexander, J., Yelon, D., Stainier, D.Y., 2000. The zebrafish bonnie and clyde gene encodes a Mix family homeodomain protein that regulates the generation of endodermal precursors. Genes Dev 14, 1279-1289.
Kimelman, D., 2006. Mesoderm induction: from caps to chips. Nat Rev Genet 7, 360-372.

Kimmel, C.B., Ballard, W.W., Kimmel, S.R., Ullmann, B., Schilling, T.F., 1995a. Stages of Embryonic Development of the Zebrafish. Developmental Dynamics 203, 253-310.
Kimmel, C.B., Ballard, W.W., Kimmel, S.R., Ullmann, B., Schilling, T.F., 1995b. Stages of embryonic development of the zebrafish. Dev Dyn 203, 253-310.
Kimmel, C.B., Warga, R.M., Schilling, T.F., 1990. Origin and organization of the zebrafish fate map. Development 108, 581-594.
Klingseisen, A., Clark, I.B., Gryzik, T., Müller, H.A., 2009. Differential and overlapping functions of two closely related Drosophila FGF8-like growth factors in mesoderm development. Development 136, 2393-2402.
Komiya, Y., Habas, R., 2008. Wnt signal transduction pathways. Organogenesis 4, 68-75.
Krause, G., Winkler, L., Piehl, C., Blasig, I., Piontek, J., Müller, S.L., 2009. Structure and function of extracellular claudin domains. Ann N Y Acad Sci 1165, 34-43.
Krauss, S., Concordet, J.P., Ingham, P.W., 1993. A functionally conserved homolog of the Drosophila segment polarity gene hh is expressed in tissues with polarizing activity in zebrafish embryos. Cell 75, 1431-1444.
Kuida, K., Haydar, T.F., Kuan, C.Y., Gu, Y., Taya, C., Karasuyama, H., Su, M.S., Rakic, P., Flavell, R.A., 1998. Reduced apoptosis and cytochrome c-mediated caspase activation in mice lacking caspase 9. Cell 94, 325-337.
Kwon, H.J., Bhat, N., Sweet, E.M., Cornell, R.A., Riley, B.B., 2010. Identification of early requirements for preplacodal ectoderm and sensory organ development. PLoS Genet 6, e1001133.
Lakkis, M.M., Golden, J.A., O'Shea, K.S., Epstein, J.A., 1999. Neurofibromin deficiency in mice causes exencephaly and is a modifier for Splotch neural tube defects. Dev Biol 212, 80-92.
Lele, Z., Folchert, A., Concha, M., Rauch, G.J., Geisler, R., Rosa, F., Wilson, S.W., Hammerschmidt, M., Bally-Cuif, L., 2002. parachute/n-cadherin is required for morphogenesis and maintained integrity of the zebrafish neural tube. Development 129, 3281-3294.
Lemay, P., Guyot, M.C., Tremblay, É., Dionne-Laporte, A., Spiegelman, D., Henrion, É., Diallo, O., De Marco, P., Merello, E., Massicotte, C., Désilets, V., Michaud, J.L., Rouleau, G.A., Capra, V., Kibar, Z., 2015. Loss-of-function de novo mutations play an important role in severe human neural tube defects. J Med Genet.
Liang, J.O., Etheridge, A., Hantsoo, L., Rubinstein, A.L., Nowak, S.J., Izpisua Belmonte, J.C., Halpern, M.E., 2000. Asymmetric nodal signaling in the zebrafish diencephalon positions the pineal organ. Development 127, 5101-5112.
Liang, J.O., Rubinstein, A.L., 2003. Patterning of the zebrafish embryo by nodal signals. Curr Top Dev Biol 55, 143-171.
Liedtke, D., Winkler, C., 2008. Midkine-b regulates cell specification at the neural plate border in zebrafish. Dev Dyn 237, 62-74.
Link, V., Shevchenko, A., Heisenberg, C.P., 2006. Proteomics of early zebrafish embryos. BMC Dev Biol 6, 1.
Liu, A., Li, J.Y., Bromleigh, C., Lao, Z., Niswander, L.A., Joyner, A.L., 2003. FGF17b and FGF18 have different midbrain regulatory properties from FGF8b or activated FGF receptors. Development 130, 6175-6185.

Londin, E.R., Niemiec, J., Sirotkin, H.I., 2005. Chordin, FGF signaling, and mesodermal factors cooperate in zebrafish neural induction. Dev Biol 279, 1-19.
Lowery, L.A., Sive, H., 2004. Strategies of vertebrate neurulation and a re-evaluation of teleost neural tube formation. Mech Dev 121, 1189-1197.
Lu, P.N., Lund, C., Khuansuwan, S., Schumann, A., Harney-Tolo, M., Gamse, J.T., Liang, J.O., 2013. Failure in closure of the anterior neural tube causes left isomerization of the zebrafish epithalamus. Dev Biol 374, 333-344.
Luo, H., Liu, X., Wang, F., Huang, Q., Shen, S., Wang, L., Xu, G., Sun, X., Kong, H., Gu, M., Chen, S., Chen, Z., Wang, Z., 2005. Disruption of palladin results in neural tube closure defects in mice. Mol Cell Neurosci 29, 507-515.
Mathieu, J., Barth, A., Rosa, F.M., Wilson, S.W., Peyrieras, N., 2002. Distinct and cooperative roles for Nodal and Hedgehog signals during hypothalamic development. Development 129, 3055-3065.
Milenkovic, L., Goodrich, L.V., Higgins, K.M., Scott, M.P., 1999. Mouse patched1 controls body size determination and limb patterning. Development 126, 4431-4440.
Mohammadi, M., McMahon, G., Sun, L., Tang, C., Hirth, P., Yeh, B.K., Hubbard, S.R., Schlessinger, J., 1997. Structures of the tyrosine kinase domain of fibroblast growth factor receptor in complex with inhibitors. Science 276, 955-960.
Monaghan, A.P., Kioschis, P., Wu, W., Zuniga, A., Bock, D., Poustka, A., Delius, H., Niehrs, C., 1999. Dickkopf genes are co-ordinately expressed in mesodermal lineages. Mech Dev 87, 45-56.
Moretti, M.E., Bar-Oz, B., Fried, S., Koren, G., 2005. Maternal hyperthermia and the risk for neural tube defects in offspring: systematic review and meta-analysis. Epidemiology 16, 216-219.
Morriss-Kay, G., Wood, H., Chen, W.H., 1994. Normal neurulation in mammals. Ciba Found Symp 181, 51-63; discussion 63-59.
Morriss, G.M., Solursh, M., 1978. Regional differences in mesenchymal cell morphology and glycosaminoglycans in early neural-fold stage rat embryos. Journal of embryology and experimental morphology 46, 37-52.
Mukhopadhyay, M., Shtrom, S., Rodriguez-Esteban, C., Chen, L., Tsukui, T., Gomer, L., Dorward, D.W., Glinka, A., Grinberg, A., Huang, S.P., Niehrs, C., Izpisúa Belmonte, J.C., Westphal, H., 2001. Dickkopf1 is required for embryonic head induction and limb morphogenesis in the mouse. Dev Cell 1, 423-434.
Murakami, T., Hijikata, T., Matsukawa, M., Ishikawa, H., Yorifuji, H., 2006. Zebrafish protocadherin 10 is involved in paraxial mesoderm development and somitogenesis. Dev Dyn 235, 506-514.
Niederreither, K., Abu-Abed, S., Schuhbaur, B., Petkovich, M., Chambon, P., Dollé, P., 2002. Genetic evidence that oxidative derivatives of retinoic acid are not involved in retinoid signaling during mouse development. Nat Genet 31, 84-88.
Ogata, H., Goto, S., Sato, K., Fujibuchi, W., Bono, H., Kanehisa, M., 1999. KEGG: Kyoto Encyclopedia of Genes and Genomes. Nucleic Acids Res 27, 29-34.
Olsen, S.K., Li, J.Y., Bromleigh, C., Eliseenkova, A.V., Ibrahimi, O.A., Lao, Z., Zhang, F., Linhardt, R.J., Joyner, A.L., Mohammadi, M., 2006. Structural basis by which

alternative splicing modulates the organizer activity of FGF8 in the brain. Genes Dev 20, 185-198.
Ota, S., Tonou-Fujimori, N., Yamasu, K., 2009. The roles of the FGF signal in zebrafish embryos analyzed using constitutive activation and dominant-negative suppression of different FGF receptors. Mech Dev 126, 1-17.
Paek, H., Gutin, G., Hébert, J.M., 2009. FGF signaling is strictly required to maintain early telencephalic precursor cell survival. Development 136, 2457-2465.
Palstra, A.P., Beltran, S., Burgerhout, E., Brittijn, S.A., Magnoni, L.J., Henkel, C.V., Jansen, H.J., van den Thillart, G.E., Spaink, H.P., Planas, J.V., 2013. Deep RNA sequencing of the skeletal muscle transcriptome in swimming fish. PLoS One 8, e53171.
Pan, Y., Wang, C., Wang, B., 2009. Phosphorylation of Gli2 by protein kinase A is required for Gli2 processing and degradation and the Sonic Hedgehog-regulated mouse development. Dev Biol 326, 177-189.
Parker, S.E., Mai, C.T., Canfield, M.A., Rickard, R., Wang, Y., Meyer, R.E., Anderson, P., Mason, C.A., Collins, J.S., Kirby, R.S., Correa, A., National Birth Defects Prevention, N., 2010. Updated National Birth Prevalence estimates for selected birth defects in the United States, 2004-2006. Birth Defects Res A Clin Mol Teratol 88, 1008-1016.
Pei, W., Feldman, B., 2009. Identification of common and unique modifiers of zebrafish midline bifurcation and cyclopia. Dev Biol 326, 201-211.
Pei, W., Williams, P.H., Clark, M.D., Stemple, D.L., Feldman, B., 2007. Environmental and genetic modifiers of squint penetrance during zebrafish embryogenesis. Dev Biol 308, 368-378.
Pfeffer, P.L., Gerster, T., Lun, K., Brand, M., Busslinger, M., 1998. Characterization of three novel members of the zebrafish Pax2/5/8 family: dependency of Pax5 and Pax8 expression on the Pax2.1 (noi) function. Development 125, 3063-3074.
Pogoda, H.M., Solnica-Krezel, L., Driever, W., Meyer, D., 2000. The zebrafish forkhead transcription factor FoxH1/Fast1 is a modulator of nodal signaling required for organizer formation. Curr Biol 10, 1041-1049.
Ragland, J.W., Raible, D.W., 2004. Signals derived from the underlying mesoderm are dispensable for zebrafish neural crest induction. Dev Biol 276, 16-30.
Raya, A., Izpisúa Belmonte, J.C., 2004. Sequential transfer of left-right information during vertebrate embryo development. Curr Opin Genet Dev 14, 575-581.
Rebagliati, M.R., Toyama, R., Haffter, P., Dawid, I.B., 1998. cyclops encodes a nodal-related factor involved in midline signaling. Proc Natl Acad Sci U S A 95, 9932-9937.
Reifers, F., Böhli, H., Walsh, E.C., Crossley, P.H., Stainier, D.Y., Brand, M., 1998. Fgf8 is mutated in zebrafish acerebellar (ace) mutants and is required for maintenance of midbrain-hindbrain boundary development and somitogenesis. Development 125, 2381-2395.
Ries, J., Yu, S.R., Burkhardt, M., Brand, M., Schwille, P., 2009. Modular scanning FCS quantifies receptor-ligand interactions in living multicellular organisms. Nat Methods 6, 643-645.
Rohner, N., Bercsényi, M., Orbán, L., Kolanczyk, M.E., Linke, D., Brand, M., Nüsslein-Volhard, C., Harris, M.P., 2009. Duplication of fgfr1 permits Fgf signaling to serve as a target for selection during domestication. Curr Biol 19, 1642-1647.

Sampath, K., Rubinstein, A.L., Cheng, A.M., Liang, J.O., Fekany, K., Solnica-Krezel, L., Korzh, V., Halpern, M.E., Wright, C.V., 1998. Induction of the zebrafish ventral brain and floorplate requires cyclops/nodal signalling. Nature 395, 185-189.
Schepis, A., Nelson, W.J., 2012. Adherens junction function and regulation during zebrafish gastrulation. Cell Adh Migr 6, 173-178.
Schier, A.F., 2003. Nodal signaling in vertebrate development. Annu Rev Cell Dev Biol 19, 589-621.
Schier, A.F., Neuhauss, S.C., Harvey, M., Malicki, J., Solnica-Krezel, L., Stainier, D.Y., Zwartkruis, F., Abdelilah, S., Stemple, D.L., Rangini, Z., Yang, H., Driever, W., 1996. Mutations affecting the development of the embryonic zebrafish brain. Development 123, 165-178.
Schier, A.F., Shen, M.M., 2000. Nodal signalling in vertebrate development. Nature 403, 385-389.
Schier, A.F., Talbot, W.S., 2001. Nodal signaling and the zebrafish organizer. Int J Dev Biol 45, 289-297.
Schmidt, R., Strahle, U., Scholpp, S., 2013. Neurogenesis in zebrafish - from embryo to adult. Neural Dev 8, 3.
Schmitz, B., Campos-Ortega, J., 1994. Dorso-ventral polarity of the zebrafish embryo is distinguishable prior to the onset of gastrulation. Roux's Arch Dev Biol 203, 374-380.
Schoenwolf, G., Colas, J., 2001. Towards a Cellular and Molecular Understanding of Neurulation. Developmental Dynamics: an official publication of the American Association of Anatomists 221, 117-145.
Seiliez, I., Thisse, B., Thisse, C., 2006. FoxA3 and goosecoid promote anterior neural fate through inhibition of Wnt8a activity before the onset of gastrulation. Dev Biol 290, 152-163.
Seller, M.J., Perkins-Cole, K.J., 1987. Hyperthermia and neural tube defects of the curly-tail mouse. Journal of craniofacial genetics and developmental biology 7, 321-330.
Shang, E., Wang, X., Wen, D., Greenberg, D.A., Wolgemuth, D.J., 2009. Double bromodomain-containing gene Brd2 is essential for embryonic development in mouse. Dev Dyn 238, 908-917.
Shimada, A., Yabusaki, M., Niwa, H., Yokoi, H., Hatta, K., Kobayashi, D., Takeda, H., 2008. Maternal-zygotic medaka mutants for fgfr1 reveal its essential role in the migration of the axial mesoderm but not the lateral mesoderm. Development 135, 281-290.
Shimizu, T., Bae, Y.K., Hibi, M., 2006. Cdx-Hox code controls competence for responding to Fgfs and retinoic acid in zebrafish neural tissue. Development 133, 4709-4719.
Shinya, M., Eschbach, C., Clark, M., Lehrach, H., Furutani-Seiki, M., 2000. Zebrafish Dkk1, induced by the pre-MBT Wnt signaling, is secreted from the prechordal plate and patterns the anterior neural plate. Mech Dev 98, 3-17.
Shinya, M., Koshida, S., Sawada, A., Kuroiwa, A., Takeda, H., 2001. Fgf signalling through MAPK cascade is required for development of the subpallial telencephalon in zebrafish embryos. Development 128, 4153-4164.
Shu, W., Guttentag, S., Wang, Z., Andl, T., Ballard, P., Lu, M.M., Piccolo, S., Birchmeier, W., Whitsett, J.A., Millar, S.E., Morrisey, E.E., 2005. Wnt/beta-catenin

signaling acts upstream of N-myc, BMP4, and FGF signaling to regulate proximal-distal patterning in the lung. Dev Biol 283, 226-239.
Shum, A.S., Copp, A.J., 1996. Regional differences in morphogenesis of the neuroepithelium suggest multiple mechanisms of spinal neurulation in the mouse. Anat Embryol (Berl) 194, 65-73.
Sleptsova-Friedrich, I., Li, Y., Emelyanov, A., Ekker, M., Korzh, V., Ge, R., 2001. fgfr3 and regionalization of anterior neural tube in zebrafish. Mech Dev 102, 213-217.
Smith, J.L., Schoenwolf, G.C., 1997. Neurulation: coming to closure. Trends Neurosci 20, 510-517.
Solnica-Krezel, L., Sepich, D.S., 2012. Gastrulation: making and shaping germ layers. Annu Rev Cell Dev Biol 28, 687-717.
Solursh, M., Morriss, G.M., 1977. Glycosaminoglycan synthesis in rat embryos during the formation of the primary mesenchyme and neural folds. Dev Biol 57, 75-86.
Stachel, S.E., Grunwald, D.J., Myers, P.Z., 1993. Lithium perturbation and goosecoid expression identify a dorsal specification pathway in the pregastrula zebrafish. Development 117, 1261-1274.
Stulberg, M.J., Lin, A., Zhao, H., Holley, S.A., 2012. Crosstalk between Fgf and Wnt signaling in the zebrafish tailbud. Dev Biol 369, 298-307.
Sun, L., Tran, N., Liang, C., Tang, F., Rice, A., Schreck, R., Waltz, K., Shawver, L.K., McMahon, G., Tang, C., 1999. Design, synthesis, and evaluations of substituted 3-[(3- or 4-carboxyethylpyrrol-2-yl)methylidenyl]indolin-2-ones as inhibitors of VEGF, FGF, and PDGF receptor tyrosine kinases. J Med Chem 42, 5120-5130.
Sun, Z., Jin, P., Tian, T., Gu, Y., Chen, Y.G., Meng, A., 2006. Activation and roles of ALK4/ALK7-mediated maternal TGFbeta signals in zebrafish embryo. Biochem Biophys Res Commun 345, 694-703.
Szeto, D.P., Kimelman, D., 2006. The regulation of mesodermal progenitor cell commitment to somitogenesis subdivides the zebrafish body musculature into distinct domains. Genes Dev 20, 1923-1932.
Tadros, W., Lipshitz, H.D., 2009. The maternal-to-zygotic transition: a play in two acts. Development 136, 3033-3042.
Talbot, W.S., Trevarrow, B., Halpern, M.E., Melby, A.E., Farr, G., Postlethwait, J.H., Jowett, T., Kimmel, C.B., Kimelman, D., 1995. A homeobox gene essential for zebrafish notochord development. Nature 378, 150-157.
Tanaka, Y., Naruse, I., Hongo, T., Xu, M., Nakahata, T., Maekawa, T., Ishii, S., 2000. Extensive brain hemorrhage and embryonic lethality in a mouse null mutant of CREB-binding protein. Mech Dev 95, 133-145.
Tawk, M., Araya, C., Lyons, D.A., Reugels, A.M., Girdler, G.C., Bayley, P.R., Hyde, D.R., Tada, M., Clarke, J.D., 2007. A mirror-symmetric cell division that orchestrates neuroepithelial morphogenesis. Nature 446, 797-800.
Thisse, B., Heyer, V., Lux, A., Alunni, A., Degrave, A., Seiliez, I., Kirchner, J., Parkhill, J.-P., Thisse, C., 2004a. Spatial and Temporal Expression of the Zebrafish Genome by Large-Scale In Situ Hybridization Screening. Meth. Cell. Biol. 77, 505-519.

Thisse, B., Heyer, V., Lux, A., Alunni, V., Degrave, A., Seiliez, I., Kirchner, J., Parkhill, J.P., Thisse, C., 2004b. Spatial and temporal expression of the zebrafish genome by large-scale in situ hybridization screening. Methods Cell Biol 77, 505-519.
Thisse, B., Pfumio, S., Furthauer, M., Loppin, B., Heyer, V., Degrave, A., Woehl, R., Lux, A., Steffan, T., Charbonnier, X.Q., Thisse, C., 2001. Expression of the zebrafish genome during embryogenesis. ZFIN Direct Data Submission.
Thisse, B., Thisse, C., 2004. Fast Release Clones: A High Throughput Expression Analysis. ZFIN Direct Data Submission, http://zfin.org.
Thisse, B., Thisse, C., 2014. In situ hybridization on whole-mount zebrafish embryos and young larvae. Methods Mol Biol 1211, 53-67.
Thisse, B., Thisse, C., Weston, J.A., 1995. Novel FGF receptor (Z-FGFR4) is dynamically expressed in mesoderm and neurectoderm during early zebrafish embryogenesis. Dev Dyn 203, 377-391.
Thisse, B., Wright, C.V., Thisse, C., 2000. Activin- and Nodal-related factors control antero-posterior patterning of the zebrafish embryo. Nature 403, 425-428.
Thisse, C., Thisse, B., 1999. Antivin, a novel and divergent member of the TGFbeta superfamily, negatively regulates mesoderm induction. Development 126, 229-240.
Thisse, C., Thisse, B., Halpern, M.E., Postlethwait, J.H., 1994. Goosecoid expression in neurectoderm and mesendoderm is disrupted in zebrafish cyclops gastrulas. Dev Biol 164, 420-429.
Tuckett, F., Morriss-Kay, G.M., 1986. The distribution of fibronectin, laminin and entactin in the neurulating rat embryo studied by indirect immunofluorescence. Journal of embryology and experimental morphology 94, 95-112.
Ueno, N., Greene, N.D., 2003. Planar cell polarity genes and neural tube closure. Birth defects research. Part C, Embryo today : reviews 69, 318-324.
Vanhauwaert, S., Van Peer, G., Rihani, A., Janssens, E., Rondou, P., Lefever, S., De Paepe, A., Coucke, P.J., Speleman, F., Vandesompele, J., Willaert, A., 2014. Expressed repeat elements improve RT-qPCR normalization across a wide range of zebrafish gene expression studies. PLoS One 9, e109091.
Vesterlund, L., Jiao, H., Unneberg, P., Hovatta, O., Kere, J., 2011. The zebrafish transcriptome during early development. BMC Dev Biol 11, 30.
Vogel, A.M., Gerster, T., 1997. Expression of a zebrafish cathepsin L gene in anterior mesendoderm and hatching gland. Deve Genes Evol 206, 477-479.
Wallingford, J.B., Harland, R.M., 2002. Neural tube closure requires Dishevelled-dependent convergent extension of the midline. Development 129, 5815-5825.
Warga, R.M., Mueller, R.L., Ho, R.K., Kane, D.A., 2013. Zebrafish Tbx16 regulates intermediate mesoderm cell fate by attenuating Fgf activity. Dev Biol 383, 75-89.
Westerfield, M., 2000a. The zebrafish book.
Westerfield, M., 2000b. The zebrafish book., A guide for the laboratory use of zebrafish (Danio rerio). 4 ed. University of Oregon Press, Eugene, Oregon.
Williams, L.J., Rasmussen, S.A., Flores, A., Kirby, R.S., Edmonds, L.D., 2005. Decline in the prevalence of spina bifida and anencephaly by race/ethnicity: 1995-2002. Pediatrics 116, 580-586.

Wolpert, L., 1969. Positional information and the spatial pattern of cellular differentiation. J Theor Biol 25, 1-47.
Xu, W., Baribault, H., Adamson, E.D., 1998. Vinculin knockout results in heart and brain defects during embryonic development. Development 125, 327-337.
Yamamoto, S., Hikasa, H., Ono, H., Taira, M., 2003. Molecular link in the sequential induction of the Spemann organizer: direct activation of the cerberus gene by Xlim-1, Xotx2, Mix.1, and Siamois, immediately downstream from Nodal and Wnt signaling. Dev Biol 257, 190-204.
Yan, Y.L., Hatta, K., Riggleman, B., Postlethwait, J.H., 1995. Expression of a type II collagen gene in the zebrafish embryonic axis. Dev Dyn 203, 363-376.
Ybot-Gonzalez, P., Cogram, P., Gerrelli, D., Copp, A.J., 2002. Sonic hedgehog and the molecular regulation of mouse neural tube closure. Development 129, 2507-2517.
Ybot-Gonzalez, P., Gaston-Massuet, C., Girdler, G., Klingensmith, J., Arkell, R., Greene, N.D., Copp, A.J., 2007. Neural plate morphogenesis during mouse neurulation is regulated by antagonism of Bmp signalling. Development 134, 3203-3211.
Yin, Z., Haynie, J., Yang, X., Han, B., Kiatchoosakun, S., Restivo, J., Yuan, S., Prabhakar, N.R., Herrup, K., Conlon, R.A., Hoit, B.D., Watanabe, M., Yang, Y.C., 2002. The essential role of Cited2, a negative regulator for HIF-1alpha, in heart development and neurulation. Proc Natl Acad Sci U S A 99, 10488-10493.
Zhang, J., Chen, F.Z., Gao, Q., Sun, J.H., Tian, G.P., Gao, Y.M., 2012. Hyperthermia induces upregulation of connexin43 in the golden hamster neural tube. Birth Defects Res A Clin Mol Teratol 94, 16-21.
Zhao, Q., Behringer, R.R., de Crombrugghe, B., 1996. Prenatal folic acid treatment suppresses acrania and meroanencephaly in mice mutant for the Cart1 homeobox gene. Nat Genet 13, 275-283.
Zohn, I.E., 2012. Mouse as a model for multifactorial inheritance of neural tube defects. Birth defects research. Part C, Embryo today : reviews 96, 193-205.